Received: 31 August 2023 | Revised: 18 December 2023 | Accepted: 21 December 2023

DOI: 10.1002/ar.25376

SPECIAL ISSUE ARTICLE

The Anatomical Record WILEY

The osteology of *Shuvosaurus inexpectatus*, a shuvosaurid pseudosuchian from the Upper Triassic Post Quarry, Dockum Group of Texas, USA

Sterling J. Nesbitt[1,2] | **Sankar Chatterjee**[2]

[1]Department of Geosciences, Virginia Tech, Blacksburg, Virginia, USA

[2]Museum of Texas Tech University, Lubbock, Texas, USA

Correspondence
Sterling J. Nesbitt, Department of Geosciences, Virginia Tech, Blacksburg, VA 24061, USA.
Email: sjn2104@vt.edu

Funding information
National Science Foundation; National Geographic Society

Abstract

A vast array of pseudosuchian body plans evolved during the diversification of the group in the Triassic Period, but few can compare to the toothless, long-necked, and bipedal shuvosaurids. Members of this clade possess theropod-like character states mapped on top of more plesiomorphic pseudosuchian character states, complicating our understanding of the evolutionary history of the skeleton. One taxon in this clade, *Shuvosaurus inexpectatus* has been assigned to various theropod dinosaur groups based on a partial skull and referred material and its postcranium was assigned to a different taxon in Pseudosuchia. After the discovery of a skeleton of a shuvosaurid with a *Shuvosaurus*-like skull and a pseudosuchian postcranial skeleton, it became clear *Shuvosaurus inexpectatus* was a pseudosuchian. Nevertheless, a number of questions have arisen about what skeletal elements belonged to *Shuvosaurus inexpectatus*, the identification of skull bones, and the resulting implication for pseudosuchian evolution. Here, we detail the anatomy of the skeleton *Shuvosaurus inexpectatus* through a critical lens, parse out the bones that belong to the taxon or those that clearly do not or may not belong to the taxon, rediagnose the taxon based on these revisions, and compare the taxon to other archosaurs. We find that *Shuvosaurus inexpectatus* possesses similar anatomy to other shuvosaurids but parts of the skeleton of the taxon clarifies the anatomy of the group given that they are preserved in *Shuvosaurus inexpectatus* but not in others. *Shuvosaurus inexpectatus* is represented by at least 14 individuals from the West Texas Post Quarry (Adamanian holochronozone) and all *Shuvosaurus inexpectatus* skeletal material from the locality pertains to skeletally immature individuals. All of the skeletons are missing most of the neural arches, ribs, and most of the forelimb. We only recognize *Shuvosaurus inexpectatus* from the Post Quarry and all other material

A recent paper describing the skull of *Shuvosaurus inexpectatus* by Lehane (2023) was published just before we submitted our work and we were not aware of this work until publication. Our work was not intended to correct or supersede Lehane's (2023) work and our paper was conducted independently from that study.

assigned to the taxon previously is better assigned to the broader group Shuvosauridae.

KEYWORDS
Archosauria, convergence, Dockum Group, Norian, Poposauroidea, Shuvosauridae

1 | INTRODUCTION

During the Triassic Period, archosaurs diversified in fantastic forms that reached all corners of Pangea (Benton, 1990a; Benton & Clark, 1988; Brusatte et al., 2010; Ezcurra, 2016; Gauthier, 1986; Gauthier & Padian, 1985; Juul, 1994; Nesbitt, 2011; Parrish, 1993; Sereno, 1991; Sereno & Arcucci, 1990). Archosaurs split into two main lineages early in the Triassic (Butler et al., 2011; Nesbitt et al., 2011), one lineage that eventually led to living crocodylians (pan-Crocodylia, Pseudosuchia, crocodile-line archosaurs) and one lineage that eventually led to birds (pan-Aves, Avemetatarsalia, bird-line archosaurs). Between these two lineages, rapid diversification into sub clades and the evolution of shape, locomotion, and ecologies led to a blossoming of body plans, and among these body plans morphological convergence was frequent across lineages (Bates & Schachner, 2012; Benton, 1986; Chatterjee, 1985; Nesbitt, 2007; Nesbitt et al., 2019, 2023; Nesbitt & Norell, 2006; Stocker et al., 2016). Consequently, discriminating the phylogenetic history and convergence of morphology has been a major goal among Triassic workers and this research has progressed as new archosaur specimens and imaging technologies (CT scanning, surface scanning) have become available.

A central example of this research has focused on the Shuvosauride, a highly divergent pseudosuchian lineage that includes members with large-eyed skulls, toothless beaks, elongated vertebral columns, bipedal locomotion, and other characteristics more in common with theropod dinosaurs than with any member of the pseudosuchian lineage (Nesbitt, 2007; Nesbitt & Norell, 2006). Within this clade, there are three recognized species, *Effigia okeeffeae* (Nesbitt & Norell, 2006), *Shuvosaurus inexpectatus* (Chatterjee, 1993), and *Sillosuchus longicervix* (Alcober & Parrish, 1997) and many occurrences throughout the Late Triassic of North America (Hunt, 2001; Lessner et al., 2018; Nesbitt, 2007; Sidor et al., 2018) or possibly in the Middle Triassic (Nesbitt, 2005a). Among the named species, *Effigia okeeffeae* served as a linchpin in referring cranial to postcranial remains to the same species and to the clade as a whole (Nesbitt, 2007; Nesbitt & Norell, 2006). Yet, there are many anatomical elements and details missing in *Effigia okeeffeae* that are preserved in the closely related species *Shuvosaurus inexpectatus*, a species known from many skeletal elements from a single bonebed (Post Quarry; MOTT VPL 3624) in the Cooper Canyon Formation of the Dockum Group in West Texas.

Shuvosaurus inexpectatus originally consisted of skull and a few elements of the postcranium, but it is now widely recognized that the postcrania of a separately named taxon, *Chatterjeea elegans* Long & Murry, 1995 belongs to the skull of *Shuvosaurus inexpectatus* (see below). However, questions remain about the attribution of elements of *Shuvosaurus inexpectatus*, how different or similar *Shuvosaurus inexpectatus* is compared to its close relatives, and what *Shuvosaurus inexpectatus* tells us about convergence of some pseudosuchians and dinosaurs. Here, we critically examine what elements that compose *Shuvosaurus inexpectatus*, rediagnose the taxon, detail the osteology of each of those skeletal parts after further preparation and extensive comparisons, illustrate those skeletal elements, and comment on its implications for further studies of Shuvosauridae. Furthermore, this work corrects a number of our previous interpretations with *Shuvosaurus inexpectatus* and its close relatives (i.e., *Effigia okeeffeae*, *Arizonasaurus babbitti*) and demonstrates personal evolutions of our previous work. With this revision, *Shuvosaurus inexpectatus* will serve as an important example of an enigmatic taxon that has undergone revision as our field incorporates new information from other taxa.

1.1 | History of interpretation of *Shuvosaurus inexpectatus*

In the early 1980s, one of the authors (Chatterjee) and his students unearthed an important fossil locality in the lower portion of the Cooper Canyon Formation (Dockum Group; see Martz et al., 2013), near the town of Post in Garza County, Texas. This locality, known as the Post Quarry (MOTT VPL 3624), preserves a rich deposit of skeletons from many Upper Triassic vertebrates from a 30-centimeter thick, fine-grained deposit (Figure 1b; Chatterjee, 1985; Martz et al., 2013). Among the multitaxic remains, the archosaur assemblage includes both pseudosuchians and avemetatarsalians preserved as

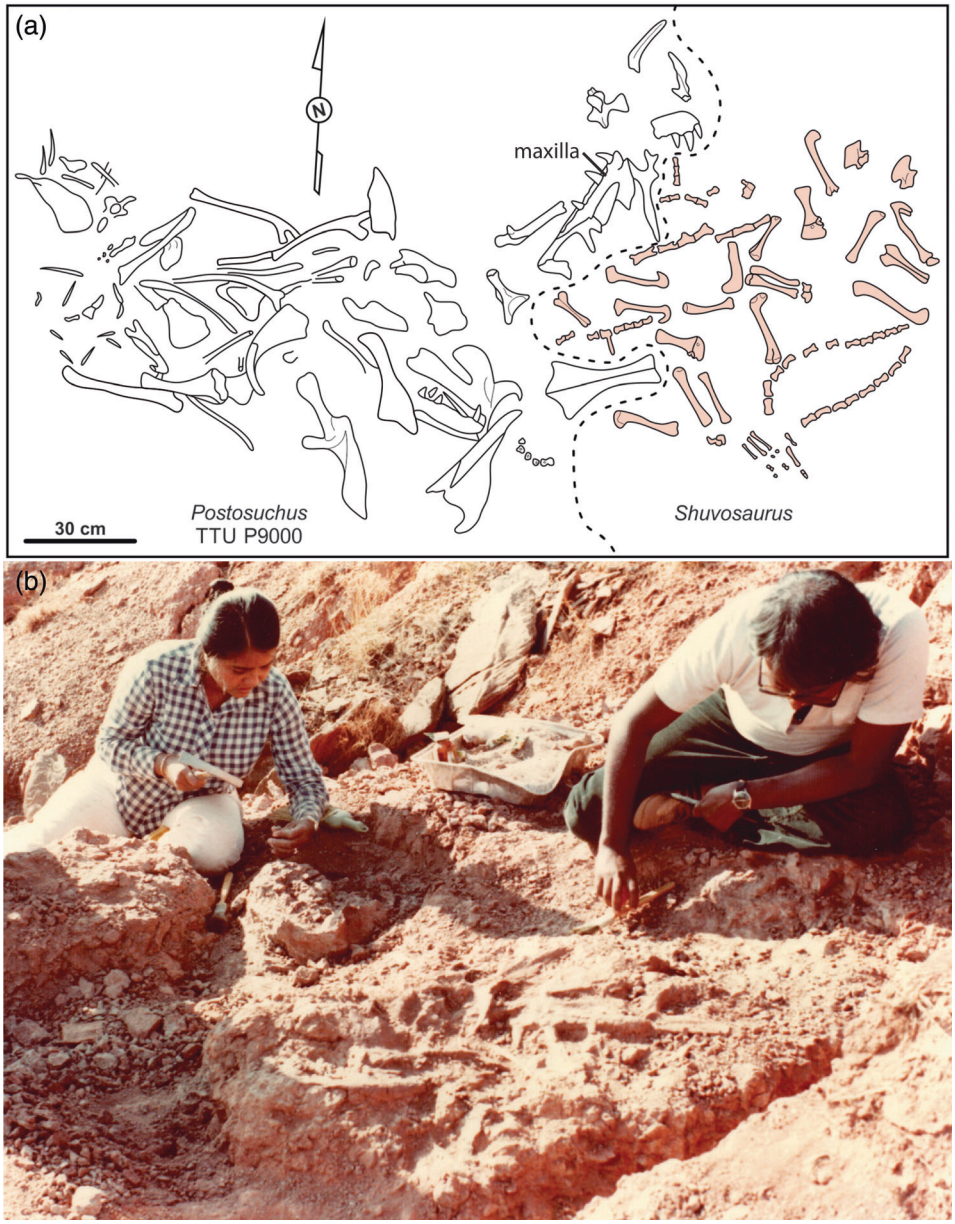

FIGURE 1 Excavation map of the Post Quarry (MOTT VPL 3624; modified from Chatterjee, 1985) demonstrating the association of material referred to *Shuvosaurus inexpectatus* in orange (a). Note, there is more than one postcranial skeleton of *Shuvosaurus inexpectatus* illustrated (e.g., four femora, four ischia) and it is not known which parts pertains to TTU-P9001 in this quarry map and if all parts of the skeleton were recorded. Photograph of the excavation of the Post Quarry by Sankar Chatterjee (right) and Sibani Chatterjee (left) in 1980 (b). The maxilla of the holotype of *Postosuchus kirkpatricki* (TTU-P9000) lies just in front of Sankar and the bones of the largely complete postcranium referred to *Shuvosaurus inexpectatus* (TTU-P9001) lies just underneath Sankar.

partial skeletons (Figure 1a; Martz et al., 2013). Soon after initial preparation, a variety of archosaurs species were named including *Technosaurus smalli* (Chatterjee, 1984), *Postosuchus kirkpatricki* (Chatterjee, 1985), and the enigmatic *Shuvosaurus inexpectatus* (Chatterjee, 1993) from a skull material and a few parts of postcranial bones (TTU-P9280, TTU-P9281, TTU-P9282) that were associated. Chatterjee (1993) referred *Shuvosaurus inexpectatus* to Theropoda and more tentatively to ?Ornithomimosauria based on a variety of features of the premaxilla, palate, and braincase. Soon after, the theropod affinities of the skull were supported by Rauhut (1997, 2003) and Osmólska (1997), but in these studies the coelurosaurian and Ornithomimosauria affinities were questioned and not supported. Hunt et al. (1998) followed by Heckert and Lucas (1998) briefly commented on the affinities of the taxon writing that the taxon did not possess any diagnostic character states of Dinosauria. A Master's thesis later reached a similar conclusion as Rauhut and found *Shuvosaurus inexpectatus* as an early diverging theropod (Lehane, 2005).

!In parallel to the timeline of the *Shuvosaurus inexpectatus* discovery, preparation, and analysis, the partial skeletons of another apparent pseudosuchian was also discovered in the Post Quarry near the remains of *Postosuchus kirkpatricki* (Figure 1b). Initially, these were interpreted as young individual of *Postosuchus kirkpatricki* (Chatterjee, 1985), but were considered "radically different in morphology" and "such differences cannot be explained by growth or sexual dimorphism" (Long & Murry, 1995, p. 161). Consequently, Long and Murry (1995) identified these skeletons as a new taxon,

Chatterjeea elegans based on a largely complete postcranial skeleton (TTU-P9001). Within the original description of *Chatterjeea elegans*, Long and Murry (1995) provided a compelling case that the cranium of *Shuvosaurus inexpectatus* belongs to the postcranium of *Chatterjeea elegans* and if their case is further supported *Shuvosaurus inexpectatus* would be the senior synonym. Their argument was supported by the discovery of *Effigia okeeffeae*, a close relative with a *Shuvosaurus inexpectatus*-like head and a *Chatterjeea elegans*-like postcranium (Nesbitt, 2007; Nesbitt & Norell, 2006). Subsequent discoveries and closer scrutinization of previously found *Shuvosaurus inexpectatus*-like material across the Upper Triassic deposits of North America and phylogenetic analyses further supported the *Shuvosaurus inexpectatus-Chatterjeea elegans* synonymy (Brusatte et al., 2010; Lehane, 2023; Nesbitt, 2007, 2011). It is now clear that *Shuvosaurus inexpectatus* consists of a toothless skull and a long-limbed and elongated body (Figure 2) belong to a group of pseudosuchian archosaurs.

1.2 | Taphonomy and preparation

Other than the taxonomic and phylogenetic history of *Shuvosaurus inexpectatus*, we want to highlight the taphonomic and preparation history of the specimens; this process has important interpretive implications for our description and the composition of *Shuvosaurus inexpectatus*. The partial Post Quarry map produced in 1982 (Figure 1a) shows the occurrence of associated postcranial skeletons of *Shuvosaurus inexpectatus* next to an associated skull and postcranial skeleton of *Postosuchus kirkpatricki*. The specimen closest to *Postosuchus kirkpatricki* represents the nearly complete postcranium referred to *Shuvosaurus inexpectatus* (TTU-P9001) we largely rely on for the description below. This detailed quarry map demonstrates that the skeletons of *Shuvosaurus inexpectatus* were (1) partially articulated, including the vertebrae and (2) clearly consist of associated skeletons (Chatterjee, 1985). Subsequent excavations for the next few years, east of the *Postosuchus kirkpatricki* specimens, produced at least nine individuals (based on postcrania, see below) in a generally similar associated condition. Unfortunately, details of the association and partial articulation of all but TTU-P9001 are now lost and more detailed bonebed maps are not available; currently the TTU *Shuvosaurus inexpectatus* collection is organized by element, not individual.

The three specimens of *Shuvosaurus inexpectatus* with cranial elements were found associated and were prepared from field jackets (Chatterjee, 1993), but the quarry location of the holotype skull (TTU-P9280) and referred cranial material (TTU-P9281, TTU-P9282) was not recorded relative to the partial postcranial skeletons. The holotype skull bones (TTU-P9280) were found disarticulated (e.g., quadrate, parietal) and some partially articulated (e.g., part of the skull roof, braincase), prepared and then assembled into an incomplete reconstructed skull (Chatterjee, 1993, fig. 4; Figures 3 and 4). During the assembly of the skull, compounds and materials were added (i.e., plaster, epoxy clay, cyanoacrylate, wire mesh in the lower jaw) to make connections and stabilize the skull whereas missing elements were sculpted. Prior to 2005, the holotype reconstructed skull was taken apart and partially reprepared (Lehane, 2005). Much of the original added compounds were removed and partially replaced with some limited "paper pulp" to either

FIGURE 2 Reconstructed skeleton of *Shuvosaurus inexpectatus*. Assembled and designed by Doug Cunningham. Photograph by Bill Mueller.

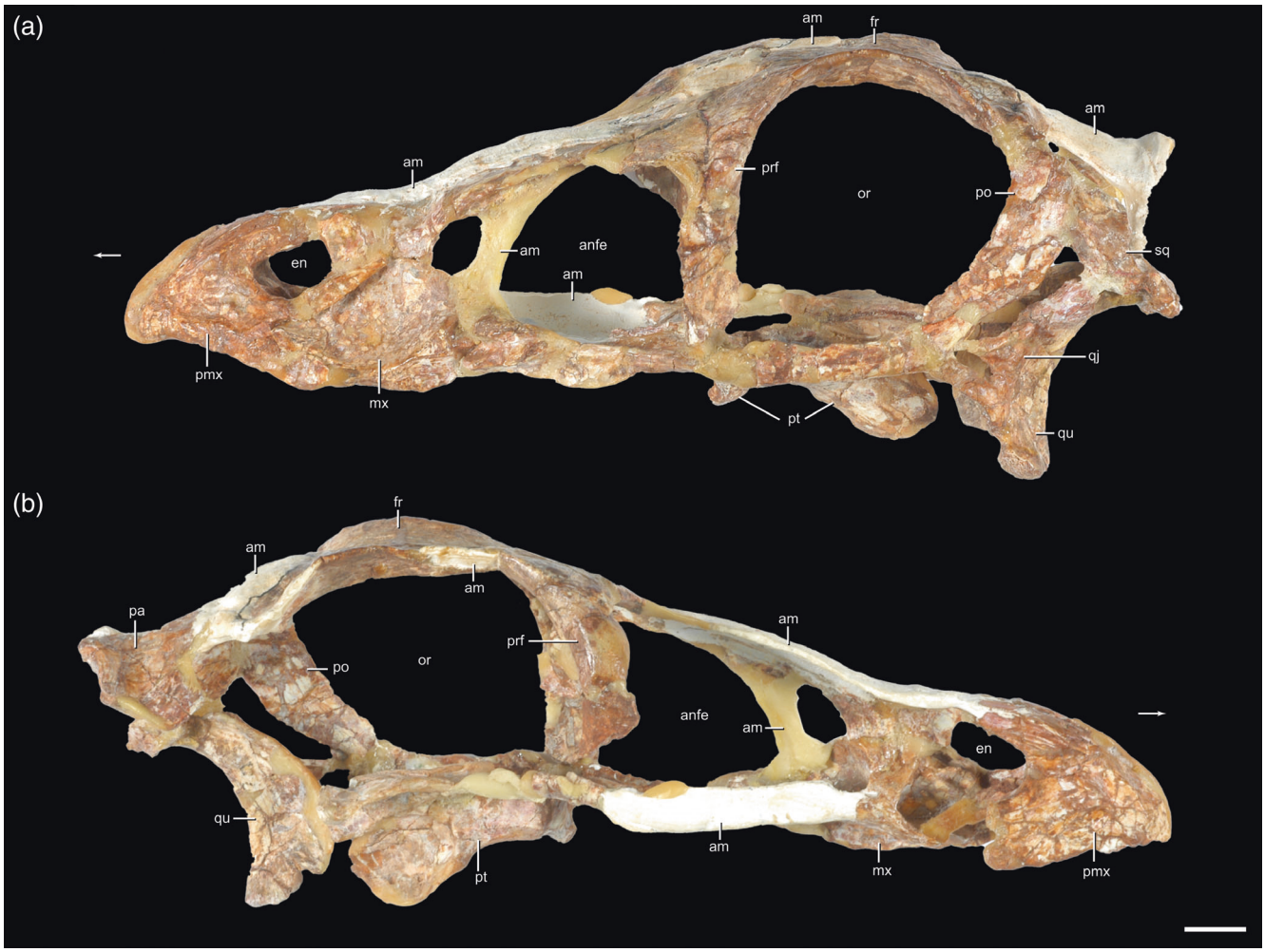

FIGURE 3 The originally reconstructed holotype skull of *Shuvosaurus inexpectatus* (TTU-P9280) prior to the naming of the taxon in left lateral (a) and right lateral (b) views with a view of the medial surfaces of many of the bones from the left side. Skull illustrations including suture interpretations by Chatterjee (1993, fig. 5) and Rauhut (1997, fig. 1) were based directly on this physical reconstruction. am, added material; anfe, antorbital fenestra; en, external naris; fr, frontal; mx, maxilla; or, orbit; pa, parietal; pmx, premaxilla; po, postorbital; prf, prefrontal; pt, pterygoid; qj, quadratojugal; qu, quadrate; sq, squamosal. Arrows indicate anterior direction. Scale bar equals 1 cm. Photographs by Bill Mueller.

rearticulate some bones (e.g., premaxillae) or to reconstruct missing areas (Lehane, 2005) within bones.

For this analysis, our team conducted further preparation of the holotype (e.g., removing adhesives, other added materials, matrix; see acknowledgments), referred cranial, and postcranial material referrable to the taxon. Additionally, we CT scanned the skull roof (TTU-P9280) and the braincase (TTUP 9282) to examine connection details of the bones. We found that some of the skull roof bones were clearly preserved articulated and have not been manipulated whereas others are separated from other bones by added material (e.g., the nasal from the prefrontal-frontal) and assembled. The latter is also the case in the braincase (TTUP 9282); the otooccipital, prootic, and supraoccipital were originally articulated, but the ?laterosphenoid, parabasisphenoid, and basioccipital were later adhered to the rest of the braincase with added materials after initial cleaning. We take all this into consideration in our description below.

1.3 | Institutional abbreviations

AMNH = American Museum of Natural History, New York, New York, USA; CMNH = Carnegie Museum of Natural History, Pittsburgh, Pennsylvania, USA; IVPP = Institute of Vertebrate Paleontology and Paleoanthropology, Beijing, China; MOTT VPL = Museum of Texas Tech University Vertebrate Paleontology Locality; MSM = Arizona Museum of Natural History, Mesa, Arizona, USA; NCSM = North Carolina Museum of Natural Sciences in Raleigh, North Carolina, USA; NMT = National Museum of Tanzania, Dar es Salaam, Tanzania; PEFO = Petrified Forest National Park, Arizona, USA; PVL = Paleontología de Vertebrados,

FIGURE 4 The originally reconstructed holotype skull of *Shuvosaurus inexpectatus* (TTU-P9280) prior to the naming of the taxon in dorsal (a) and ventral (b) views with a view of the ventral surfaces of many of the bones from the skull roof. Skull illustrations including suture interpretations by Chatterjee (1993, fig. 5) and Rauhut (1997, fig. 1) were based directly on this physical reconstruction. am, added material; ect, ectopterygoid (previously identified as the palatine); fr, frontal; mx, maxilla; pa, parietal; pmx, premaxilla; po, postorbital; prf, prefrontal; pt, pterygoid; qj, quadratojugal; qu, quadrate; sq, squamosal. Arrows indicate anterior direction. Scale bar equals 1 cm. Photographs by Bill Mueller.

Instituto "Miguel Lillo," San Miguel de Tucumán, Argentina; PVSJ = División de Paleontología de Vertebrados del Museo de Ciencias Naturales y Universidad Nacional de San Juan, San Juan, Argentina; TTU-P = Texas Tech University Paleontology, Lubbock, Texas, USA; USNM = National Museum of Natural History (formerly United States National Museum), Smithsonian Institution, Washington, D.C., USA; YPM = Yale Peabody Museum, New Haven, Connecticut, USA.

1.4 | Methods

1.4.1 | Strategy for identifying which bones belong to *Shuvosaurus inexpectatus*

The anatomical and taxonomic identification of the specific elements of *Shuvosaurus inexpectatus* has changed since their initial identification and description (Chatterjee, 1985; Long & Murry, 1995; Nesbitt & Norell, 2006; see above). Consequently, what skeletal elements pertain to *Shuvosaurus inexpectatus* is not always clear because of missing and ambiguous information. Therefore, we choose a deliberate strategy to identify *Shuvosaurus inexpectatus* bones, especially the identification of cranial bones. Our strategy is also enhanced by new tools for comparing other extinct archosaurs including CT information and 3D models generated from high precision optical laser scanners of comparative material.

We used the following strategy for the identification of skull bones of *Shuvosaurus inexpectatus*. First, we used the original association/composition of each specimen (i.e., TTU-P9280, TTU-P9281, TTU-P9282) from Chatterjee (1993) as a starting point. In that original description, the holotype cranial material was listed as

a "nearly complete skull, left lower jaw" without an inventory of which specific skull bones were part of the holotype. Therefore, we used the original reconstructed holotype skull as a guide (Figures 3 and 4). We then assessed each skull bone of the holotype to determine which side of the skull the bone came from to eliminate potential duplicates. Next, we carefully compared our assessed skull bones of *Shuvosaurus inexpectatus* with that of the nearly complete skull of the close relative *Effigia okeeffeae*, the only other shuvosaurid with skull material (Nesbitt, 2007; Nesbitt & Norell, 2006). From this comparison, we determined which bones matched between the two taxa (Table 1), which could not be confirmed because

TABLE 1 Identifications of the skull bones of *Shuvosaurus inexpectatus* from previous interpretations and our interpretations.

Original identifications in Chatterjee (1993) type series	Identifications of Lehane (2023)	Holotype (TTU P9280), our identifications)	Referred, our identifications	Present in *Effigia?*
Premaxilla	Premaxilla	l + r	TTU-P9282	Yes
Maxilla	r	l, but not clear	None	No
Nasal	Attached to the skull roof	Maybe a piece on the frontal	None	No
Lacrimal	l + r, attached to the skull roof	Not located	None	No
Jugal	l, and attached to postorbital	l, but not clear	TTU-P15378	Yes, as referred
Frontal	l + r	l + r	TTU-P9281, TTU-P9282	Yes
Prefrontal	l + r	l + r	None	Yes
Postorbital	l, attached to the skull roof and attached to jugal	l	Partial on TTU-P9282 and TTU- P9281	Yes
Parietal	r	r	TTU-P9282	Yes
Squamosal	r	l, could not locate	TTU-P9282	Yes
Quadrate	l	l	TTU-P9282	Yes
Quadratojugal	l	l	None	No
ectopterygoid	l (misidentified, we reidentify this as the pterygoid)	r	None	Yes
Pterygoid	r (misidentified, we reidentify this as possibly the palatine)	l + r	None	Yes
Palatine	l (misidentified, we reidentify this as the ectopterygoid)	Possibly	None	Yes
Vomers	not mentioned	Not located	None	No
Laterosphenoid	TTU-P9282	Absent	Present but misidentified	No
Basioccipital	TTU-P9282	Absent	TTU-P9282	Yes
Parabasisphenoid	TTU-P9282	Absent	TTU-P9282	Yes
Supraoccipital	TTU-P9282	Yes	TTU-P9282	No
Otoccipital	TTU-P9282	Yes	TTU-P9282	No
Prootic	TTU-P9282	l + r	TTU-P9282	Yes
Dentary	l	l	TTU-P9281	Yes
Surangular	l	l	TTU-P24873	Yes
Angular	l	l	None	Yes
Articular	l	l, highly eroded	TTU-P24873	Yes

Abbreviations: l, left; r, right.

those bones are not present in *Effigia okeeffeae* (e.g., quadratojugal), and which bones did not match (e.g., jugal, laterosphenoid) between the two taxa. Consequently, we reidentified all of the originally identified palatal bones of *Shuvosaurus inexpectatus* based on the more complete palatal bones of *Effigia okeeffeae*.

Our strategy for the identification of postcranial bones of *Shuvosaurus inexpectatus* is similar to that stated for the crania. The postcrania of *Shuvosaurus inexpectatus* was partially mapped (Figure 1a), some of the material was articulated (e.g., TTU-P9001), and is easily differentiated from the other taxa present in the Post Quarry (Martz et al., 2013). Additionally, the postcrania was compared directly to the holotype and referred specimens of *Effigia okeeffeae*. Through this process, we were able to identify a few parts of the anatomy of *Shuvosaurus inexpectatus* that were not originally reported (e.g., distal tarsal three).

1.5 | Computer tomography

The skull roof of the holotype (TTU-P9280) and the dentaries (TTU-P9281), premaxillae (TTU-P9282), and the braincase (TTU-P9282) of referred specimens were CT scanned using a Nikon XT H 225 CT high-resolution micro-computed tomographic scanner at the Shared Materials Instrumentation Facility of Duke University. We digitally segmented the μCT data using Materialize Mimics v20.0 (Materialise, Leuven, Belgium) (https://www.materialise. com/mimics). The μCT scans of these specimens and their parameters can be found through MorphoSource (https://www.morphosource.org).

2 | SYSTEMATIC PALEONTOLOGY

ARCHOSAURIA Cope, 1869 sensu Gauthier & Padian, 1985

PSEUDOSUCHIA Zittel 1887-90, sensu Gauthier & Padian, 1985

POPOSAUROIDEA Nopcsa, 1923 sensu Nesbitt, 2011

SHUVOSAURIDAE Chatterjee, 1993 sensu Nesbitt, 2011

Shuvosaurus inexpectatus Chatterjee, 1993

Figures 1–45

Holotype—TTU-P9280, left and right premaxillae, right ectopterygoid, pterygoid fragments, left quadrate, left quadratojugal, skull roof including the frontals and prefrontals, left postorbital, right parietal (not listed in the holotype originally, but incorporated into the original reconstruction), partial braincase including supraoccipital, partial prootics, and otooccipitals, left dentary, left posterior portion of the jaw including the articular, surangular and possibly the angular. Other possible bones that are either missing or their identification is tenuous include a left maxilla, jugal fragment, left squamosal (missing), and other fragments.

Paratypes—TTU-P9281, left squamosal, right frontal, nearly complete left dentary with attached partial right side of the dentary; TTU-P9282; left and right premaxilla, partial skull roof formed of frontals and partial postorbitals, left squamosal, right quadrate, partial braincase including basioccipital, supraoccipital, partial prootics, otooccipitals, and parabasisphenoid, partial atlas and axis components.

Referred specimens—TTU-P24873, left postdentary bones; TTU-P9001, "*Chatterjeea elegans*" holotype, nearly complete atlas and axis, at least five other cervical vertebrae, at least 10 trunk vertebrae, four partially coossified sacral vertebrae, at least 26 partial caudal vertebrae (mostly middle to posterior but missing the posteriormost vertebrae), left and right partial scapulocoracoids, left humerus, left ilium, right pubis, left and right coossified ischia, left femur, left and right tibia, right fibula, left astragalus, left calcaneum, left distal tarsal four, left metatarsals I-V, right metatarsals I-IV, phalanges from the left pes, one ungual from digit 1; TTU-P19950, third and fourth cervical vertebrae; TTU-P23422, two neural arches from trunk vertebrae; TTU-P23438, sacrum; TTU-P23873-TTU-P23875, posterior caudal vertebrae; TTU-P23903, cervical rib; TTU-P19577, trunk rib; TTU-P18424, right scapula; TTU-P9003, right ilium; TTU-P18927, proximal portions of the left and right pubes; TTU-P18414, left and right coossified ischia; TTU-P18309, right femur; TTU-P18322, right calcaneum; TTU-P18304 right astragalus; TTU-P24024, left distal tarsal three; TTU-P9296, pedal ungual; TTU-P9297, pedal ungual; TTU-P18323, TTU-P18368, TTU-P18380, TTU-P18381, TTU-P18382, TTU-P18383, TTU-P19010, TTU-P19012, TTU-P19275, TTU-P19575, TTU-P22577, TTU-P22578, left calcanea; TTU-P15186, TTU-P18305, TTU-P18306, TTU-P18307, TTU-P18308, TTU-P18310, TTU-P18311, TTU-P18312, TTU-P18316, TTU-P18480, TTU-P18481, TTU-P18483, TTU-P18490, TTU-P18493, right femora. Additionally, there are many unprepared bones referrable to *Shuvosaurus inexpectatus* from the Post Quarry in collections at MOTT. We do not formally refer any element to *Shuvosaurus inexpectatus* from outside the Post Quarry (see discussion).

Locality and age—Post (= Miller) Quarry (MOTT VPL 3624), lower part of the type section of the Cooper Canyon Formation in southern Garza County, western Texas. Adamanian holochronozone based on the presence of the phytosaur genus *Leptosuchus* and stratigraphically below the phytosaur genus *Machaeroprosopus* (Martz et al., 2013). None of the Dockum Group

FIGURE 5 The holotype skull of *Effigia okeeffeae* (AMNH FR 30578) in left lateral (a) and right lateral (b) view. ar, articular; de, dentary; ect, ectopterygoid; fr, frontal; ju, jugal; la, lacrimal; mx, maxilla; na, nasal; or, orbit; pa, parietal; pal, palatine; pmx, premaxilla; po, postorbital; prf, prefrontal; pt, pterygoid; qu, quadrate; sq, squamosal; su, surangular. Arrows indicate anterior direction. Scale bar equals 1 cm. Photographs by Mick Ellison.

sediments have high precision radioisometric dates like that of the Chinle Formation, but the Adamanian is early to middle Norian in the Chinle Formation (Irmis et al., 2011; Martz & Parker, 2017; Ramezani et al., 2011; Rasmussen et al., 2021).

Archosaurs found with *Shuvosaurus inexpectatus* from the Post Quarry include the phytosaur *Leptosuchus*, aetosaurs (*Calyptosuchus wellesi*, *Typothroax coccinarum*, *Paratypothorax*, and *Desmatosuchus smalli*), paracrocodylomorphs (*Postosuchus kirkpatricki* and Crocodylomorpha), and avemetatarsalians (*Dromomeron gregorii*, *Technosaurus smalli*, Herrerasauridae, Neotheropoda) (for full assemblage see Martz et al., 2013; Sarigül, 2017).

Revised diagnosis—Given the complications of holotypes, paratypes, and referred specimens and non-overlapping elements among each, we diagnose *Shuvosaurus inexpectatus* in a number of categories to prevent confusion in the future. We start with a differential diagnosis.

Based on the holotype: *Shuvosaurus inexpectatus* differs from all other archosaurs other than *Effigia okeeffeae* based on the following combination of character states: Clear tomia (cutting edge) in an edentulous premaxilla and dentary (also in *Lotosaurus adentus*, see below); anterior process of the nasal fits into slot on the lateral side of the anterior process of the premaxilla (also in *Lotosaurus adentus*, see below); prefrontal ventral process expanded to more than 80% the dorsolateral height of the orbit (estimated based on the curvature of the orbital margin in *Shuvosaurus inexpectatus*); postfrontal absent; ventral process of the postorbital mediolaterally compressed and greater than 50% the length of the postorbital-jugal bar; quadrate with a concave ventral surface that corresponds to a convex articular surface of the articular; pterygoid possesses a

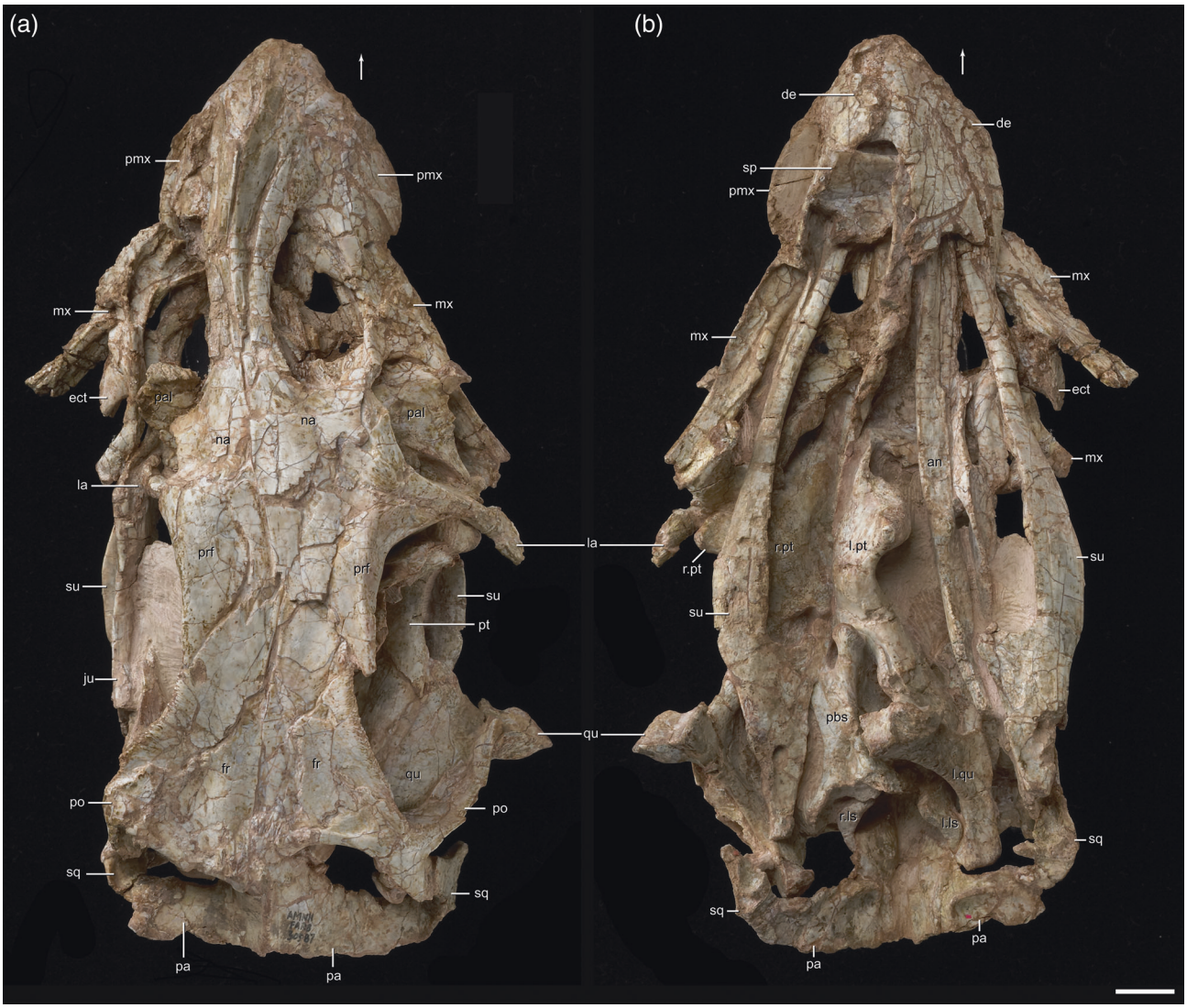

FIGURE 6 The holotype skull of *Effigia okeeffeae* (AMNH FR 30578) in dorsal (a) and ventral (b) views. an, angular; de, dentary; ect, ectopterygoid; fr, frontal; ju, jugal; l., left; la, lacrimal; ls, laterosphenoid; mx, maxilla; na, nasal; pa, parietal; pal, palatine; pbs, parabasisphenoid; pmx, premaxilla; po, postorbital; prf, prefrontal; pt, pterygoid; qu, quadrate; r., right; sp, splenial; sq, squamosal; su, surangular. Arrows indicate anterior direction. Scale bar equals 1 cm. Photographs by Mick Ellison.

lateral process with a laterally rounded margin with small dimples on the surface; ectopterygoid dorsoventrally compressed so that the length is five times longer than height where it meets the jugal; edentulous dentary with medially expanded shelf; dorsally arched surangular.

Based on the paratypes and referred cranial material: *Shuvosaurus inexpectatus* differs from all other archosaurs other than *Effigia okeeffeae* based on the following combination of character states: posterodorsal process of the premaxilla much shorter than the anterodorsal process; anteroposterior elongated parabasisphenoid that is longer than wide at its posterior portion; exoccipital portion of the otooccipital do not meet at the midline on the basioccipital; deep, well defined pockets lateral to the cultriform process on the anterior portion of the parabasisphenoid; anterior process of the jugal much longer than the posterior process of the jugal.

Based on the referred postcranial material: *Shuvosaurus inexpectatus* is different from all other archosaurs other than *Effigia okeeffeae* based on the following combination of character states: low neural spine of the cervical centra (less than 25% the height of the neural arch); posterior cervical and anterior trunk vertebrae with prezygodiapophyseal lamina, or transverse processes, that are triangular in dorsal view and posterolaterally terminate in processes; epipophyses in the presacral vertebrae absent; sacral series consisting of at least three sacrals where the sacral centra are much wider than tall; sacral neural spines coossified; caudal vertebrae with anterior processed that are at least ¼ the length of the preceding

centrum; well defined fossa on the lateral edge of the glenoid of the scapula; posterior expanded, postglenoid process of the coracoid and a fossa on the dorsal process of the process; ventral margin of the scapula anteroposteriorly longer than any of the scapular blade; humeral head greater that 75% the mediolateral length of the proximal surface; proximal and distal ends about or less expanded than twice the width of midshaft; anterior process (prepubic) of ilium longer than the anteroposterior width of the acetabulum; supraacetabular ridge present on the dorsolateral surface and arcs anteriorly; pubic "boot" (posterior expansion) greater than 50% the length of the long axis of the pubis; ridge present on the lateral side of the shaft of the pubis; ischia meet at midline for the length of the elements with a swelling at the midline dorsally and a sharp ridge ventrally; proximal portion of the femur with a posterolaterally expanded anteromedial tuber (largest of the proximal tubera); ridge for attachment of the caudifemoralis muscles (= 4th trochanter) absent; proximal portion of the fibula much longer anteroposteriorly than wide mediolaterally with an anterior edge that curves medially; medial edge of the distal end of the fibula possesses a medially expanded rim; astragalar peg medially expanded with a concave surface; anterior hollow reduced to a foramen; distal tarsal four with a tongue-like ventral process; metatarsals I and IV subequal in length and metatarsals II and III subequal in length; metatarsal V with a flange on the anteromedial side of the shaft; at least ungual from digit 1 wider than tall and hoof-like.

Further character states that *Shuvosaurus inexpectatus* possesses that are poorly known or unknown in *Effigia okeeffeae* (across all type and referred material) that could be a shared character state or a unique character states of either taxon: supraoccipital highly constricted at the midline to form a ridge; posteroventrally deflected paroccipital processes of the otooccipital; anteroventral portion of the quadratojugal with a clear notch; proportionally longer dentary; axis centrum articular facet height by length ration, longest of the presacral series; proportionally longer cervical vertebrae measured by height of the centrum versus length; well defined ridge on the anterior half of the ventral midline in cervical centra, this ridge could expand laterally or could be blade-like further ventrally; rimmed fossa on the anterior half of the lateral side of the cervical centra; rimmed fossa on the posterior half of the lateral side of the cervical centra (less common); far posterior caudal centra with a ratio eight times longer than centrum height; pronounced lateral ridge in the posterior caudal vertebrae; calcaneum tuber much taller (proximodistally) than wide (mediolaterally); calcaneum tuber tapers proximally to an acute tip.

Shuvosaurus inexpectatus differs from *Effigia okeeffeae* by: the anterior processes of parietal extends much more anteriorly into the frontal than that of *Effigia okeeffeae*; lateral (= orbital) rim of the frontal is sharp and lacks rugosity in contrast to the broader, rugose lateral margin in *Effigia okeeffeae*; orbital rim of frontal dorsally raised relative to the midline whereas the frontal is nearly flat in *Effigia okeeffeae*; anterior (= postorbital process) of the squamosal proportionally much longer than tall than the corresponding process in *Effigia okeeffeae*; tapered posterior process of the squamosal present and absent in *Effigia okeeffeae*; small fossa on posterolateral side of squamosal that is absent in *Effigia okeeffeae*; the parabasisphenoid in *Shuvosaurus inexpectatus* is proportionally longer relative to the width compared to that of *Effigia okeeffeae*; the basipterygoid processes are more anteriorly projected and pointed in *Shuvosaurus inexpectatus*; a ridge on the midline ventral surface of the parabasisphenoid that divides the basipterygoid processes in *Effigia okeeffeae* is absent in *Shuvosaurus inexpectatus*; the coracoid foramen of *Shuvosaurus inexpectatus* is proportionally much larger than that of *Effigia okeeffeae*; *Shuvosaurus inexpectatus* lacks the prominent proximodistally oriented ridge on the anterolateral side of the proximal portion of the femur that is clearly present in *Effigia okeeffeae*; a shallow concavity lies just distal to a ridge posterolateral surface of the proximal portion of metatarsal I which is absent in *Effigia okeeffeae*.

Similarities and differences with *Lotosaurus adentus*: *Lotosaurus adentus* also possesses an edentulous premaxilla and dentary with a clear tomia at the edges of these elements. *Shuvosaurus inexpectatus* and *Effigia okeeffeae* have a deeper fossa dorsal to the medial palatal shelf in the premaxilla and a larger fossa ventral to the dentary shelf in the anterior portion of the dentary. *Lotosaurus adentus* also possesses an anterior process of the nasal fits into slot on the lateral side of the anterior process of the premaxilla. *Lotosaurus adentus* does possess many character states of shuvosaurids (see scorings in Nesbitt, 2011 dataset and iterations) but possesses more plesiomorphic states within Poposauroidea compared to *Shuvosaurus inexpectatus* and *Effigia okeeffeae* including an anteroposteriorly short parabasisphenoid, a quadrate with two condyles that are wide mediolaterally, and a small postfrontal. Further comparisons will be detailed elsewhere.

Ontogenetic age—The holotype skull has been previously reported to be a "juvenile" (see Griffin et al., 2020 for problematic language associated with the term for reptiles) based on visible and open sutures (Chatterjee, 1993; Rauhut, 1997), as an adult based on the absence of external sutures (Lehane, 2005), and lastly as "not juveniles" based on suture "obliteration" (Lehane, 2023) following recent studies on birds (Bailleul et al., 2016; Plateau & Foth, 2021). With our close examination of the cranial bones of *Shuvosaurus inexpectatus*, we found that almost all of the sutures between skull bones were either open (= suture contacts

were visible) (e.g., otooccipital-supraoccipital) and disarticulated along the sutural surfaces (e.g., parietal, dentary), easily discernible (e.g., prefrontal-frontal), or the bones were glued together (e.g., premaxillae). The only suture that is absent between skull elements in the holotype is the exoccipital-opisthotic suture, as also pointed out by Lehane (2023); this suture is absent early in archosaur ontogeny (Griffin et al., 2020). Therefore, we conclude that nearly all sutures are open and the ontogenetic age of the holotype is better constrained as skeletally immature. Regardless, suture closure pattern as an indicator of ontogenetic age in early archosaurs is poorly constrained (Bailleul et al., 2016; Griffin et al., 2020). It should also be noted that the skull of *Effigia okeeffeae* (AMNH FR 30587) also has clearly defined sutures among nearly all skull bones and that the braincase is completely disarticulated. Furthermore in *Effigia okeeffeae*, histology of the femur (AMNH FR 30587 [incorrectly referred to 30589 by Nesbitt, 2007]) indicates that at least four lines of arrested growth (= LAGs) separated by faster growth intervals. This pattern of growth implies that the sutures of *Effigia okeeffeae* remain open well after hatching. Whether skull sutures remains open after the rapid growth stage (see Griffin et al., 2020), well into skeletal maturity, or never fuse in *Shuvosaurus inexpectatus* is not currently known.

Postcranially, all of the vertebrae from the presacral series and the sacrum either have no attached neural arch and an exposed neurocentral suture (e.g., post axial presacral vertebrae of TTU-P9001) or have clearly defined neurocentral sutures (i.e., the elements are in contact and a suture is clearly visible; sensu Brochu, 1996) (e.g., axis of TTU-P9001, sacrum, TTU-P23438) between the centra and neural arches. Some caudal vertebrae (e.g., TTU-P9001, TTU-P23875) have closed neurocentral sutures (i.e., the elements are fused with no suture present at the juncture; sensu Brochu, 1996). Neurocentral suture closure patterns typical for some crocodile-line archosaurs proceed from tail to head (Brochu, 1996; but see some exceptions in Irmis, 2007) suggesting that *Shuvosaurus inexpectatus* may follow the same pattern in its vertebrae. We did not observe any coossifications between the scapula and coracoid or coossifications among any of the pelvic elements, either. The femoral length of the *Shuvosaurus inexpectatus* individuals from the Post Quarry only differ by ~15% so most individuals are about the same size. This indicates that most individuals may be about the same developmental stage using size as a general proxy (see Griffin et al., 2020).

Combining the evidence from the skull and postcrania and comparisons to other reptiles, it appears that all of the *Shuvosaurus inexpectatus* remains from the Post Quarry pertain to skeletally immature individuals. Histological analyses of *Shuvosaurus inexpectatus* was not conducted for this study. We also note that there are no published skeletally mature shuvosaurid individuals and all known individuals we observed possessed skeletally immature states at death, even though some of the individuals of shuvosaurids may reach 4–10 meters in length (Nesbitt, 2011).

3 | DESCRIPTION

Premaxilla—The premaxillae are known from the holotype (TTU-P9280; Figure 7a–c) and the paratype (TTU-P 9282; Figure 7d–g) and both specimens contain both the

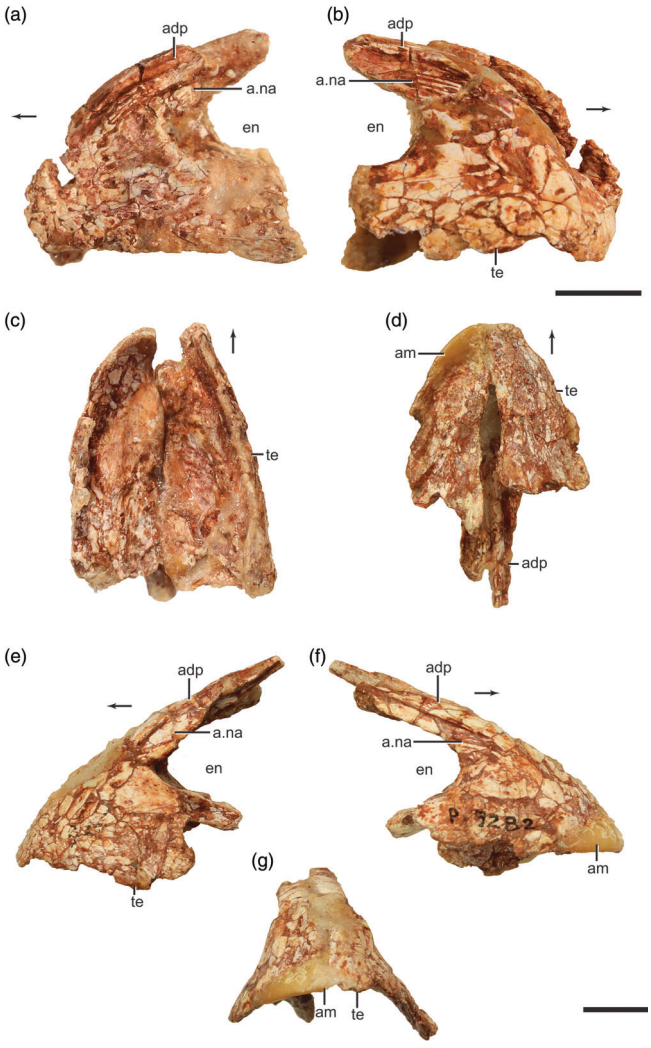

FIGURE 7 Premaxillae of *Shuvosaurus inexpectatus*. Left and right elements of the holotype (TTU-P9280) in left lateral (a), right lateral (b), and ventral (c) views. Referred left and right elements (TTU-P9282) in ventral (d), left lateral (e), right lateral (f), and anterior (g) views. a., articulates with; adp, anterodorsal process; am, added material; en, external naris; na, nasal; te, tomial edge. Arrows indicate anterior direction. Scale bars equal 1 cm.

right and left sides. The premaxillae are held together at the midline with epoxy and paper pulp in both specimens. It is not clear if the premaxillae were conjoined at discovery, taken apart for preparation, and then reconjoined, or if the premaxillae elements were found separated and then put together after preparation. Between the two specimens, nearly the entire anatomy of the premaxillae is known, but some of the surfaces are poorly preserved. Like *Effigia okeeffeae* (AMNH FR 30587) and *Lotosaurus adentus* (IVPP V48013), the premaxillae are edentulous with a sharp ventral ridge (i.e., tomia) and most of the lateral surfaces are covered in small foramina (Figure 7). The foramina are more concentrated in the anterior portion of the premaxillae than the posterior portion. The ventral edge of the lateral margin (= tomia) is nearly straight and in the same horizontal plane in *Shuvosaurus inexpectatus* (Figure 7a), as originally reconstructed for *Effigia okeeffeae* (Nesbitt & Norell, 2006), but in contrast to the more pointed beak of *Effigia okeeffeae* as reconstructed by Bestwick et al. (2021). The uniformly thin ventral margin (= tomia) continues from the anterior to the posterior edges.

The premaxilla bears a long anterodorsal (= nasal) process and a shorter posterodorsal (= maxillary) process like that of *Effigia okeeffeae* (AMNH FR 30587) and *Lotosaurus adentus* (IVPP V4783). The anterodorsal process tapers posterodorsally posteriorly beyond the rest of the element. A slot at the base of the anterodorsal process penetrates the main body of the premaxilla clearly marks the anterior extension of a nasal process (Figure 7a,e,f; a.na), identical to the condition in *Effigia okeeffeae* (Nesbitt, 2007) and in *Lotosaurus adentus* (IVPP V48013). Consequently, the anterodorsal process of the premaxilla does not participate in the external naris. The short posterodorsal process extends posteriorly and contacts the maxilla as in *Effigia okeeffeae* (Nesbitt, 2007). This process, though broken in both specimens, does not appear to be as long or as anterodorsally tapered as originally reconstructed (Figure 3; Chatterjee, 1993; Rauhut, 1997; Lehane, 2023) and is in contrast to the long process of *Lotosaurus adentus* (IVPP V4783). The smooth posterodorsal edge of the main body of the premaxilla indicates that the premaxilla formed the anterior and ventral portion of the external naris. After repreparation, we could not find evidence for a posterior process located at the ventral edge of the premaxilla as illustrated in Rauhut (1997) and Lehane (2023).

In ventral view, the lateral margins of the premaxillae gently arc laterally to medially to form a rounded anterior end. A premaxillary shelf extend medially where the deepest portion is located at the medial edge in ventral view (Figure 7c,d). The premaxillae only meet at the midline anteriorly in TTU-P9282 (Figure 7d) and there is a clear gap at the midline for most of the length of the premaxillary shelf; this gap may fit the vomers, but none of the vomer is preserved. A gap at the midline appears absent in TTU-P9280 (Figure 7e) and it is not clear if this a real absence or the premaxillae were adhered together incorrectly. Posteriorly, the medial premaxillary shelf terminates in a pointed process near the midline (Figure 7d). The medial surface of the process is dorsoventrally expanded relative to the rest of the premaxillary shelf. A gap between the medial process and the posterodorsal process likely fits the anterior (= palatal) process of the maxilla, similar to *Effigia okeeffeae* (Nesbitt, 2007).

Maxilla—The proposed maxilla of *Shuvosaurus inexpectatus* in the reconstruction (Figures 3 and 8a,b) and further described by Lehane (2005, 2023), represents one of the elements that cannot unambiguously assigned to the taxon in its proposed form. The proposed right maxilla is damaged and lacks possible posterior and dorsal (= ascending) processes and other surfaces of the bone are abraded, making homology of its features difficult. The interpreted lateral surface appears to have a lateral fossa (? = antorbital fossa, as previously identified) and the ventral edge is similar to that of the premaxilla. However, the main body is mediolaterally thickened unlike other archosauriforms, *Effigia okeeffeae* (AMNH FR 30587), and *Lotosaurus adentus* (IVPP V4783). Alternatively, this fragment of bone, if a maxilla, may be the anteriormost portion of the maxilla and the lateral fossa may be equivalent to a lateral fossa present in *Effigia okeeffeae* (AMNH FR 30587; Figure 5) anterior to the dorsal process and the antorbital fossa. If this is the case, the maxillae of *Shuvosaurus inexpectatus* and *Effigia okeeffeae* are more similar to each other than previously stated in Nesbitt (2007). Given the poor preservation of this element, we cannot confirm this element as the maxilla as originally interpreted and urge caution when making comparisons to this element.

Jugal—A long fragment of bone was originally assigned as the holotype jugal of *Shuvosaurus inexpectatus* (Chatterjee, 1993) (Figure 8c,d). This long bone is much more gracile (longer, dorsoventrally narrower) than that of *Effigia okeeffeae*, but lacks any dorsal or posterior process. Thus, the bone does not bear any hallmarks of typical archosaur jugals or clear articulation surfaces with other bones and should not be considered the jugal of *Shuvosaurus inexpectatus* unambiguously. Instead, we located a jugal (TTU-P15378; Figure 8e,f) from the Post Quarry that we assign to *Shuvosaurus inexpectatus* based on appropriate size and similarity to the jugal of *Effigia okeeffeae*. This jugal has a short dorsal (= ascending) process, a short and tapered posterior process that presumably would contact the quadratojugal, and a long anterior process that would sit ventral to the orbit. This anterior process has a dorsal horizontal border,

similar to that of the anteriorly elongated jugal of *Effigia okeeffeae* (Figure 5a).

Lehane (2005, 2023, fig. 10) identified the dorsal process of the jugal in articulation with the postorbital. We disagree with this identification because we do not think that there is a suture within this fragment. Instead, we identify this whole piece of bone (Figure 8i,j) as the ventral process of the postorbital (see below).

Quadratojugal—The quadratojugal of *Shuvosaurus inexpectatus* is represented by a nearly complete left element from the holotype (TTU-P9280; Figure 8g,h). Unfortunately, a quadratojugal is not known in *Effigia okeeffeae*, so our identification here cannot be confirmed with independent evidence, but we do agree with the original identification based on a consistent size with other skull bones and the similar general shape it has in comparison with other archosaurs (e.g., *Qianosuchus mixtus*; Li et al., 2006).

The element is broadly triangular in lateral view with a clear notch on the anterior side near the ventral border. The medial surface is concave where it would presumably meet the quadrate. The shape of the quadratojugal has played an important role in the reconstruction and shape of the infratemporal fenestra (= lower temporal fenestra). For example, Chatterjee (1993) stated that the quadratojugal has two anterior progs that divide the infratemporal fenestra into two subsidiary spaces whereas others agreed and pointed out that this feature is unique (Rauhut, 1997). We generally agree with this interpretation but also offer an alternative interpretation, that the anterior notch between the two processes accepted the short posterior process of the jugal (Figure 8e,f). If this is the case, the feature would still be unique to *Shuvosaurus inexpectatus* save for the possibly similar condition in *Effigia okeeffeae*.

Lastly, we note that we disagree with the interpretation of the element put forth by Lehane (2005, 2023) where the quadratojugal in Figure 8g,h is an amalgamation of the quadratojugal and the ventral process of the squamosal (Lehane, 2023, fig. 12). We could not reproduce the proposed sutural contact of the two elements on both the lateral and medial sides and note that the ventral process of the squamosal is much shorter in the nearly complete squamosal (see below) so that the process would not extend as far ventrally. Consequently, it is not clear if or how far the squamosal-quadratojugal articulation projected into the infratemporal fenestra.

Nasal—As originally reconstructed, the holotype nasal (TTU-P9280) of *Shuvosaurus inexpectatus* articulated with the frontal posteriorly, formed part of the antorbital fenestra, and articulated with the premaxilla anteriorly (Figures 3 and 4). However, the proposed nasal that lies dorsal to the maxilla and contacts the premaxilla in the reconstruction could not be located after the skull was disassembled. The only remains of a possible nasal are near the anterior end of the left frontal (Figure 9a–d) but it does not have any clear bone contact with the frontal and the two elements are separated from each other by some kind of added material (i.e., epoxy, plaster). Our CT data further supports the lack of a bony contact between the elements (Figure 9e). The features of the possible nasal fragment are not diagnostic. Therefore, we conclude the nasal of *Shuvosaurus inexpectatus* cannot not be confirmed to be that element.

Frontal—The frontals of *Shuvosaurus inexpectatus* are represented by the holotype (TTU-P9280; Figure 9), partial frontals and partial postorbitals (TTU-P9282; Figure 10a,b), and a partial right frontal and postorbital fragment (TTU-P9281; Figure 10c–e). The most complete frontals (TTU-P9280) consist of the left and right frontals and are attached to the left and right prefrontals, a fragment of the left postorbital (Figure 9) and possibly a piece of the nasal (see above). It is clear that the frontal, postorbital fragment, and much of the prefrontals are from one individual (Figure 9). Unfortunately, plaster, epoxy, and possible other compounds were added to TTU-P9280 originally, so it is not clear if the nasal was added to frontal-prefrontal portions (Figure 9e). Furthermore, the bone surfaces are not preserved well and sutures are difficult to discern.

The frontals form the dorsal portion of the orbit and are separated at the midline across a smooth surface (Figure 9). The midline region is slightly concave relative to the slightly raised lateral margins of frontals (i.e., the orbital margin). The skull roof is reported as flat in *Effigia okeeffeae* (Bestwick et al., 2021), but this condition may be the result of crushing whereas the skull roof of *Shuvosaurus inexpectatus* is three dimensionally preserved. Posteriorly, the frontals are more concave at the midline relative to the raised orbital rim and the posterior portion of the frontal is deflected posteroventrally. The posterolateral margin of the frontals is met by the postorbital in a complex suture that cannot be easily discerned in either *Shuvosaurus inexpectatus* or *Effigia okeeffeae* (Nesbitt, 2007). A clear fossa is present on the dorsal surface of the frontal between the contact with the postorbital and the articulation surface with the parietals (Figures 9d,e and 10). This depression is present in *Effigia okeeffeae* (Nesbitt, 2007), but is not as deep likely because of the skull roof is compressed in the specimen. Posteriorly, the parietals extend into the frontals at the midline; the exact morphology of this contact is not clear because all of the specimens of *Shuvosaurus inexpectatus* are damaged or filled in with plaster (Figures 4a, 9e, and 10). However, a similar anteriorly expanded parietal is

present in *Effigia okeeffeae* (Nesbitt, 2007). Nevertheless, the anterior processes of *Shuvosaurus inexpectatus* extend much more anteriorly into the frontal than that of *Effigia okeeffeae*.

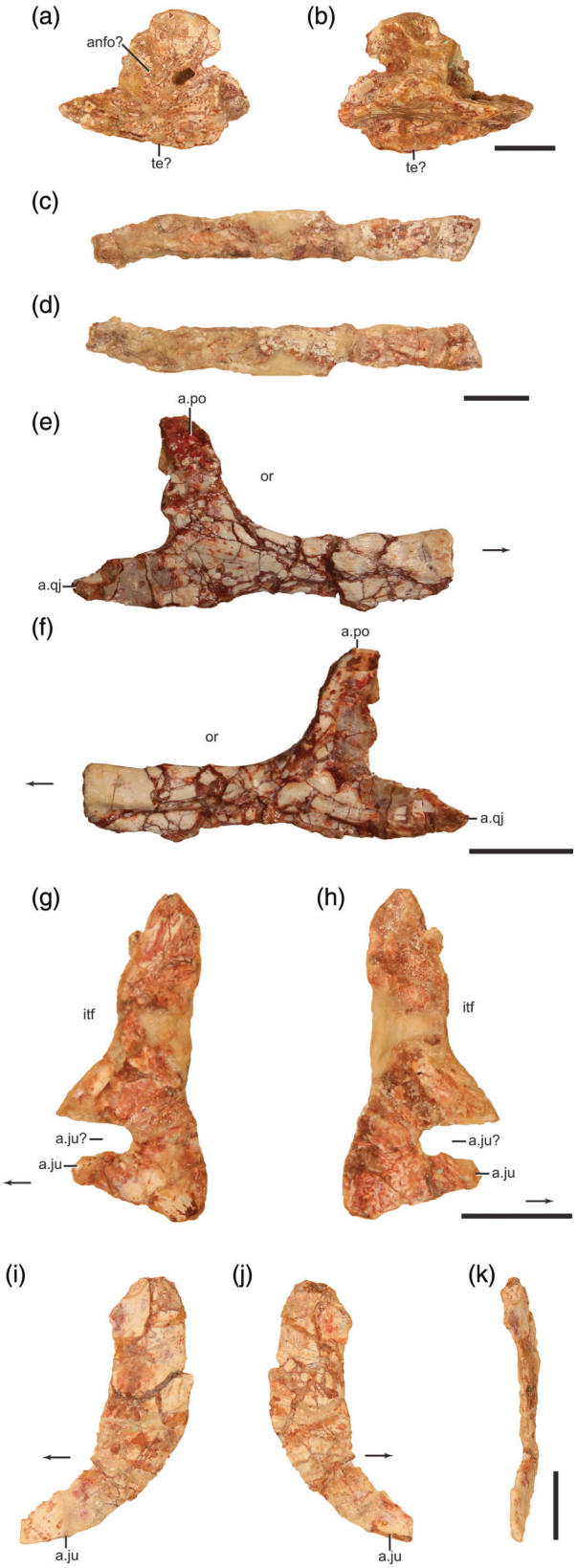

Anteriorly and laterally, the frontals meet the large prefrontals (Figure 9). What is preserved anteriorly suggests that the anterior end of the frontals likely tapered to a point in *Shuvosaurus inexpectatus* like that of *Effigia okeeffeae* (Nesbitt, 2007), but this region is damaged in all known specimens.

Ventrally, the frontals have a well-defined orbital margin marked with a curved rim (Figures 9 and 10). The region medial of the curved rim is nearly flat anteriorly and in the anteroposterior middle of the orbit whereas it becomes concave posteriorly near the contact with the parietals. Within the orbital fossa, the bone tapers laterally to a sharp lateral edge. This lateral edge is much sharper in *Shuvosaurus inexpectatus* than the scalloped and more blunt lateral edge of *Effigia okeeffeae* and *Shuvosaurus inexpectatus* lacks the laterally oriented lines on the ventral surface of the orbital fossa, like those of *Effigia okeeffeae*. Posteriorly, the orbital rim continues onto the ventral surface of the postorbital. Just posterior to this, there is a clear fossa that may be an articulation facet for the laterosphenoid (Figure 10b).

Prefrontal—The large prefrontal of the holotype (TTU-P9280) attaches to the lateral edge of the frontal just anterior of the anteroposterior middle of the orbit (Figure 9). The prefrontal gradually arcs anteroventrally in a smooth transition that mirrors the posterior half of the orbital margin (in lateral view). The sharp posterior lateral margin of the prefrontal gives way to a much rounder lateral margin anteriorly, similar to that of *Effigia okeeffeae* (AMNH FR 30587). It is not clear if the ventral portion of the prefrontal of TTU-P9280 original pertains to the prefrontal (Figure 9) or to the lacrimal (i.e., the interpretation of Chatterjee, 1993; Lehane, 2023; Rauhut, 1997) given the long length. However, the ventral processes of the prefrontals of *Effigia okeeffeae* (AMNH FR 30587) are proportionally similar in length and the shape of the lacrimal in that taxon is mediolaterally expanded rather than the proposed sheet-like mediolaterally thin lacrimal of *Shuvosaurus inexpectatus* (see below). Medially, the prefrontals have a concave surface.

FIGURE 8 Skull bones of the holotype of *Shuvosaurus inexpectatus* (TTU-P9280). Putative left maxilla (TTU-P9280) in lateral (a) and medial (b) views. Putative left jugal in lateral (a) and medial (b) views and a referred right jugal (TTU-P15378) in lateral (c) and medial (d) views. Left quadratojugal of the holotype of *Shuvosaurus inexpectatus* (TTU-P9280) in lateral (e) and medial (f) views. Partial left postorbital of *Shuvosaurus inexpectatus* (TTU-P9280) in lateral (e), medial (f), and anterior (g) views. a., articulate with; anfo, antorbital fossa; itf, infratemporal fenestra; ju, jugal; or, orbit; po, postorbital; qj, quadratojugal; te, tomial edge. Arrows indicate anterior direction. Scale bars equal 1 cm.

Postorbital—The fragment of the postorbital of TTU-P9280 (Figure 9) and TTU-P9282 (Figure 10) indicates that no postfrontal was present in *Shuvosaurus inexpectatus* as observed by previous authors (Lehane, 2023; Rauhut, 1997). In comparison, a postfrontal is absent in *Effigia okeeffeae* (Nesbitt, 2007) and a sliver of a postfrontal is present between the frontal and postfrontal in the close relative *Lotosaurus adentus* (IVPP V48013). The postorbital has a medial process that forms the supratemporal fenestra (= upper temporal fenestra) and thus, excludes the frontal from participating in the opening. The medial process has a dorsally rounded edge, like that of *Effigia okeeffeae* (Nesbitt, 2007). In dorsal view, the postorbital of *Shuvosaurus inexpectatus* is mediolaterally narrow like that of *Effigia okeeffeae* (Nesbitt, 2007). The main body of the postorbital is small relative to the frontals and is divided into ventral and posterior processes near its contact with the frontal. Unfortunately, the posterior process is missing in all specimens.

A tapered piece of bone from the holotype (TTU-P9280) was originally included in the reconstructed holotype as the ventral process of the postorbital (Figure 3) and then disarticulated during further preparation (Lehane, 2005). Overall, the bone is consistent with and proportional in size and shape with that of the ventral process of the postorbital of *Effigia okeeffeae* (left side of AMNH FR 30587), but there are no other features to confirm this identification; we tentatively accept the identification of this element as much of the ventral process of the postorbital. The mediolaterally thin and anteroposteriorly wide fragment is curved. The anterior and posterior edges appear to be complete, but the ventral tip is missing. Recently, this entire fragment was interpreted as the descending process of the postorbital and the dorsal (= ascending, = postorbital) process of the jugal (Lehane, 2023). We disagree with this identification because; (1) what is identified as a suture between the two elements does not carry through the entire bone; (2) the shape of the resulting dorsal process of the jugal would taper ventrally and anterior, which is not consistent with other archosaurs that we have observed (e.g., Nesbitt, 2011); and (3) the shape and length of the entire piece of bone is consistent with the ventral process of the closest relative of *Shuvosaurus inexpectatus*, *Effigia okeeffeae*. Consequently, *Shuvosaurus inexpectatus* and *Effigia okeeffeae* share a postorbital bar that is largely composed of the ventral process of the postorbital.

Squamosal—The left squamosal in the original reconstruction of the holotype (Figures 3 and 4) is missing, but the element is well represented in the paratypes from the left side (TTU-P9282, Figure 11a,b: TTU-P9282, Figure 11c–e) and are nearly complete. The squamosal has four projections visible in lateral view and one medial

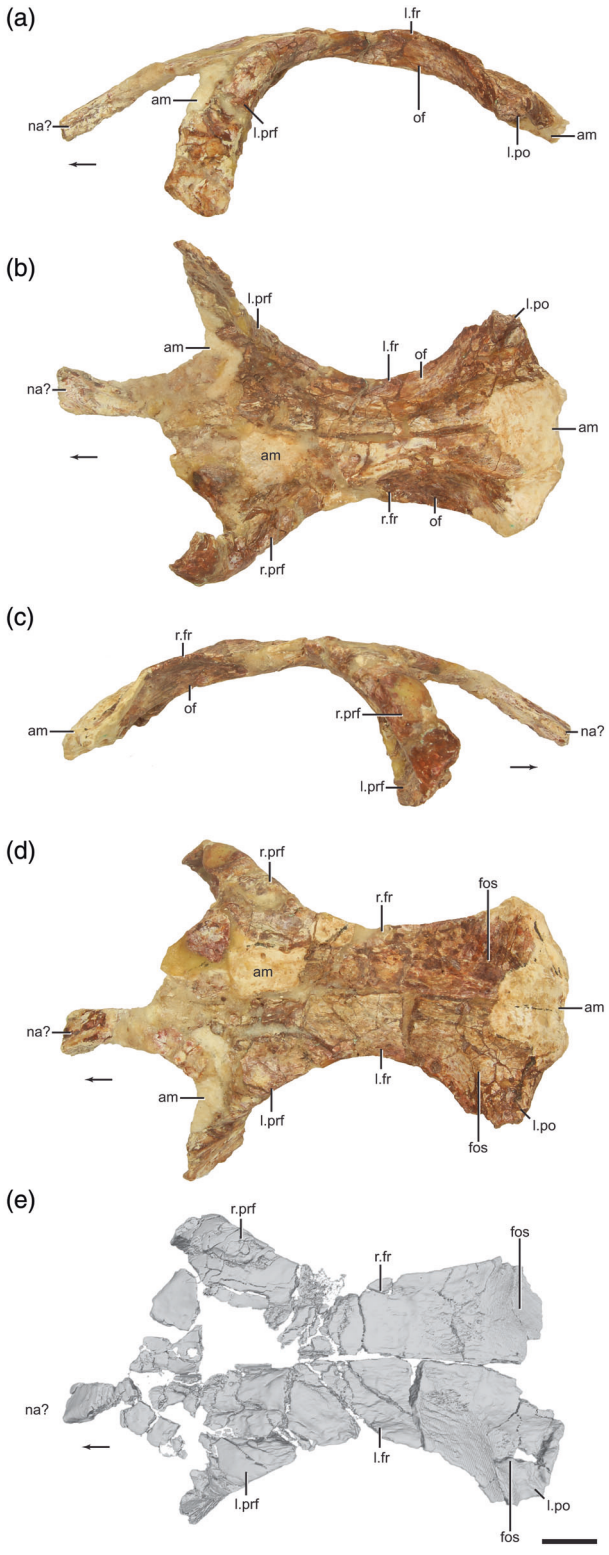

FIGURE 9 Skull roof of the holotype of *Shuvosaurus inexpectatus* (TTU-P9280) in left lateral (a), ventral (b), right lateral (c), and dorsal (d) views. Dorsal view (e) of a surface rendering of the same skull roof (TTU-P9280) derived from CT data where the lower density added material (e.g., epoxy, plaster) was removed. am, added material; fos, fossa; fr, frontal; l., left; na, nasal; of, orbital fossa; po, postorbital; prf, prefrontal; r., right. Arrows indicate anterior direction. Scale bar equals 1 cm.

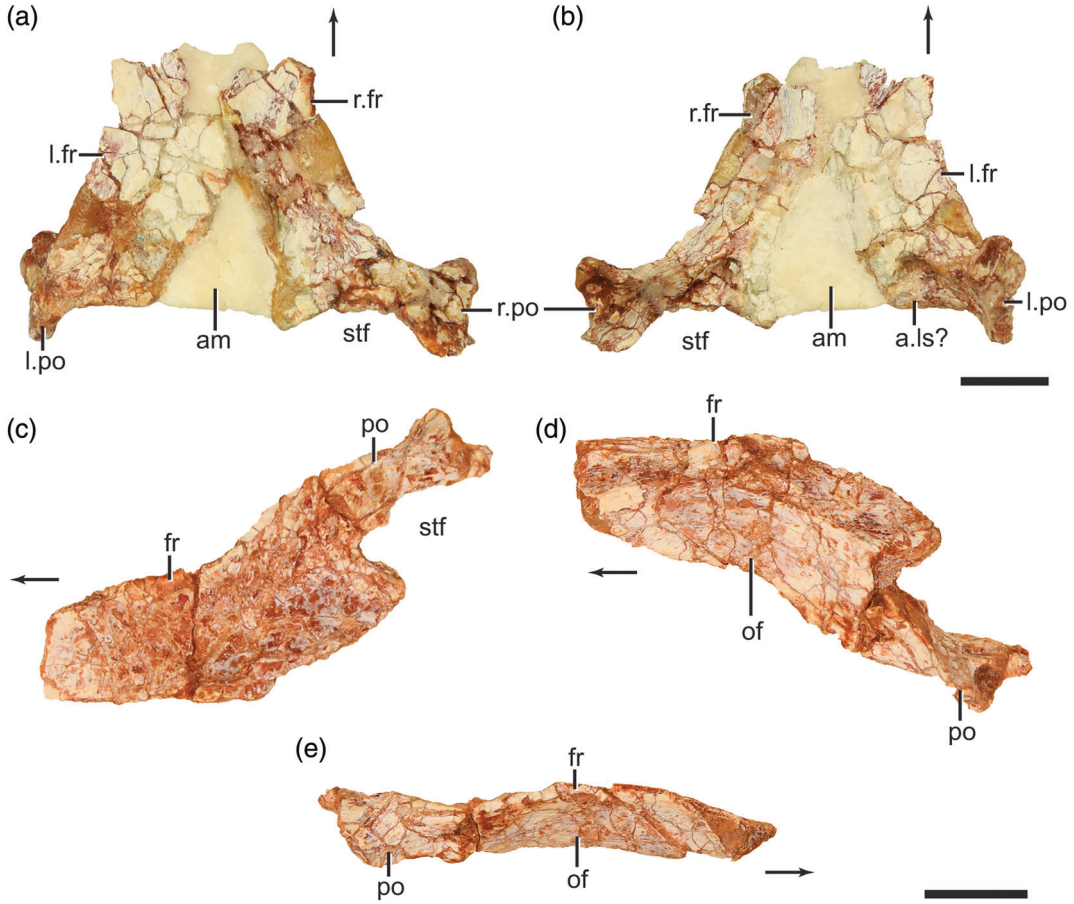

FIGURE 10 Frontals of referred specimens of *Shuvosaurus inexpectatus*. Conjoined partial frontals and partial postorbitals (TTU-P9282) in dorsal (a) and ventral (b) views. Right frontal (TTU-P9281) in dorsal (c), ventral (d), and lateral (e) views. a., articulates with; am, added material; fr, frontal; l., left; ls, laterosphenoid; na, nasal; of, orbital fossa; po, postorbital; prf, prefrontal; r., right; stf, supratemporal fenestra. Arrows indicate anterior direction. Scale bars equal 1 cm.

process. The anterior process articulates with the postorbital. The anterior end of this process is broken, thus the exact articulation arrangement of the squamosal-postorbital is not clear. The process is mediolaterally compressed and with nearly parallel dorsal and ventral sides. Overall, the length and height of the process is more gracile than its comparative process in *Effigia okeeffeae* (Figure 5). The ventral process tapers like that of *Effigia okeeffeae* (AMNH FR 30587) and presumably meets the quadratojugal on the posteroventral surface. As mentioned above, the ventral process in our view is much shorter than that interpreted by Lehane (2023) given that the process is nearly complete in TTU-P9281 (Figure 11c–e). Posteriorly, a prominent pointed process tapers in both specimens, but is slightly laterally expanded and rugose in the larger example (TTU-P9282). This posterior process in *Shuvosaurus inexpectatus* is absent in *Effigia okeeffeae* (Nesbitt, 2007). The posteromedial process curves anteromedially to contact the parietal. This posteromedial process thins ventrally and is broken in both examples. A prominent depression on the posterodorsal portion of this process in *Effigia okeeffeae* is absent in *Shuvosaurus inexpectatus*.

Medially, a posterodorsally opening fossa marks the contact surface with the paroccipital process of the braincase. This fossa extends on both the posterior side of the posteromedial process and the medial surface of the prominent posterior process. The glenoid for articulation with the dorsal head of the quadrate is ventral of the posterodorsal process, just anterior of the posterior process, and at the dorsal base of the ventral process (Figure 11). The rounded pit that forms the glenoid opens ventrally, and continues ventrally as a groove on the posteroventral portion of the ventral process. A weakly developed medial process at the medial margin of the glenoid marks the medial extent of the squamosal.

Lacrimal—In the original reconstruction of the holotype of *Shuvosaurus inexpectatus* (Figures 3 and 4), a lacrimal forms much of the anterior border of the orbit and forms a hood dorsal and posterior to the antorbital fenestra, similar to other archosaurs. This reconstruction was

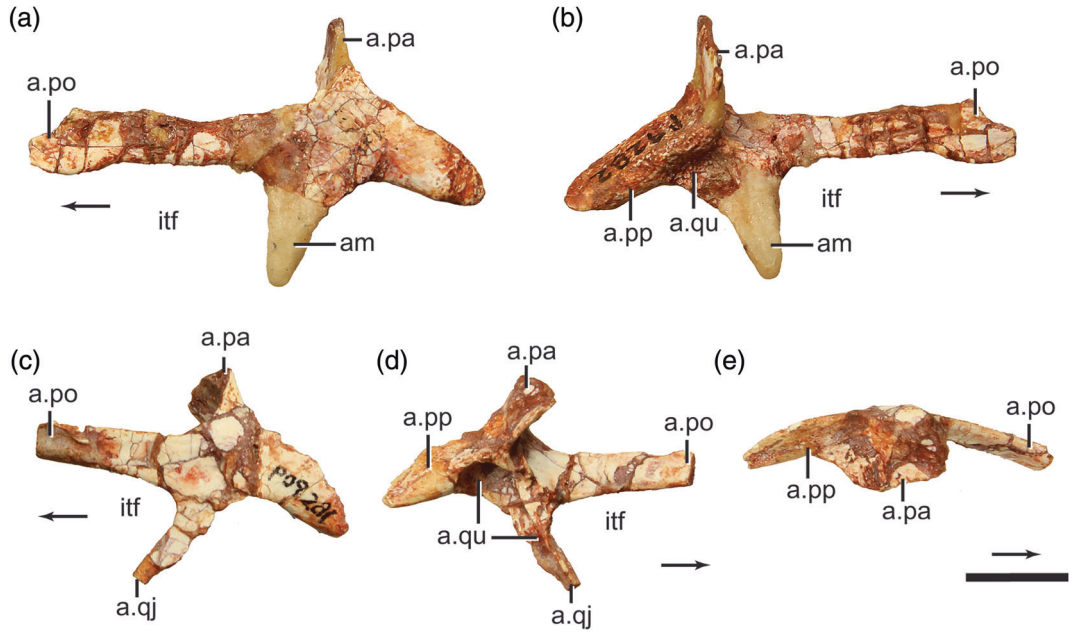

FIGURE 11 Squamosals referred to *Shuvosaurus inexpectatus*. Left element (TTU-P9282) in lateral (a) and medial (b) views. Left element (TTU-P9281) in lateral (c), medial (d), and dorsal (e) views. a., articulates with; am, added material; itf, infratemporal fenestra; pa, parietal; po, postorbital; pp, paraoccipital process of the otooccipital; qj, quadratojugal; qu, quadrate. Arrows indicate anterior direction. Scale bar equals 1 cm.

followed by Rauhut (1997) and Lehane (2023). The dorsal portion of the purported lacrimal (Figures 3 and 4) could not be located after repreparation of the holotype. The main body of the lacrimal was reconstructed extending to the ventral margin of the orbit to the jugal (Lehane, 2023) based on the holotype (TTU-P9280). As briefly stated above, we do not agree with that interpretation and could not reliably identify the lacrimal in the holotype (Figure 9). More specifically, we could not clearly find a sutural contact between the prefrontal and the purported lacrimals on both sides of the skull. Furthermore, we note the mediolaterally thin purported lacrimal and how different that it is in shape compared to the close relative *Effigia okeeffeae* (Figures 5 and 6). Alternatively, we think this projection is all a ventrally elongated prefrontal. Therefore, we suggest that the lacrimal of *Shuvosaurus inexpectatus* is currently unknown.

Quadrate—The quadrate of *Shuvosaurus inexpectatus* is represented by a left element in the holotype (TTU 9280; Figure 12a–d) and a complete right element from the paratype (TTU-P9282; Figure 12e–h; this bone was incorrectly identified as a left element and cited an incorrect specimen number in Nesbitt, 2007, fig. 17). The quadrate possesses a well-rounded dorsal head that articulated with the squamosal, an anteriorly arched main body, and a ventral end with two articular facets that contacted the articular. The rounded dorsal head of the quadrate slightly slants medially in posterior view (Figure 12c,g) and is longer anteroposteriorly than mediolaterally in dorsal view. In articulation with the squamosal, part of the posterior portion of the head must have been visible in lateral view, as indicated by the size of the glenoid of the squamosal. Anteriorly, the dorsal head bears two rami separated by a groove; the more lateral ramus becomes the squamosal ramus and the more medial ramus becomes the pterygoid ramus. The more expanded pterygoid ramus is not complete in any specimen but is mediolaterally thin throughout most of its length. The anterior termination is the anterior extent of the quadrate and the ventral portion of this process is slightly expanded mediolaterally. The lateral surface of the ventral third of the pterygoid ramus bears a slight fossa that opens laterally. The anterolaterally deflected squamosal ramus is shorter anteriorly than the quadrate ramus. The squamosal ramus terminates about dorsoventral midlength of the quadrate body. Medially, the surface of the quadrate is flat (Figure 12).

The lateral surface of the main body of the quadrate has a slight laterally opening fossa just ventral to the termination of the squamosal ramus. A shallow groove originating on the posterior portion of the ventral condyles expands anterodorsal, just ventral to the laterally opening fossa. This groove may indicate that a subtle and likely small quadrate foramen was present, but this could only

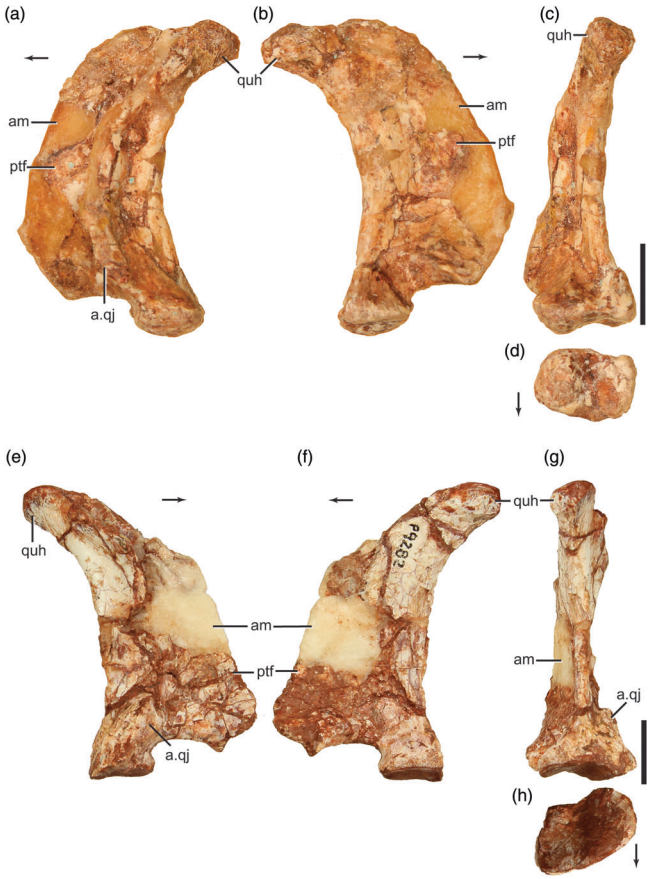

FIGURE 12 Quadrates referred to *Shuvosaurus inexpectatus*. Left element (TTU-P9280) in lateral (a), medial (b), posterior (c), and ventral (d) views. Right element (TTU-P9282) in lateral (e), medial (f), posterior (g), and ventral (h) views. a., articulates with; am, added material; ptf, pterygoid flange; qj, quadratojugal; quh, quadrate head. Arrows indicate anterior direction. Scale bars equal 1 cm.

be confirmed with an articulated quadratojugal; it is not clear if *Effigia okeeffeae* may have a small quadrate foramen based on this new observation. The ventral portion of the lateral side expands laterally and medially and the lateral edge of quadrate bears a clear facet for articulation with the quadratojugal; the facet is deeper posteriorly and extends to the ventralmost margin of the more lateral condyle.

The posterior edge of the quadrate arches anteriorly between the dorsal head and the ventral condyles. In posterior view, the main shaft is mediolaterally compressed only expanded at the dorsal and ventral ends. In articulation with the squamosal the entire body angles posterodorsally so that the ventral condyles are far anterior of the head, as stated by Chatterjee (1993).

In ventral view, the ventral surface is rectangular, like that of *Effigia okeeffeae* (Lehane, 2005, 2023; Nesbitt, 2007, fig. 17A). The ventral surface is divided into two portions, a lateral portion that is convex anteroposteriorly and a more medial portion that is concave anteroposteriorly (Figure 12d,h). The lateral condyle of the holotype (TTU-P9280; Figure 12d) is rounded in lateral view, but this rounding appears to be damaged; the referred specimen (TTU-P9282; Figure 12h) has a complete lateral margin and this matches that of *Effigia okeeffeae* (AMNH FR 30587). The medial surface corresponds precisely to the convex glenoid of the articular (see below). The largely concave ventral surface of the quadrate is similar to the configuration of *Effigia okeeffeae* and possibly similar to that of *Lotosaurus adentus* (IVPP V4791.3). This concave and convex shape in shuvosaurids is in contrast to that of other pseudosuchians in which the ventral condyles are uniformly convex, as stated in Lehane (2023).

We could not reidentify the two pneumatic openings in the quadrate mentioned by Chatterjee (1993).

Palate—The palate of *Shuvosaurus inexpectatus* was reconstructed based on the holotype (Figure 4) and was critical to interpreting the relationships of the taxon initially (Chatterjee, 1993). The identifications of the bones were followed by subsequent authors (Lehane, 2023; Rauhut, 1997). Here, we completely reinterpret the palatal bone identifications and shapes based on the skull of *Effigia okeeffeae* (Figures 5 and 6). All of the palatal bones of *Shuvosaurus inexpectatus* are from the holotype (TTU-P9280).

The bone originally identified as the palatine (Chatterjee, 1993; Lehane, 2023) of *Shuvosaurus inexpectatus* is reidentified as a right ectopterygoid (Figure 13a–c) based on the similarity of it to that of the ectopterygoids of *Effigia okeeffeae* (Nesbitt, 2007). The ectopterygoid possesses a lateral head that articulates with the jugal and a partial medial process that would articulate with the pterygoid. The slightly concave surface that would articulate with the jugal is much more anterodorsally longer than dorsoventrally high, like that in *Effigia okeeffeae* (Nesbitt, 2007). The dorsoventrally thin main body of the ectopterygoid arcs posteromedial, like that of *Effigia okeeffeae* (Nesbitt, 2007).

The bone originally identified as the ectopterygoid (Chatterjee, 1993; Lehane, 2023) of *Shuvosaurus inexpectatus* is reidentified as a partial right pterygoid (Figure 13d,e) based on the similarity of it to that of the large pterygoids of *Effigia okeeffeae* (Bestwick et al., 2021; Nesbitt, 2007). The surface previously interpreted as a ventral pocket (Chatterjee, 1993; Lehane, 2023; Rauhut, 1997) and allied with the feature in theropods (Chatterjee, 1993; Rauhut, 1997), is the ventrolateral surface of the quadrate wing of the pterygoid; the depth of the pocket was increased with a slight rim of epoxy on part of the bone. The previously identified head of the ectopterygoid (see Lehane, 2023, figs. 4 and 15) is reinterpreted as the robust lateral flange of the pterygoid and is nearly identical to that of *Effigia okeeffeae* (Nesbitt, 2007).

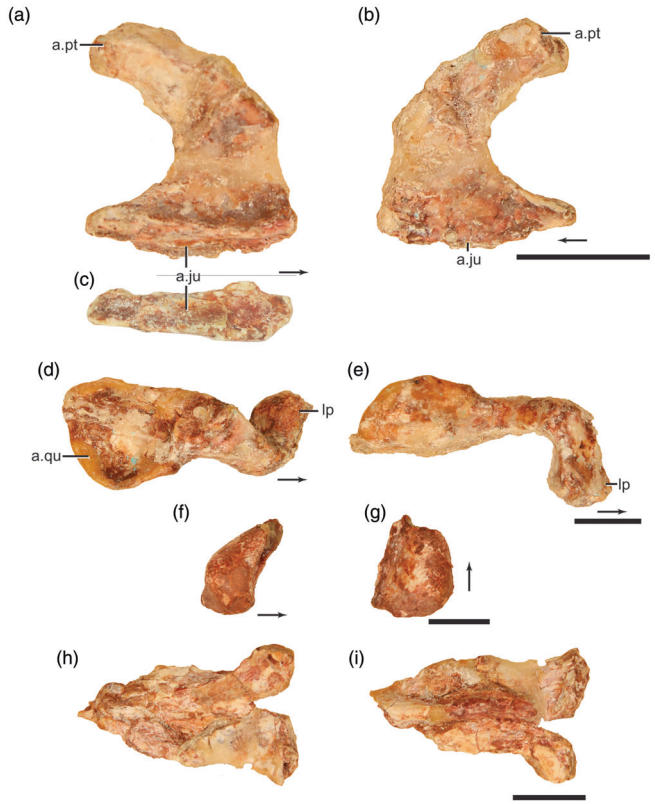

FIGURE 13 Palatal bones of *Shuvosaurus inexpectatus*. Right ectopterygoid of the holotype (TTU-P9280) in dorsal (a), ventral (b), and lateral (c) views. Right partial pterygoid (TTU-P9280) in ventral (d) and dorsal (e) views. Lateral process of a ?right pterygoid (TTU-P9280) in lateral (f) and ventral (g) views. Possible palatine (TTU-P9280) in two views (h and i). a., articulates with; ju, jugal; lp, lateral process; pt, pterygoid; qu, quadrate. Arrows indicate anterior direction. Scale bars equal 1 cm.

Small dimples on the lateral side of the lateral process on the right pterygoid (Figure 13d) further support this reidentification given the prominent feature in *Effigia okeeffeae* (Figures 5 and 6); the lateral side of the left pterygoid was identified among the holotype material based on these small dimples covering a rounded surface (Figure 13f,g). Our reidentification conclusively shows that the large pterygoid of *Shuvosaurus inexpectatus* is present and nearly identical to that of *Effigia okeeffeae*.

We cautiously reinterpret the fragmentary bone originally identified as a pterygoid (Chatterjee, 1993; Lehane, 2023) of *Shuvosaurus inexpectatus* as a possible palatine. This interpretation is based on the large lateral articulation with the maxilla in *Effigia okeeffeae* with that of the articular head of *Shuvosaurus inexpectatus* (Figure 13H,I) and the overall proportional size with that of other elements and the bone in *Effigia okeeffeae*. However, this identification is tentative and should not be relied on when making comparisons to *Shuvosaurus inexpectatus*.

No vomer, as mentioned in the original description by Chatterjee (1993), was reidentified among the holotype material by us.

Braincase—The holotype braincase (TTU-P9280) consists of the complete supraoccipital, right and left prootics, and left paraoccipital (missing the lateralmost end) that clearly represent the same individual (Figure 14). The referred braincase (TTU-P9282; Figure 15) consists of a complete parabasisphenoid, basioccipital, left otooccipital and the prootic, and a supraoccipital. Repreparation and CT information indicate that the more complete braincase TTU-P9282 was partially rearticulated with epoxy and other compounds; it is clear that the left otooccipital, the prootic, and a supraoccipital were articulated and the parabasisphenoid and basioccipital were isolated and added to the braincase. Regardless, all of the braincase elements in TTU-P9282 either identical to the holotype braincase (otooccipital and the prootic, and the supraoccipital) or are strikingly similar to that of *Effigia okeeffeae* (Nesbitt, 2007), with the exception of a fragment interpreted as the laterosphenoid (Chatterjee, 1993, fig. 5). Among shuvosaurids, *Shuvosaurus inexpectatus* is the only member of the clade to preserve the supraoccipital and otooccipital, all other bones are represented in *Effigia okeeffeae*.

The supraoccipital of *Shuvosaurus inexpectatus* bears a pronounced ridge at the midline that expands dorsally where it terminates (Figures 14 and 15). In dorsal view, the supraoccipital is compressed across the midline and expands anteriorly as two paramedian ridges that surround a midline depression. These ridges continue anteriorly onto the prootic. In comparison, the braincase of other poposauroids like *Arizonasaurus babbitti* (Gower & Nesbitt, 2006) and *Xilousuchus sapingensis* (Nesbitt et al., 2011) possess a much broader supraoccipital ridge. Laterally, the supraoccipital extends posteriorly to contact the otooccipital and both TTU-P9280 and TTU-P9282 have a clear suture defining this contact. The supraoccipital clearly forms the dorsal part of the foramen magnum unlike that of other poposauroids (Gower & Nesbitt, 2006; Nesbitt et al., 2011). Anterolaterally, the supraoccipital forms a concave surface that continues onto the otooccipital and the prootic. The anteromedial portion of the otooccipital forms half of the dorsally opening auricular recess.

The otooccipital consists of a fused opisthotic and exoccipital and no suture is visible between the two in both TTU-P9280 (Figure 14) and TTU-P 9282 (Figure 15). The exoccipital region consists of posteriorly expanded, but not laterally expanded "foot" that sat on the dorsolateral surface of the basioccipital. The position of the exoccipital foot indicates that the other exoccipital foot would

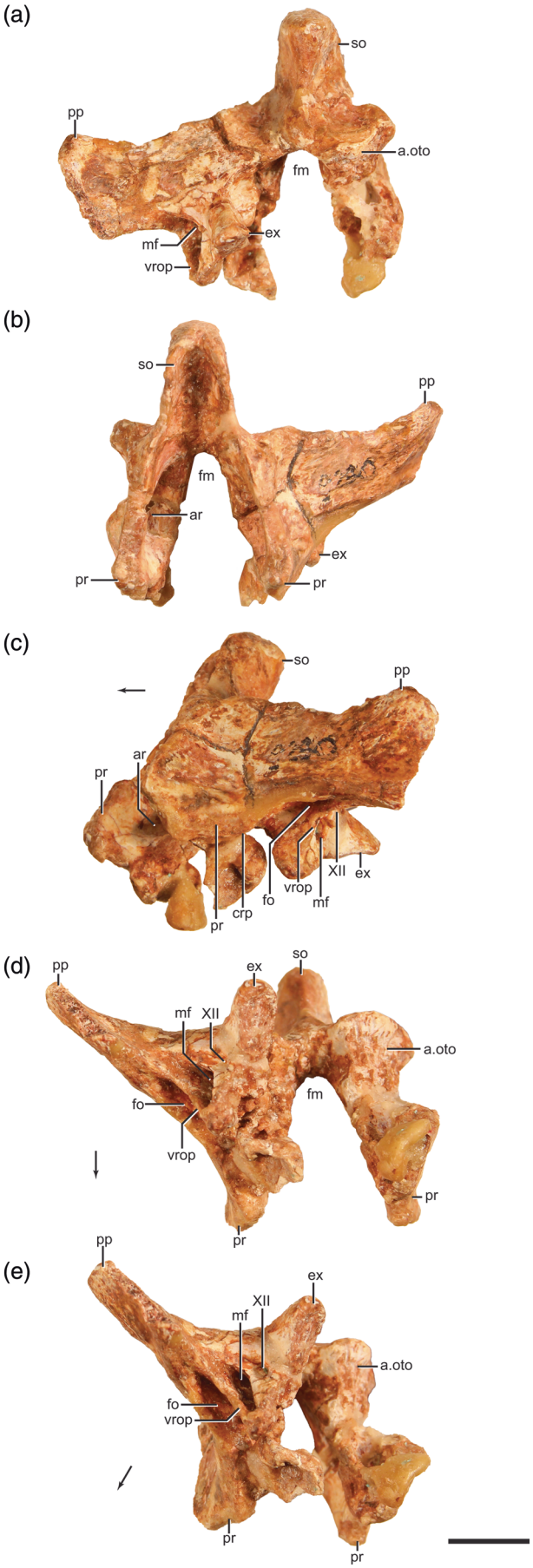

have been clearly separated for the length of the elements when in articulation with the basioccipital, as with *Effigia okeeffeae* (Nesbitt, 2007; Nesbitt & Norell, 2006). The lateral surface of the exoccipital "foot" only bears a single exit for cranial nerve XII in the holotype (Chatterjee, 1993; Lehane, 2023), but part of the lateral surface is broken through the element and the area is damaged in TTU-P9282. Therefore, we could not confirm if a second exit was present or absent. A anteroposteriorly thin ridge separates the exit for cranial nerve XII anteriorly from the metotic foramen and this ridge continues laterally to form the anterolateral portion of the exoccipital foot. Medially, the surface of the exoccipital foot bears a small foramen at its dorsal border, just posterior of the metotic foramen (Figure 14d). A laterally expanded ventral ramus of the opisthotic separates the metotic foramen from the otic region and this lamina is clearly visible in posterior view (Figure 14a).

The paroccipital process of the otooccipital expands posterolaterally in dorsal view and ventrolaterally in posterior view, a character state shared between *Shuvosaurus inexpectatus* with theropod dinosaurs (Nesbitt, 2007; Rauhut, 1997). Laterally, the paroccipital process slightly expands dorsally and ventrally compared to the more medial part. The anterior surface of the lateral part of the paroccipital process is concave in TTU-P9282 and the tapered lateral process of the prootic fails to reach the lateral portion of the anterior surface of the paroccipital process. A small, dorsally opening foramen is present just lateral of the exoccipital foot. The dorsal region of the otic region is concave the cranial exit for nerve VII in the holotype is not visible, but a clear foramen is present in the referred specimen TTU-P9282 in the same position as that of *Effigia okeeffeae* (AMNH FR 30587). In TTU-P9282 and in *Effigia okeeffeae* (AMNH FR 30587), a thin lamina of bone (= crista prootica of Chatterjee, 1993; Nesbitt, 2007) separates the lateral surface of the prootic with the region that possesses the exit of cranial nerve VII.

The anterior portion of the prootic is damaged and this area is difficult to interpret in the holotype (TTU-P9280) but is better preserved in the referred

FIGURE 14 Partial braincase of the holotype of *Shuvosaurus inexpectatus* (TTU-P9280) in posterior (a), anterior (b), left lateral (c), ventral (d), and ventrolateral (e). a., articulates with; ar, auricular recess; crp, crista prootica; ex, exoccipital part of the otooccipital; fm, foramen magnum; fo, fenestra ovalis; mf, metotic foramen; oto, otooccipital; pp, paraoccipital process of the otooccipital; pr, prootic; so, supraoccipital; vrop, ventral ramis of the otooccipital; XII, exit for cranial nerve XII (hypoglossal). Arrows indicate anterior direction. Scale bar equals 1 cm.

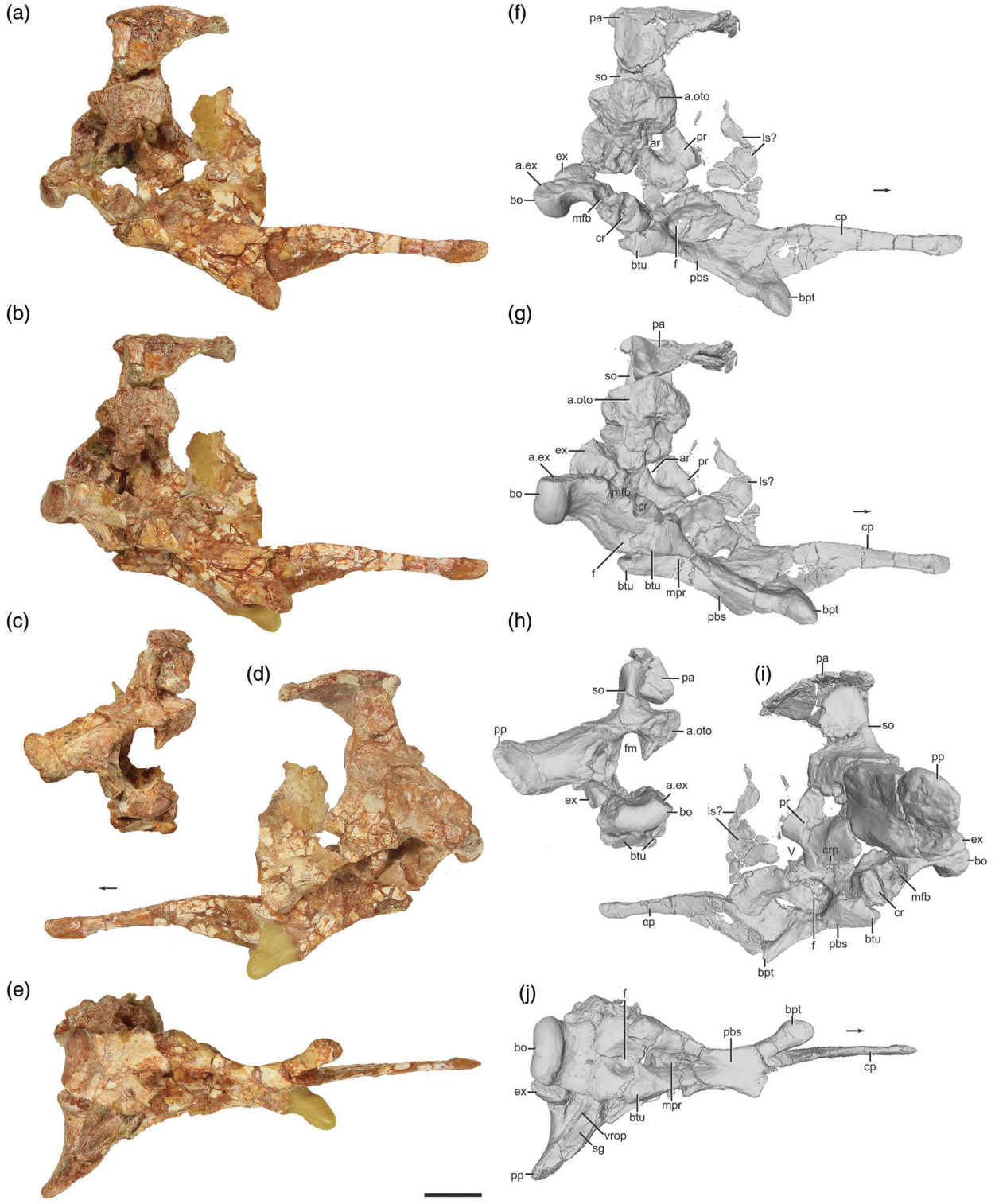

FIGURE 15 Partial braincase (TTU-P9282) referred to *Shuvosaurus inexpectatus* and an artificially adhered right parietal of the holotype (TTU-P9280) of *Shuvosaurus inexpectatus* as photographs in right lateral (a), ventrolateral (b), posterior (c), left lateral (d), and ventral (e) views and as CT surface renderings in right lateral (f), ventrolateral (g), posterior (h), left lateral (i), and ventral (j) views. Note that the anatomical views in a–e are not exactly the anatomical views in f–j. a., articulates with; ar, auricular recess; bo, basioccipital; btu, basitubera; bpt, basipterygoid process; cp, cultriform process; cr, cochlear/lagenar recess; crp, crista prootica; ex, exoccipital part of the otooccipital; f, fossa; fm, foramen magnum; fo, fenestra ovalis; ls, laterosphenoid; mf, metotic foramen; mfb, mf, metotic foramen base; mpr, median pharyngeal recess; oto, otooccipital; pa, parietal; pbs, parabasisphenoid; pp, paraoccipital process of the otooccipital; pr, prootic; so, supraoccipital; sg, stapedial groove; V, exit for cranial nerve V (trigeminal); vrop, ventral ramis of the otooccipital. Arrows indicate anterior direction. Scale bar equals 1 cm.

specimen (TTU-P9282). The articulation with the laterosphenoid slightly extends medially and laterally in the anterior direction. The prootic forms the anterior and ventral parts of the auricular recess. The exit for cranial nerve V is partially formed by the anterodorsal portion of the prootic just ventral of the anteriormost articulation surface with the laterosphenoid. A small ridge on the lateral surface of the prootic converges with the process for the ventral border of the exit of cranial nerve V. It is not clear if *Shuvosaurus* had a ossified medial wall of the inner ear region because this delicate area is damaged in the holotype and referred specimen. Because of poor preservation, we did not observe the exits of cranial nerves VI and VIII through the prootic, like in other archosaurs (e.g., *Arizonasaurus babbitti*; Gower & Nesbitt, 2006).

The parabasisphenoid is complete and well-preserved in the paratype specimen (TTU-P9282). Like that of *Effigia okeeffeae* (AMNH FR 30587), the main body of the element is oriented horizontally where the basitubera are in a near horizontal plane with that of the basipterygoid processes; this orientation contrasts with nearly all other early archosaurs (Gower, 2002) including members of Poposauroidea (Gower & Nesbitt, 2006; Nesbitt et al., 2011). The proportions of the main body of the parabasisphenoid of *Shuvosaurus inexpectatus* are generally similar to that of *Effigia okeeffeae* in that it is twice as long (measuring from the posteriormost portion to the anterior end of the basipterygoid process) than wide (at its widest point at the posterior end). Comparatively, the parabasisphenoid in *Shuvosaurus inexpectatus* is proportionally longer than that of *Effigia okeeffeae* (AMNH FR 30587). This anteroposterior elongation of the main body of the parabasisphenoid in shuvosaurids is unique among pseudosuchians. In ventral view, the main body of the parabasisphenoid is nearly X-shaped with a highly waisted anteroposterior middle (Figure 15e,j). A deep fossa lies at the midline just anterior of the anteroposterior middle, and a similarly deep fossa (= median pharyngeal recess of Witmer, 1997) is present in *Effigia okeeffeae*; this depression is not divided in both taxa. The midline depression in *Shuvosaurus inexpectatus* is longer, but less defined than that of *Effigia okeeffeae*. The basitubera processes expand posteroventrally, flanking the deep fossa. The posterodorsal portion of the basitubera processes are cup-shaped and contact the basitubera components of the basioccipital. Anteriorly, the main body of the parabasisphenoid expands into clear basipterygoid processes (the left process is broken and reconstructed with epoxy putty; Figure 15e,j). The right basipterygoid is anterolaterally pointed in lateral view and bears a clear articulation surface on its anterolateral surface. In comparison with *Effigia okeeffeae*, the basipterygoid processes are more anteriorly projected and pointed in *Shuvosaurus inexpectatus*. A ridge on the midline ventral surface of the parabasisphenoid that divides the basipterygoid processes in *Effigia okeeffeae* (Nesbitt, 2007, figs. 19 and 20) is absent in *Shuvosaurus inexpectatus*.

Laterally, the main body of the parabasisphenoid has deep depressions that are only separated by a thin lamina of bone at the midline. After repreparation and CT analysis, we revise the interpretation of Nesbitt (2007), and conclude that the deep lateral depressions are nearly identical on the right and left sides and biological features of the parabasisphenoid. Furthermore, we find that the lateral depressions have both posterior and anterior subdepression components similar to the original interpretation by Chatterjee (1993, fig. 5). The surface preservation within the posterior depressions is poor, but it appears that there is a foramen in the center of the deepest part of the lateral fossa. It is not clear if the entrance for the internal carotid arteries pass through here as interpreted by Nesbitt (2007) for *Effigia okeeffeae*, but is likely. We could not trace this foramen to the inferred exit through the hypophyseal fossa as originally described by Chatterjee (1993) because of breakage. More anteriorly, the anteroposterior middle of the main body of the parabasisphenoid is concave in dorsal view and the fossae are only divided by a thin lamina of bone. It is not clear if these depression were pneumatic like that theropod dinosaurs (Rauhut, 2003).

Like that of *Effigia okeeffeae*, the basipterygoid process of *Shuvosaurus inexpectatus* originates on the lateral surface of the parabasisphenoid and there are deep pockets medial to the basipterygoid process "stalk" (Figure 15). These deep pockets that open anteriorly are only present in *Shuvosaurus inexpectatus* and *Effigia okeeffeae*. The cultriform process originates between the deep pockets and extends anteriorly with a dorsal groove present at the midline. The ventral half of the process is extremely thin and the dorsal surface bears a clear groove. Prior to anterior termination, the cultriform process slightly expands ventrally in both *Shuvosaurus inexpectatus* and *Effigia okeeffeae*.

Anteriorly, the dorsal surface splits into symmetrical rami across the midline. A deep groove lies between the two rami and this space likely represents the hypophyseal fossa (Chatterjee, 1993; Lehane, 2023).

The basioccipital is complete and well-preserved in TTU-P9282 (Figure 15). Overall, the basioccipital of *Shuvosaurus inexpectatus* is nearly identical to that of *Effigia okeeffeae* (AMNH FR 30587). The occipital condyle of *Shuvosaurus inexpectatus* is dorsolaterally compressed like that of *Effigia okeeffeae* in contrast to the much more circular structure in other archosaurs. The posterolateral sides of the basioccipital are flat and dorsolaterally

slanted for articulation with the exoccipital "foot" of the otooccipital and it is clear that the exoccipital "feet" are well separated by a concave surface, as seen in posterior view. Other than *Effigia okeeffeae*, the degree of separation of the exoccipital "feet" across the midline is the widest of any known Triassic-aged archosaur we have observed. The concave surface between the exoccipital "feet" expands laterally to form a concave floor to the posterior portion of the brain. A small lamina of bone is present at the midline in the anterior half of the element in *Shuvosaurus inexpectatus*, just like in *Effigia okeeffeae* (Nesbitt, 2007, fig. 22B). The platform for the exoccipital "feet" is rectangular in dorsolateral view, with a convex dorsal border and a concave ventral border. More anteriorly, there are two deep fossae on the dorsolateral surface of the anterior portion of the element. These depressions were interpreted as the ventral base of metotic recess (metotic foramen in Nesbitt, 2007), posteriorly and the cochlear recess, anteriorly for *Effigia okeeffeae* (Nesbitt, 2007) and we accept this interpretation here for *Shuvosaurus inexpectatus* (Figure 15). The ventral base of metotic recess is circular and opens anterolaterally whereas the cochlear recess is bigger that the base of the metotic recess and opens more laterally. A thin lamina of bone separates the ventral base of metotic recess and the cochlear recess.

Ventrally, the occipital condyle continues from the lateral surface to the ventral surface. The neck of the occipital condyle is well developed and the surface between the occipital condyle and the rest of the basioccipital in simply concave in lateral view. Confined to just the ventral surface, the basitubera are low swollen structures, less expanded ventrally in comparisons with *Effigia okeeffeae* (Nesbitt, 2007, fig. 22A); the basitubera slightly expand laterally where the width of the basioccipital also expands. A deep, circular fossa is present between the basitubera at the midline, similar to *Effigia okeeffeae* (AMNH FR 30587).

A left laterosphenoid was illustrated attached to the prootic in the assembled paratype braincase (TTU-P9282; Chatterjee, 1993, fig. 5) and this identification was later followed by others (Lehane, 2023). After a closer examination, we cannot substantiate the identification of the laterosphenoid. The mediolaterally thin bone lacks any anatomical detail that indicates it is a laterosphenoid (e.g., a cotylar crest, a unambiguous border of the exit for cranial nerve V, a postorbital process) and the dorsal process is thin and differs from the much more mediolaterally expanded portion in the close relative *Effigia okeeffeae* (AMNH FR 30587). Finally, it appears that the bone was not originally articulated to the rest of the braincase, as revealed through CT information (Figure 15).

Parietal—A small piece of bone attached to the supraoccipital by added material (i.e., epoxy) to TTU-P9282 (Figure 15a,b) is the holotype parietal (TTU-P9280) present in the original skull reconstruction. This bone is just a portion of the main body of the parietal, missing the lateral process. The preserved shape overall is similar to that of *Effigia okeeffeae* (AMNH FR 30587) in that the bone in TTU-P9282 is anteroposteriorly short and appears to preserve part of the sagittal crest at the midline; the rest of the surfaces are broken.

Although not preserved, we infer that the anterior process of the parietal was longer than *Effigia okeeffeae* and divided the posterior portions of the frontals along the midline. This inference was made based on the large gap between the frontals at their posterior margins.

Hemimandible—Parts of the hemimandible of *Shuvosaurus inexpectatus* are present in the holotype (TTU-P9280), a paratype (TTU-P9281), and part of the holotype of *Technosaurus smalli* (previously TTU-P9021, now TTU-P24873; Chatterjee, 1984, fig. 1f). The holotype hemimandible was assembled from a disarticulated left dentary and the posterior portion consisting of the surangular, angular, articular, and possibly the prearticular (Figure 16). The long length of the reconstructed hemimandible was made to match the length of the reconstructed skull, thus much of the length of the hemimandible is composed of added compounds. If the hemimandible of *Shuvosaurus inexpectatus* is more like that of *Effigia okeeffeae*, the hemimandible would be proportionally shorter and much of the length would be composed of the surangular and angular (Nesbitt, 2007, fig. 24).

The anterior half of the dentaries (TTU-P9820, Figure 16; TTU-P9281, Figure 17) are well-preserved although none of the posterior processes are completely preserved in any specimen. Like *Effigia okeeffeae* and *Lotosaurus adentus* (Zhang, 1975), the dentaries are edentulous. In lateral view, the sharp lateral margin (= tomia) is largely horizontal with a slightly sinuous profile with a slight upturned anteriormost end in TTU-P9280 (Figure 16d) and a slight anterior ventral deflection in TTU-P9282 (Figure 17a). Foramina dot the lateral surface of the dentary and, like the premaxilla, the highest concentration is in the anterior portion. The dentaries meet in an interdigitating midline suture signifying a type III articulation of the hemimandible (see Holliday & Nesbitt, 2013), similar to *Lotosaurus adentus* (IVPP V4800). This contact includes portions of the ventral and anterior edges, and the medial expansion of a dentary shelf (Figures 16 and 17).

In dorsal view, the articulated dentaries form a broad U-shaped articulation (Figure 17c). The medial portion of the dentary expands to form a medial shelf and this shelf is largely dorsally flat at the midline. A series of foramina lie on the dorsal surface in two distinct lines, one that is

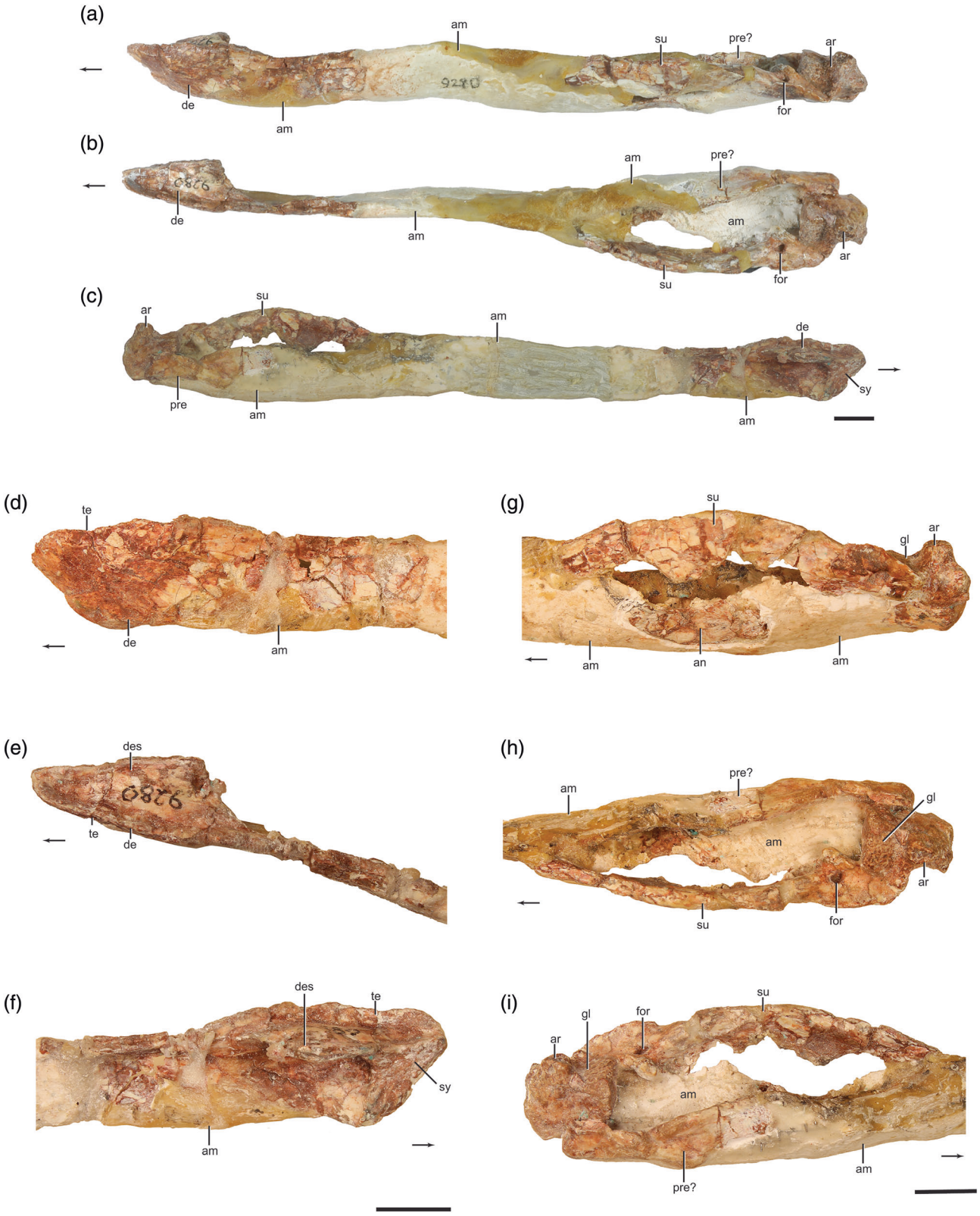

FIGURE 16 The originally reconstructed left hemimandible of the holotype of *Shuvosaurus inexpectatus* (TTU-P9280) in dorsolateral (a), dorsal (b), and medial (c) views with close up photographs of the anterior portion in lateral (d), dorsal (e), and medial (f) views and the posterior portion in lateral (g), dorsal (h), and medial (i) views. am, added material; an, angular; ar, articular; de, dentary; des, dentary shelf; for, foramen; gl, glenoid; pre, prearticular; su, surangular; sy, symphysis; te, tomial edge. Arrows indicate anterior direction. Scale bars equal 1 cm. Photos A-C by Bill Mueller.

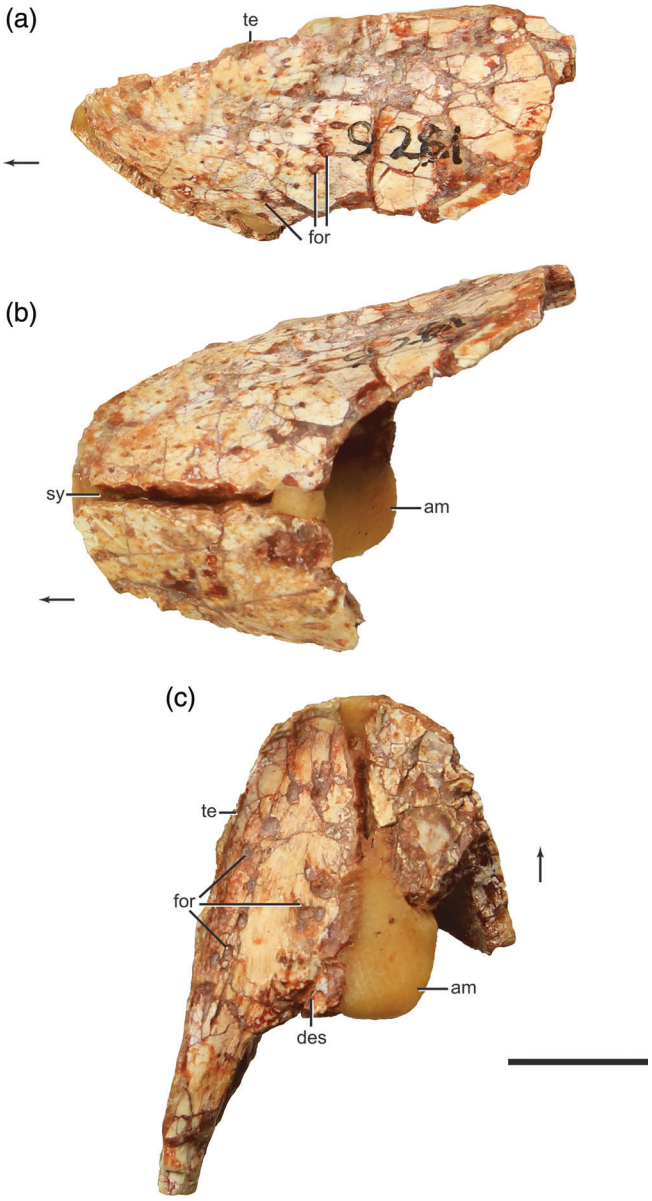

FIGURE 17 Dentaries referred to *Shuvosaurus inexpectatus* (TTU-P9281) in left lateral (a), ventral (b) and occlusal (c) views. am, added material; des, dentary shelf; for, foramen; sy, symphysis; te, tomial edge. Arrows indicate anterior direction. Scale bars equal 1 cm.

close to and parallel to the lateral margin and one that is on the medial edge (Figure 17c). Ventral to the medial shelf, a posteriorly opening fossa is present, like that of *Effigia okeeffeae* (Nesbitt, 2007), but larger than that of *Lotosaurus adentus* (IVPP V4800). The dorsal edge of the dentary is mediolaterally thick and rounded relative to the ventral three quarters of the mediolaterally thin ventral portion. The ventral edge of the anterior portion of the dentary is slightly expanded compared to the more posterior part in TTU-P9280, but no expansion is present in the paratype (TTU-P9281). Therefore, we do not agree with the ventrally extended "chin" illustrated in the reconstruction of Lehane (2023). We do note that a clear ventral "chin" is present in *Lotosaurus adentus* (IVPP V4800).

The extension of the posterior dentary is not clear in *Shuvosaurus inexpectatus*. A sheet of bone in the holotype (TTU-P9280; Figure 16d) extends much further in the specimens of *Effigia okeeffeae* (Nesbitt, 2007) and this length cannot be confirmed in the paratype (TTU-P9281) because the posterior portion is broken. A more posteriorly elongated dentary with a tomia is present in *Lotosaurus adentus* (IVPP V4800) which is clearly proportionally longer than that of *Effigia okeeffeae*. If the shape in the holotype represents the actual shape in *Shuvosaurus inexpectatus*, this would be a clear difference between the taxon and *Effigia okeeffeae*.

The posterior portion of the hemimandible is represented by the holotype (TTU-P9280; Figure 16) and a referred specimen (TTU-P24873) originally assigned to *Technosaurus smalli* (Figure 18; see Nesbitt et al., 2007). The surangular arches dorsally in the anterior direction and frames a large mandibular fenestra ventrally, like that of *Effigia okeeffeae* (Nesbitt, 2007) and *Lotosaurus adentus* (IVPP V4800). Posteriorly, the surangular tapers and lies on the lateral side of the articular. In TTU-P24873, there is a large lateral foramen (Figure 18a) nearly identical to that of *Effigia okeeffeae* (Nesbitt, 2007). In the holotype, a similarly large foramen cannot be seen laterally, but there is a large foramen opening dorsally (Figure 16h); it is possible that this foramen is homologous with that of the lateral foramen, but was twisted in preservation and possibly in preparation. Ventrally, the posterior portion of the angular also seems to frame the mandibular fenestra (Figure 16g), but most of the element remains buried in plaster. A potential prearticular is also present in the holotype (Figure 16i), but many of the details are obscured by added material. The prearticular seems to extend ventral to the articular.

The articular of the holotype is poorly preserved with abraded surfaces so the description here relies on the much better preserved referred specimen (TTU-P24873; Figure 18). The articular surface with the quadrate is convex like that of *Effigia okeeffeae*, but the articulation surface bears cortical (= internal) bone and no original surfaces. In TTU-P24873, the convex glenoid surface mirrors that of the largely concave surface of the ventral end of the quadrate, as in *Effigia okeeffeae* (AMNH FR 30587). The circular shape of the articulation surface bears a notch on the posterior side and matches that of *Effigia okeeffeae* (AMNH FR 30587) well. Medially, the articular lacks the large medial, "tongue-like" processes of other paracrocodylomorphs (Gower, 1999; Nesbitt et al., 2013). Posterior to the glenoid surface, a retroarticular process

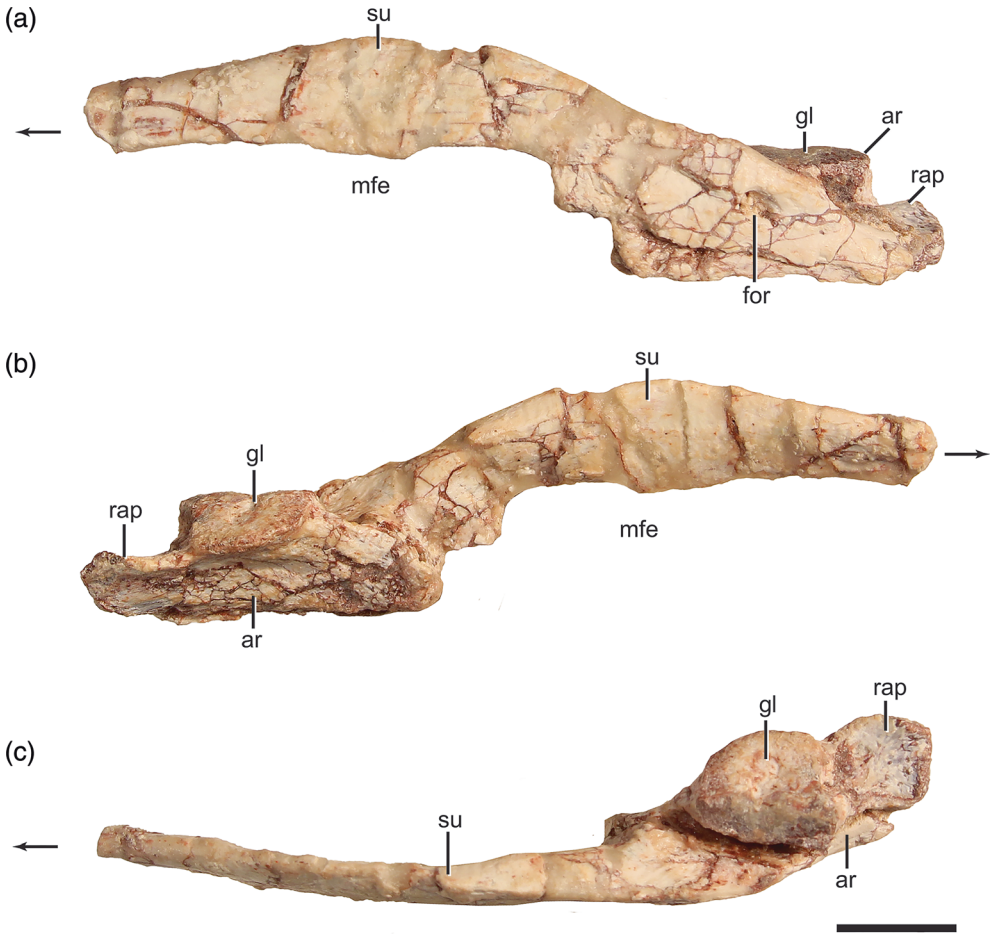

FIGURE 18 Postdentary bones of *Shuvosaurus inexpectatus* from the left side (TTU-P24873) in lateral (a), medial (b), and dorsal (c) views. ar, articular; for, foramen; gl, glenoid; mfe, mandibular fenestra; rap, retroarticular process; su, surangular. Arrows indicate anterior direction. Scale bar equals 1 cm.

extends posteriorly and slightly mediodorsally at its posterior margin in TTU-P24873. The mediodorsal process is similar to *Effigia okeeffeae* (AMNH FR 30587) but seems to be slightly shorter; this mediodorsal process may be homologous with the much greater mediodorsal processes of other poposauroids (e.g., *Arizonasaurus babbitt*, Nesbitt, 2005b). We find that the abraded dorsal expansion posterior to the glenoid surface in the holotype is a preservational artifact, and not representative of the shape of the articular of the taxon. Therefore, the quadrate was not braced and locked posteriorly by the articular, as postulated previously (Lehane, 2023).

3.1 | Vertebral column

Cervical vertebrae—The cervical vertebrae of *Shuvosaurus inexpectatus* are represented by a partial series from a referred skeleton (TTU-P9001) and other examples from the Post Quarry (e.g., TTU-P19950). In nearly all cases, the exact position of the vertebrae in the neck are not known but are estimated.

The atlas and axis are represented by a nearly complete axis-atlas complex (TTU-P9001; Figure 19a–e) and partial atlases (TTU-P9282; Figure 19g–j) preserved with the type series. The atlas consists of a complete odontoid, intercentrum, and a partial right neural arch whereas the axis consists of a small intercentrum and a complete axis pleurocentrum with neural arch. The wedge-shaped atlas intercentrum consists of a sharp rim anteriorly and a much dorsoventrally thicker posterior end. In ventral view, the posterior margin is nearly straight across the midline whereas the anterior edge arcs across the midline (Figure 19j). The dorsal surface is concave and there is little distinction between the medial portion of the bone and the articulation facets with the neural arches. The lateral surfaces do not appear to have an articulation surface with an atlantal rib.

The anterior portion of the neural arch has a concave facet that is a continuation of the articular surface of the atlas intercentrum with the occipital condyle of the skull (Figure 19e,h). In lateral view, a notch separates the articulation surface with the atlas intercentrum from that of the medially expanded portion (Figure 19b,i). The medial portion thins dorsoventrally like that of *Effigia okeeffeae* (AMNH FR 30587). The odontoid is slightly longer than wide and the anterior portion is rounded in dorsal view (Figure 19d). The dorsal portion is flat and extends from

the centrum of the axis at the ventral level of the neural canal. Much of the ventral surface is covered, but it is clear that the odontoid expands posteroventrally to contact much of the articular face of the axis.

The axis intercentrum sits as a wedge of bone between the atlas intercentrum and the axis centrum (Figure 19a–c). The small bone is ~33% the size of the atlas intercentrum. The complete axis pleurocentrum has an elongated centrum with a length almost five times longer (42 mm long vs. 9 mm high) than the height of the posterior articular facet of the centrum. This ratio is the greatest of all of the cervical vertebrae in *Shuvosaurus inexpectatus* and is not matched in any other pseudosuchian with a comparative part of the skeleton. In lateral view, the anterior portion bears a shallow depression that is shallower than other cervical vertebrae (see below) whereas the posterior portion is flat and not concave as in more posterior cervical vertebrae (Figure 19a,b). There appear to be both diapophyses and parapophyses at the anterior end of the centrum and both are closely appressed without distinct articular facets for a cervical rib. Ventrally, there are two parallel ridges separated by a longitudinal depression at the midline, a character state that seems to be unique to *Shuvosaurus inexpectatus* (unknown in *Effigia okeeffeae*) within poposauroids, but is also shared in rauisuchids (Nesbitt, 2011). The D-shaped posterior articular surface of the centrum is concave. The anterior portion of the neural arch extends anteriorly of the centrum and creates dorsolateral platforms for articulation with the posterior processes of the neural arches of the atlas. A ridge from the ventral portion of this platform extends posteriorly to mark the lateral margins of the postzygapophysis (Figure 19a,b). The postzygapophysis terminates at the posterior margin of the centrum and no epipophyses are present on the dorsal surface. In lateral view, the thin neural spine is nearly horizontal anteroposteriorly (Figure 19a,b) with a slight gradual expansion at its posterior end. In

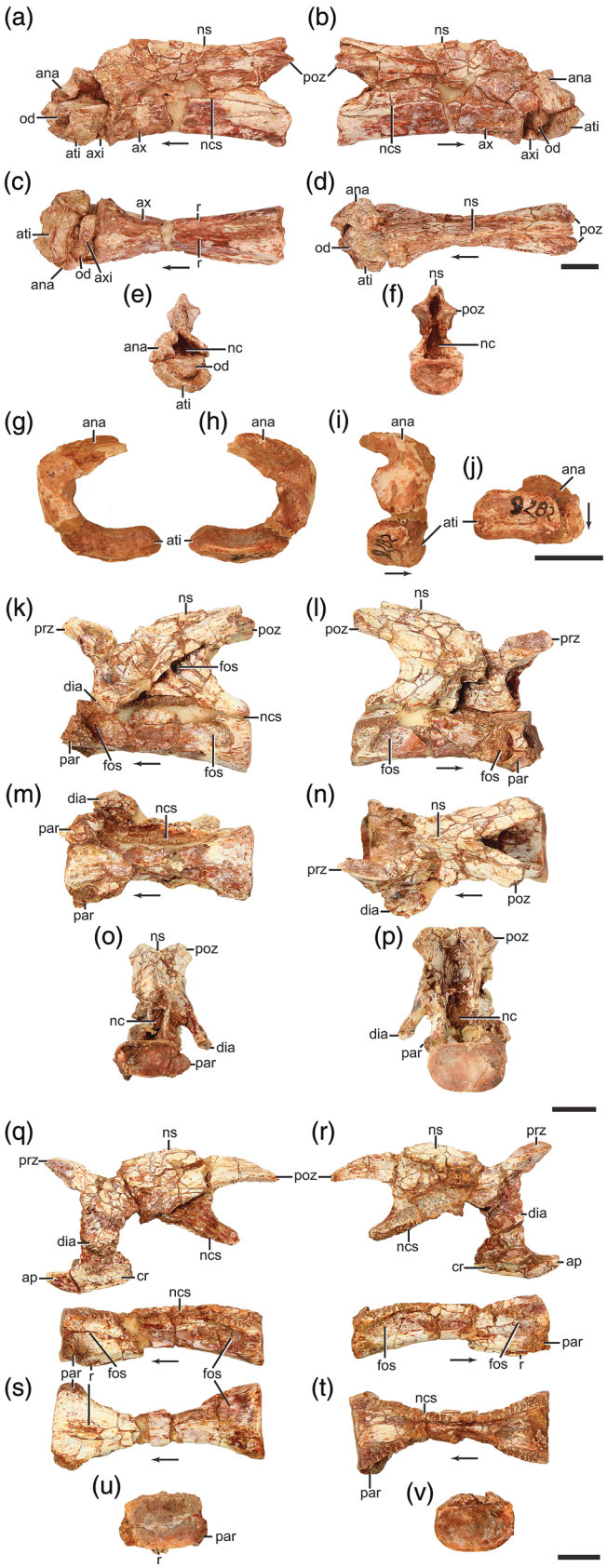

FIGURE 19 Anterior cervical vertebrae referred to *Shuvosaurus inexpectatus*. Articulated atlas and axis (TTU-P9001) in left lateral (a), right lateral (b), ventral (c), dorsal (d), anterior (e), and posterior (f) views. Partial atlas components (TTU-P9282) in anterior (g), posterior (h), right lateral (i), and ventral (j) views. Third cervical vertebra (TTU-P19950) in left lateral (k), right lateral (l), ventral (m), dorsal (n), anterior (o), and posterior (p) views. Fourth cervical vertebra (TTU-P19950) in left lateral (q) and right lateral (r) and centrum in ventral (s), dorsal (t), anterior (u), and posterior (v) views. ana, atlantal neural arch; ap, anterior process; ati, atlas intercentrum; ax, axis pleurocentrum; axi, axis intercentrum; cr, cervical rib; dia, diapophysis; fos, fossa; nc, neural canal; ncs, neurocentral suture; ns, neural spine; od, odontoid process of the atlas; par, parapophysis; poz, postzygapophysis; prz, prezygapophysis; r, ridge. Arrows indicate anterior direction. Scale bars equal 1 cm.

posterior view, a deep gap separates the postzygapophyses and this gap reaches the dorsal margin of the neural spine (Figure 19f).

Two anterior vertebrae (TTU-P19950; Figure 19k–v) represent the anterior cervical vertebrae, likely in the third and fourth position. The two vertebrae, which were once articulated, bear both the centrum and the neural arch. The two articulated anterior cervical vertebrae have long centra with a height to length ratio of 4.2 for the first and 4 for the second. Among pseudosuchians, the long length of the cervical centra of *Shuvosaurus inexpectatus* are only matched by *Sillosuchus longicervix*, being longer that what is preserved in *Effigia okeeffeae* (AMNH FR 30587). In lateral view, the centra of *Shuvosaurus inexpectatus* have clear rimmed fossae at the anterior end, medial and dorsal of the parapophysis and, at the posterior end of the centrum; a shallow lateral fossa connects the two. The circular depressions open posteriorly and anterior respectively and a laterally projected ridge binds the ventral surface. A similar feature is present in the fragmentary anterior vertebrae of *Effigia okeeffeae* (Nesbitt, 2007) and in both taxa, the surrounding rim does not create a pocket like those of archosaurs with pneumatic openings (= pleurocoels) (see Britt, 1993; Rauhut, 2003). In lateral view, the dorsal and ventral edges of the centra are straight with little arching between the two ends contrasting with the ventrally waisted condition in *Sillosuchus longicervix* (Alcober & Parrish, 1997) and the parallelogram-shaped anterior cervical vertebrae of *Arizonasaurus babbitti* (MSM P4590), *Qianosuchus mixtus* (Li et al., 2006), and crocodylomorphs (*Hesperosuchus agilis*, AMNH FR 6758). The parapophyses are present at the ventral margin of the anterior edge of the centrum and extend ventrally of the centrum surface. The anterior and posterior articular surfaces are deeply concave and oval. The neurocentral suture in both these vertebrae are open (sensu Brochu, 1996). The first of the articulated series bears a distinct ridge on the midline in the anterior half of the centrum whereas the second in the series lacks any ridge on the ventral. This ventral ridge slightly expands laterally at its ventral margin in the first of the series.

The two anterior articulated vertebrae have partial neural arches, which are rarely preserved among the *Shuvosaurus inexpectatus* material. The neural arch possesses the diapophysis and the diapophysis extends anteroventral, ventral to the neurocentral suture. The oval articular facet of diapophysis faces anterolaterally (Figure 19k–u). A ridge on the posterior edge of the diapophysis extends posterodorsally to meet the anterior portion of the postzygapophysis. This ridge serves as the dorsal roof a deep mediodorsally fossa in the anteroposterior middle of the neural arch and a deep anteromedially directed fossa on the posterolateral surface of the neural arch. The central fossa is not reported in *Effigia okeeffeae* (Nesbitt, 2007), but this portion of the vertebral column is fragmentary in that taxon, is unknown in *Sillosuchus longicervix* (PVSJ 85) and *Poposaurus gracilis* (YPM 57100), and is definitely absent in *Arizonasaurus babbitti* (MSM P4590) and *Qianosuchus mixtus* (IVPP V13899). The posterior fossa is present in the anterior cervical vertebrae of *Effigia okeeffeae* (Nesbitt, 2007, fig. 28c) but are absent in other poposauroids with the preserved anterior cervical vertebrae. It appears that a deep fossa is lateral to the neural canal bound laterally by the prezygapophysis process in *Shuvosaurus inexpectatus*, but this area is poorly preserved. If present, these deep fossae are much more like those in neotheropod dinosaurs than any other pseudosuchian (Nesbitt, 2007).

The oval prezygapophyses are anteroposteriorly elongated with sharp anterior and lateral rims (Figure 19). The articular surface is slightly bowed dorsally. Similarly, the oval postzygapophyses are anteroposteriorly elongated with an articular surface that is concave dorsally to match that of the bowed articular surface of the prezygapophyses. The dorsal portion of the postzygapophyses bear ridges that converge dorsomedially. No posteriorly-extending epipophysis is preserved in *Shuvosaurus inexpectatus*. A deep fossa lies at the midline between the postzygapophyses. This fossa extends to the anteroposterior middle of the centra and we have not seen any other feature like this in other archosaurs. None of the neural spines are complete, but they appear mediolaterally thin and only occupy a bit more than ~33% the length of the centrum, over the anteroposterior center of the centrum.

Isolated anterior to posterior cervical centra (Figure 20) were identified in the referred skeleton (TTU-P9001) based on: the (1) the similarity of shape of the centrum of the articulated anterior vertebrae (TTU-P19950; Figure 19k–v); (2) the presence of a parapophysis on the ventral portion of the anterior end of the centrum; and (3) general length versus centrum height (at the posterior articular surface) ratio. The centra possess a wide parapophysis that expands more laterally than any other portion of the centrum (Figure 20c,i,o). In anterior view, these paraphyses laterally expand the oval shape of the centrum compared to the more circular posterior articular facet. All of the centra have a clear fossa on the lateral side of the centrum like that of the more anterior centra (e.g., Figure 19k) whereas the posterior fossa (Figure 20) disappears. A pronounced ridge is present in the anterior half of the centrum on the ventral surface in some of the cervical centra (Figure 20g–k,s–u), but absent in others (Figure 20a–e,m–q). The centra with the ridges have a

variable depth (Figure 20g–k vs. s–u) and variable lateral expansion (Figure 20g–k vs. s–u). The neurocentral sutures are all exposed in these vertebrae as uniform peaks and valleys along the lateral side of the dorsal portion of the centrum. In lateral view, the neurocentral suture is nearly horizontal with a small peak in the anteroposterior middle. All of the articular facet of the centrum are slightly concave and the articular facets are in the same horizontal plane in contrast to taxa with long cervical vertebrae where the articular facets are offset (= parallelogram-shaped, e.g., *Arizonasaurus babbitti*, Nesbitt, 2005b).

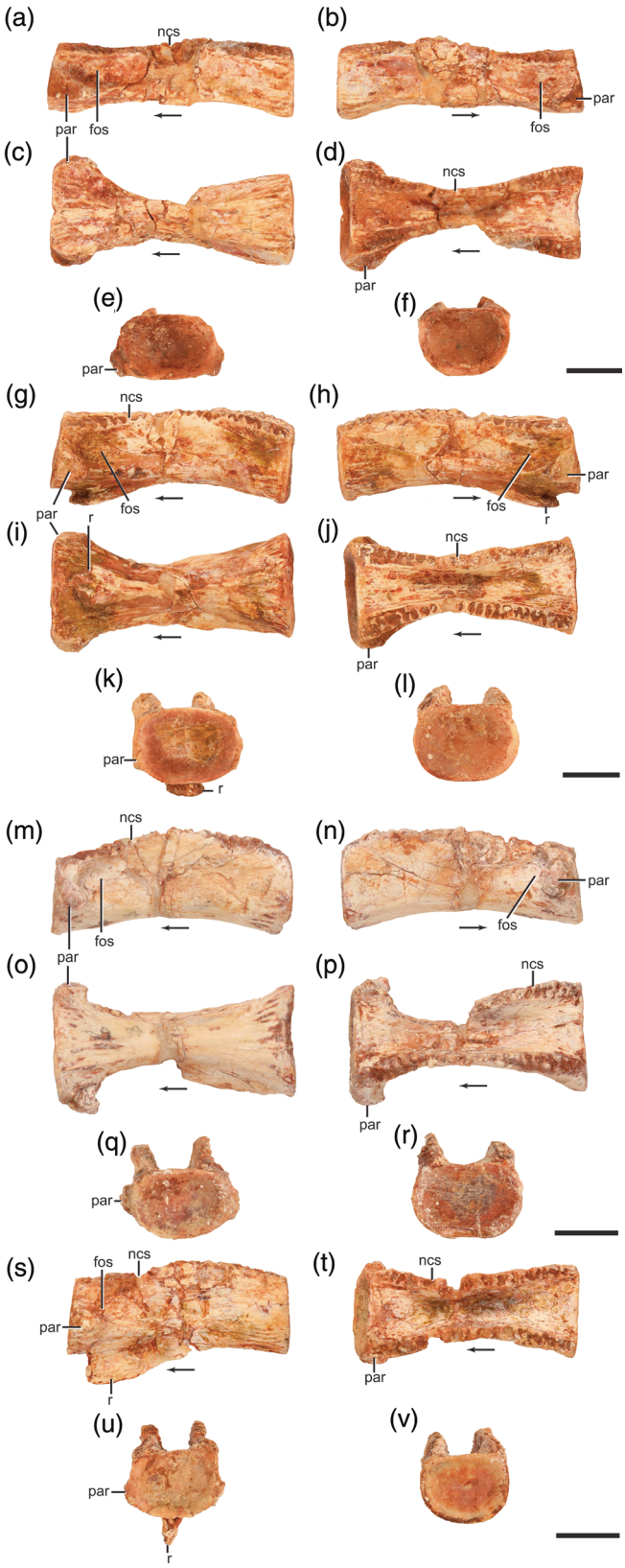

FIGURE 20 Cervical centra of an associated skeleton referred to *Shuvosaurus inexpectatus* (TTU-P9001). Centrum in left lateral (a), right lateral (b), ventral (c), dorsal (d), anterior (e), and posterior (f) views. Centrum in left lateral (g), right lateral (h), ventral (i), dorsal (j), anterior (k), and posterior (l) views. Centrum in left lateral (m), right lateral (n), ventral (o), dorsal (p), anterior (q), and posterior (r) views. Centrum in left lateral (s), ventral (t), anterior (u), and posterior (v) views. Order of centra in the figure does not indicate anterior–posterior anatomical order. fos, fossa; ncs, neurocentral suture; par, parapophysis; r, ridge. Arrows indicate anterior direction. Scale bars equal 1 cm.

Trunk vertebrae—At least 12 vertebrae from the trunk region are present in the referred skeleton of *Shuvosaurus inexpectatus* (TTU-P9001; Figure 21). With the exception of one attached partial neural arch, all trunk centra in TTU-P9001 are disarticulated from the neural arches across the neurocentral suture; the neural arches were not recovered in nearly all cases. The absence of neural arches is common among nearly all of the trunk vertebrae assignable to *Shuvosaurus inexpectatus* from the Post Quarry, and the number of trunk centra far outnumber that of neural arches (Figure 22). Given the lack of attached neural arches and the anteroposterior symmetry of the trunk centra, the anterior direction cannot be determined easily. Moreover, the position within the trunk series is not known either, although the difference in centrum size, length, and shape of the articular facets hint at possible shape changes throughout the series, possibly similar to close relatives (see Schachner et al., 2020).

The centra have circular articular facets in contrast to the oval articular facets in the close relative *Poposaurus gracilis* (Schachner et al., 2020). The lengths of the centrum versus height of the articular facets vary from ~2 in the longer centra to ~1.4 in the larger centra; most centra are the same length regardless of potential position. The articular facets are slightly concave like that of the cervical centra. In ventral view, the mid portions of the centra are highly waisted (Figure 21) like that of other paracrocodylomorphs (Schachner et al., 2020) and the centrum rims are sharp, like that of *Poposaurus gracilis* (YPM 57100). Fine radiating ridges aligned anteroposteriorly decorate the lateral and ventral surface of the centrum

near the rims. No ridge is present on the midline of the ventral surface (Long & Murry, 1995). A shallow fossa is present on the lateral side, just ventral to the neurocentral suture. The exposed neurocentral sutures are nearly horizontally oriented in lateral view (Figure 21) with a small central peak in some (e.g., Figure 21h). In dorsal view, the neural canal is deepest in the anteroposterior middle of the centrum, like in the cervical centra (Figure 20).

Two nearly complete neural arches were found together (TTU-P23422; Figure 22). The exact position within the presacral column is not known, but a posterior process of the transverse processes are present in the posterior cervical to anterior trunk vertebrae (Nesbitt, 2007, figs. 28 and 29) in *Effigia okeeffeae* (Nesbitt, 2007) suggesting that these vertebrae are in the anterior portion of the trunk series. The prezygapophyses are well separated from each other indicating that a hypantrum was present (see Stefanic & Nesbitt, 2018), a similar condition is present in *Effigia okeeffeae* (Nesbitt, 2007) and *Poposaurus gracilis* (Schachner et al., 2020). Posteriorly, the postzygapophyses are separated at the midline, but both have a small and ventrally extended lamina of bone; this modified hyposphene fits the definition of a hyposphene found in other archosaurs (see Stefanic & Nesbitt, 2018). The wide prezygapophyses are nearly horizontally oriented (Figure 22c) and the lateral margin is continuous with a prezygodiapophyseal lamina (sensu Wilson, 1999) that expands laterally. The prezygodiapophyseal lamina dorsally caps the anterior centrodiapophyseal and posterior centrodiapophyseal laminae. The prezygodiapophyseal laminae, or transverse processes, are triangular in dorsal view (Figure 22a, ppr) and posterolaterally terminate in processes, identical to that of *Effigia okeeffeae* (Nesbitt, 2007). A dorsally opening fossa is present at the base of the neural spine in the anteroposterior middle of the dorsal surface, like that of *Effigia okeeffeae* (Nesbitt, 2007, fig. 29); the depth and shape of this fossa varies (Figure 22a vs. e). The neural spine sits in the anteroposterior middle of the neural arch, is low with a horizontally flat dorsal margin, and vertical fossae excavate the anterior and posterior ends. The neural canal is much taller than wide.

Sacral vertebrae and ribs—The sacrum is represented by a skeleton referred to *Shuvosaurus inexpectatus*

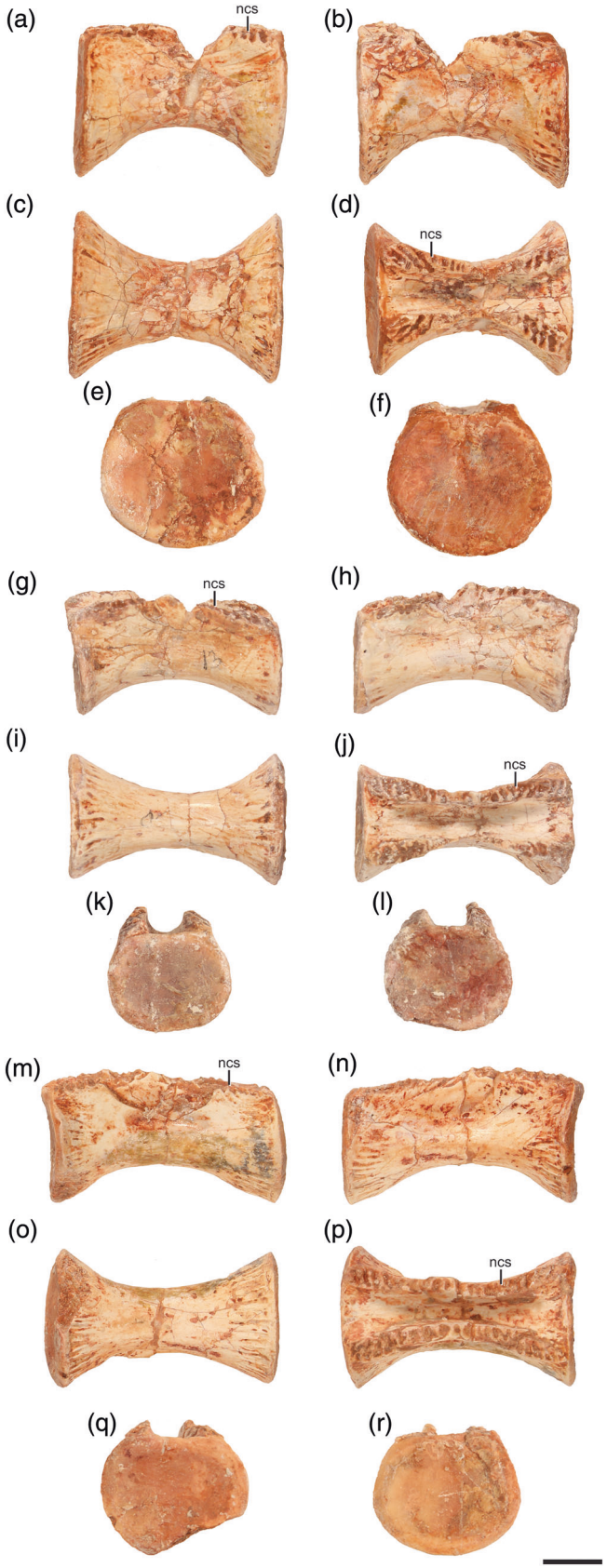

FIGURE 21 Trunk centra of an associated skeleton referred to *Shuvosaurus inexpectatus* (TTU-P9001). Centrum in lateral (a and b), ventral (c), dorsal (d), and articular ends (e and f). Centrum in lateral (g and h), ventral (i), dorsal (j), and articular ends (k and l). Centrum in lateral (m and n), ventral (o), dorsal (p), and articular ends (q and r). Note, the symmetry of the centra does not allow the anterior direction to be unambiguously determined, and the order of the centra in the figure does not indicate anterior–posterior anatomical order. ncs, neurocentral suture. Scale bar equals 1 cm.

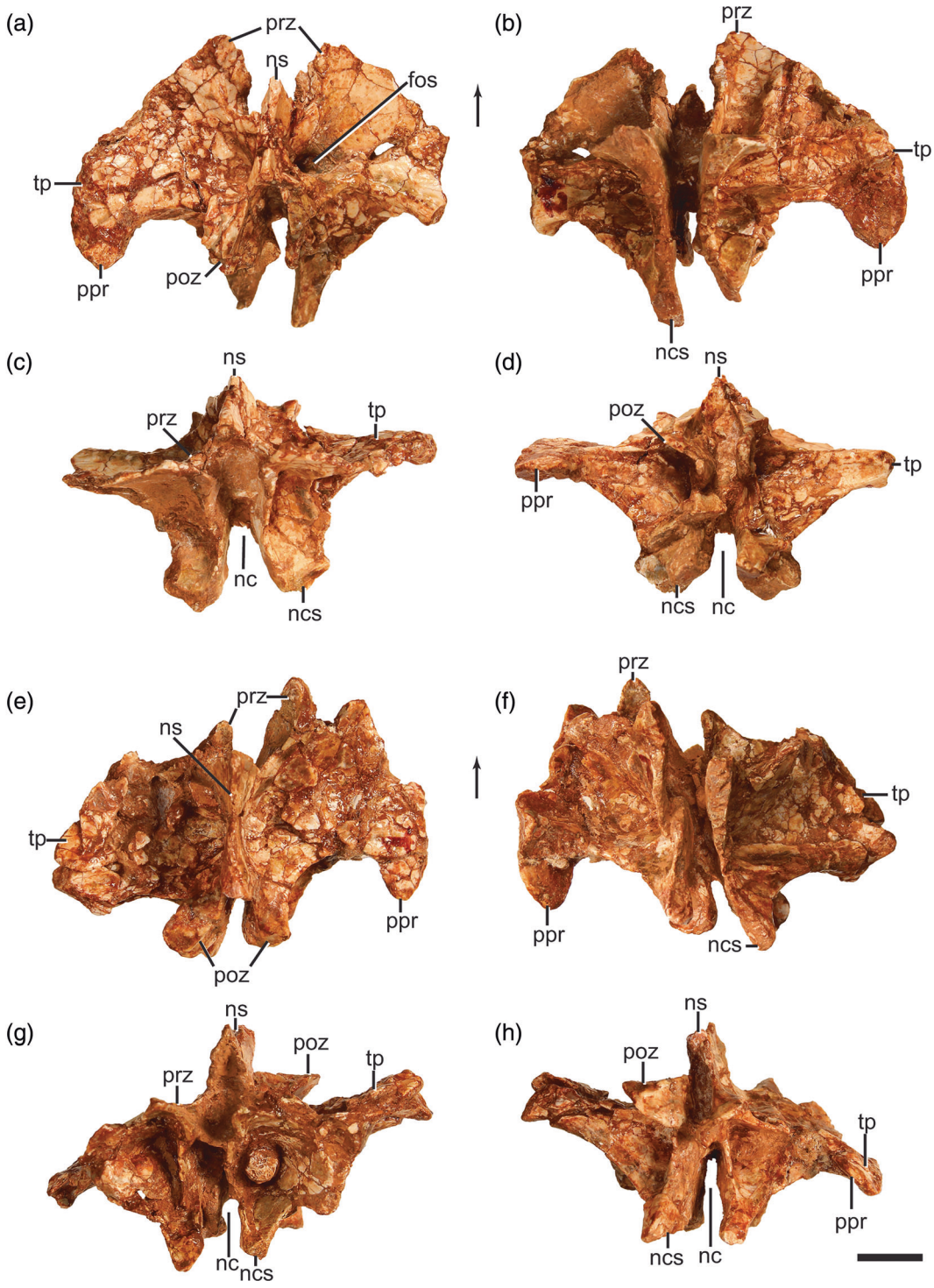

FIGURE 22 Trunk neural arches referred to *Shuvosaurus inexpectatus*. Neural arch (TTU-P23422) in dorsal (a), ventral (b), anterior (c), and posterior (d) views. Neural arch (TTU-P23422) in dorsal (e), ventral (f), anterior (g), and posterior (h) views. fos, fossa; nc, neural canal; ncs, neurocentral suture; ns, neural spine; poz, postzygapophysis; ppr, posterior process; prz, prezygapophysis; tp, transverse process. Arrows indicate anterior direction. Scale bar equals 1 cm.

(TTU-P9001; Figure 23) containing four partial sacral vertebrae, and a well-preserved sacrum with three sacral vertebrae with neural arches and mostly intact sacral ribs (TTU-P23438; Figure 24). The sacrum of *Shuvosaurus inexpectatus* consists typically of four firmly coossified centra in TTU-P9001 (Long & Murry, 1995; followed by Nesbitt, 2007) with only a slight ridge marking contact between the centra; the anteriormost sacral vertebra is

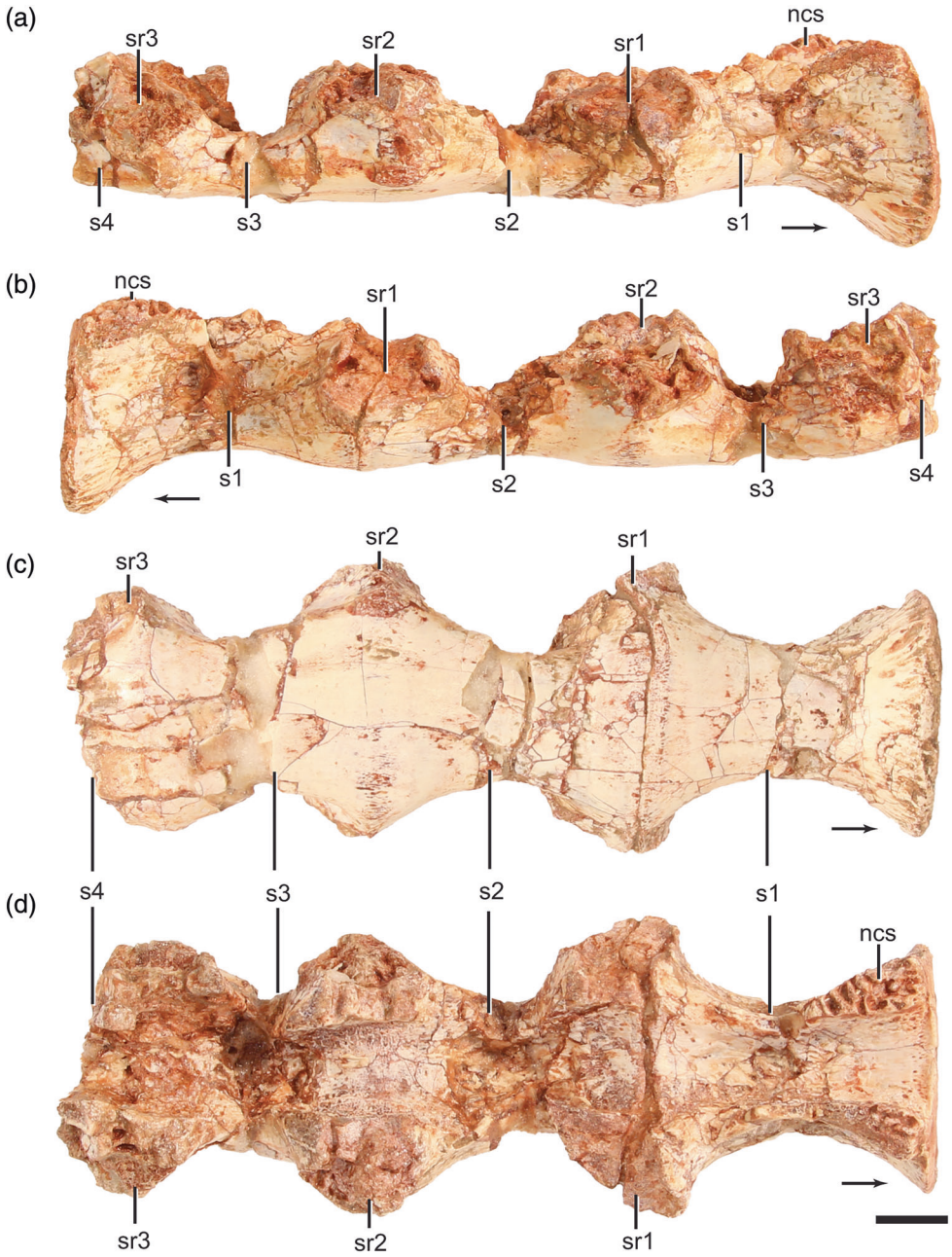

FIGURE 23 Sacrum of an associated skeleton referred to *Shuvosaurus inexpectatus* (TTU-P9001) in right lateral (a), left lateral (b), ventral (c), and dorsal (d) views. ncs, neurocentral suture; s#, sacral # in relative order; sr# sacral rib # in relative order. Arrows indicate anterior direction. Scale bar equals 1 cm.

only partially preserved (Figure 23). In TTU-P23438, there are only three preserved with no sign of coossification of a fourth. However, the posterior articular surface of the centrum of the last sacral vertebra of TTU-P23438 is flat and rugose suggesting that the fourth sacral vertebra would have been present at the posterior portion of this specimen, but not coossified. Also, there is a dorsal expansion on the posterior edge of the posterior articular facet of the centrum, suggesting that there was a shared sacral rib with the next sacral vertebra. Therefore, TTU-P23438 represents the first three sacral vertebrae compared to the four in TTU-P9001. In comparison, both specimens of *Effigia okeeffeae* have four sacral vertebrae (Nesbitt, 2007) and *Sillosuchus longicervix* (Alcober & Parrish, 1997) has at least five coossified sacral centra. No articulated series of presacral vertebrae are known from *Shuvosaurus inexpectatus*, so it is possible that a fourth sacral vertebra was added through ontogeny or the number of sacral vertebrae represents variation in the population. The identification of homologous sacral vertebrae from *Shuvosaurus inexpectatus* to other pseudosuchians is not clear using the strategy outlined by Nesbitt (2011) largely because of the loss of identifying plesiomorphic character states of the centra, the shift of the sacral ribs to between vertebrae, and the divergent features of sacral ribs (see below).

The centra articular facts of the sacrum are wider than tall with a nearly flat ventral surface (Figures 23

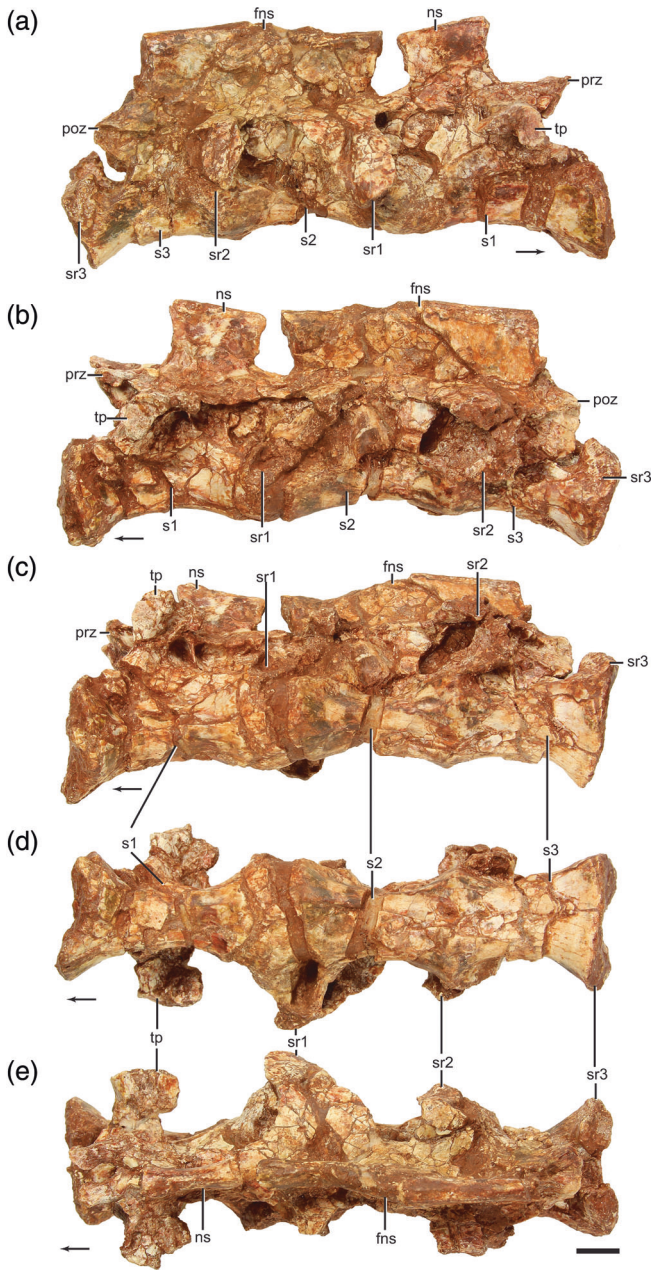

FIGURE 24 Sacrum referred to *Shuvosaurus inexpectatus* (TTU-P23438) in right lateral (a), left lateral (b), left ventrolateral (c), ventral (d), and dorsal (e) views. fns, fused neural spines; ns, neural spine; poz, postzygapophysis; prz, prezygapophysis; s#, sacral # in relative order; sr# sacral rib # in relative order; tp, transverse process. Arrows indicate anterior direction. Scale bar equals 1 cm.

and 24). Similar to *Effigia okeeffeae* (AMNH FR 30587), only an expanded rim of bone marks where the centra meet with the sacrum in *Shuvosaurus inexpectatus*; the anterior rim of the first sacral vertebra and the posterior rim of the last sacral vertebra are expanded like trunk and caudal vertebrae, respectively. The length of the centra are similar throughout (~3 cm) and similar to the trunk vertebrae. Sacral ribs are shared between the sacral vertebrae where they are coossified, similar to *Effigia okeeffeae* (Nesbitt, 2007), some dinosauriforms (*Silesaurus opolensis*, Dzik, 2003), and dinosaurs (Langer & Benton, 2006). TTU-P9001 preserves the dorsal surface of centra and shows that there are deep fossa at the midline at the anteroposterior middle of each vertebra (Figure 23d). The lateral side of the centra have fossae that are deeper than that of the trunk vertebrae.

Like the centra and sacral ribs, the neural arches and some of the neural spines are also coossified in TTU-P23438 (Figure 24). The sacral ribs and neural arches are incompletely preserved and because of the coossification, some features are difficult to interpret. The sacral ribs extend laterally from the centra joints and the lateral surface between the sacral ribs is slightly concave. The laterally directed first sacral rib is the best preserved of the series and the articular surfaces for attachment with ilium are preserved as a comma shaped surface with a flat dorsal surface. This first rib is located in the anterior third of the centrum and bears a number of thin lamina and deep fossa to the posterior side of it (left side Figure 24b). The second sacral rib expands more laterally than the first, but is crushed ventrally on the left side (Figure 24b). The more complicated second sacral rib has two main parts, a ventral portion that lies on the contact between the second and third centrum and a more dorsal portion that is dorsoventrally thin and more anteroposteriorly wide. The more ventral part has a deep ventrally opening fossa just posterior to contact between the second and third centrum. A vertical lamina of bone bridges the two components of the second sacral rib and both the anterior and posterior sides of this lamina are excavated with the more dorsal process roofing the excavations. The more dorsal component is horizontal anteroposteriorly along its dorsal margin and connects the prezygapophysis and postzygapophysis regions of the neural arch. The third sacral rib, like the second, has two main components separated by a vertical lamina of bone (Figure 24a). Overall, the preserved morphology looks like the second sacral rib. Almost nothing of the fourth sacral rib is preserved except for its dorsolaterally directed articulation surface between the third and fourth sacral centra.

The sacral rib scars on the ilium (see below) are difficult to determine, so the exact articulation points of the sacrum with the ilium cannot be determined. However, the laterally and horizontally directed first sacral rib indicates that the ilium must have been oriented vertically like that of dinosaurs and not downturned, typical of pseudosuchians and archosaur outgroups (Ezcurra, 2016; Nesbitt, 2011).

The articular surface of the prezygapophysis of the first sacral vertebra is flat and horizontally oriented and there is a large gap between the two articular surfaces (Figure 24). The postzygapophysis of the last preserved sacral vertebra are proportionally smaller than the others in the series, deflected laterally at ~40° angle relative to horizontal, and are separated by a wide peg of bone at the midline. The neural spines have flat lateral walls and the dorsal surface is flat in lateral view. In TTU-P23438, the first neural spine is free from the others whereas the neural spines of the second and third centra are completely coossified into a sheet of bone, similar to that of *Effigia okeeffeae* (Nesbitt, 2007). The dorsal part of the neural spines have rounded lateral edges and have a fine rugose texture on them that is not present on other parts of the neural spine.

TTU-P9001 and TTU-P23438 are about the same size, yet, TTU-P9001 lacks all of its neural arches whereas the neural arches and some of neural spines are coossified in TTU-P23438, demonstrating some variable timing of coossification or variation within the population. Also, after coossification of the fourth sacral vertebra, the centrum rims are reduced so it looks more like the centra rims within the sacrum.

Caudal vertebrae—The caudal vertebrae are largely represented in the referred skeleton by at least 28 vertebrae (TTU-P9001; Figure 25), but the posterior caudal vertebrae are missing; the posterior caudal vertebrae are represented by a partially articulated series and other isolated vertebrae (TTU-P23873; TTU-P23874; TTU-P23875; Figure 26). Like the presacral vertebrae, most of the anterior and some of the middle caudal vertebrae lack neural arches because either the neural arches became disarticulated along the neurocentral sutures or are broken. The anterior caudal vertebrae (e.g., Figure 25a–d) are just longer than the height of the articular facet. In lateral view, the posterior articular facet is slightly more ventral than the anterior articular facet resulting in a parallelogram-shaped centrum, similar to the anterior caudal vertebrae of *Effigia okeeffeae* (AMNH FR 30588). The ventral surface lacks a midline groove or the groove is very shallow (Long & Murry, 1995). This is in contrast to most archosauromorphs where there is a clear groove in most caudal vertebrae (Ezcurra, 2016). The chevron facets project posteroventrally. The transverse process extends laterally and partially dorsally. None of the neural spines are completely present in TTU-P9001.

The middle caudal vertebrae are represented by a few complete examples (e.g., TTU-P9001; Figure 25e–j). These vertebrae have neural arches and the neurocentral sutures are absent. The middle caudal vertebrae (e.g., Figure 25e–j) are much longer (~2.5) than the height of the articular facet. The centrum articular facets

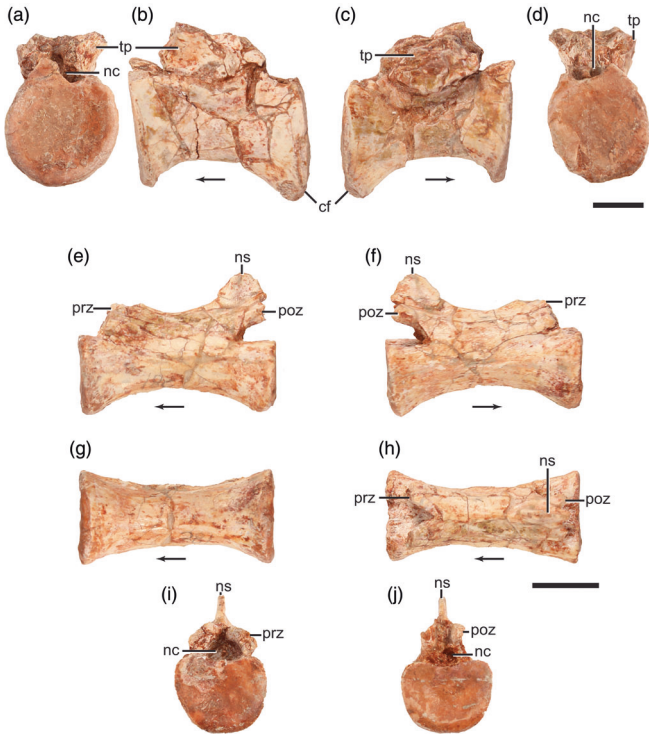

FIGURE 25 Caudal vertebrae referred to *Shuvosaurus inexpectatus* (TTU-P9001). Proximal caudal in anterior (a), left lateral (b), right lateral (c), and posterior (d) views. Middle caudal in left lateral (e), right lateral (f), ventral (g), dorsal (h), anterior (i), and posterior (j) views. cf, chevron facet; nc, neural canal; ns, neural spine; poz, postzygapophysis; prz, prezygapophysis; tp, transverse process. Arrows indicate anterior direction. Scale bars equal 1 cm.

are "bean"-shaped with a slight notch on the dorsal surface (Figure 25i,j). The anteroposterior asymmetry of the centrum in the anterior caudal vertebrae is not present in the middle caudal vertebrae. The ventral portion of the centrum lacks any groove and the chevron faces are nearly imperceptible suggesting that chevron may not be present in this part of the tail. The prezygapophyses are broken but start to show the elongated pattern present in the posterior caudal vertebrae (see below) as evidenced by a dorsolateral-ventromedial compression of the process (Figure 25i). The postzygapophyses are short and likely did not extend posterior of the border of the centrum. The neural spine is asymmetrically expanded posteriorly, just dorsal to the postzygapophyses (Figure 25e,f). The dorsal tip of the neural spines is thin in dorsal view.

The posterior caudal vertebrae are represented by articulated examples (TTU-P23874 and TTU-P23875; Figure 26a–h) and far posterior and complete examples (TTU-P23873; Figure 26k–t). Moving posteriorly, the centra elongate dramatically. From the preserved caudal vertebrae, the length to height ratio transforms from twice

as long (TTU-P23875) to nearly eight times longer (TTU-P23873). This elongation among pseudosuchians is unique and is similar to some dinosaurs (e.g., diplodocoid sauropods). The centrum rims are sharp and there is no ventral groove on the midline or any clear facet with a chevron. The more anterior posterior caudal vertebrae have long prezygapophyses like those of *Effigia okeeffeae* (AMNH FR 30588) and overlap 25% to ~50% the length of the proceeding centrum, like that in some theropod dinosaurs (Nesbitt, 2007). The postzygapophyses are completely obscured laterally by the prezygapophyses in articulation in most cases, but appear to be rather small. The articular surface with the prezygapophyses extends anteriorly of the postzygapophyses and attaches to the lateral side of the neural arch. Dorsally, the neural spine is expressed as an anterior peak at the base of the prezygapophyses and an equally high posterior peak; the two peaks are separated by a trough visible in lateral view (Figure 26e). A similar condition is present in *Effigia okeeffeae* (AMNH FR 30588; Nesbitt, 2007, fig. 34).

The preserved posteriormost caudal vertebrae radically differ from other pseudosuchians in their length and intervertebral articulation mode. The dorsal and ventral view, the centra are rectangular because a lateral ridge is present for the length of the centrum (Figure 26i–t). This ridge continues anteriorly to form the ventral edge of the prezygapophyses. In lateral view, the centrum is slightly wasted at its ventral surface between the articular ends. The centrum articular ends have sharp lateral rims, and the oval articular surfaces are flat, indicating that there was little to no gap between each centrum. Two parallel, weakly defined ridges are present on the ventral surface of some of the posterior caudal vertebrae (Figure 26k). Like the more anterior posterior caudal vertebrae, the prezygapophyses extend far anteriorly to overlap the proceeding vertebra. Although the anterior portions of the prezygapophyses are not preserved, a depression on the lateral sides of the neural arches indicate that the prezygapophyses extend to ~50% the length of the centrum (Figure 26i,j,l,o,p,r). In anterior view, the prezygapophyses are dorsolaterally thin laminae nearly reaching each other at the midline near their bases. Distinct postzygapophyses are absent, but the articulation surface with the

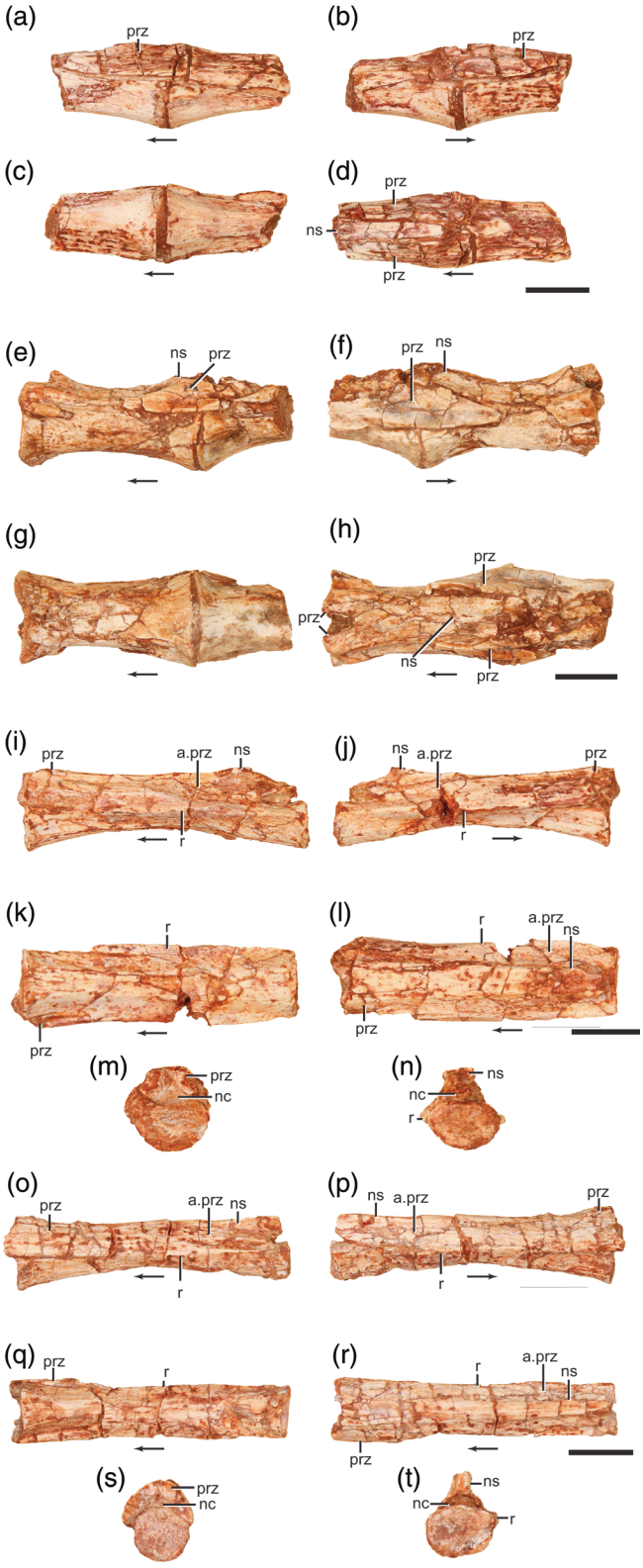

FIGURE 26 Posterior caudal vertebrae referred to *Shuvosaurus inexpectatus*. Articulated partial caudals (TTU-P23875) in left lateral (a), right lateral (b), ventral (c), and dorsal (d) views. Articulated partial caudals (TTU-P23874) in left lateral (e), right lateral (f), ventral (g), and dorsal (h) views. Posterior caudal vertebra (TTU-P23873) in left lateral (i), right lateral (j), ventral (k), dorsal (l), anterior (m), and posterior (n) views. Posterior caudal vertebra (TTU-P23873) in left lateral (o), right lateral (p), ventral (q), dorsal (r), anterior (s), and posterior (t) views. a., articulates with; nc, neural canal; ns, neural spine; poz, prz, prezygapophysis; r, ridge. Arrows indicate anterior direction. Scale bars equal 1 cm.

prezygapophyses are clear. The neural spine lacks the anterior peak present in the more anterior caudal vertebrae (Figure 26e,f), but they possess a dorsal expansion at the posterior portion. The lateral sides of the neural spine are closely flanked by the prezygapophyses of the preceding vertebra, and the dorsal surface of the neural spine is flat.

Ribs—Ribs are exceptionally rare among the *Shuvosaurus inexpectatus* material from the Post Quarry and only a partially articulated cervical rib (TTU-P19950; Figure 19q,r) can be confirmed as belonging to the taxon. We tentatively attribute a nearly complete cervical rib (TTU-P23903; Figure 27a,b) and a trunk rib (TTU-P19577; Figure 27c,d) to the taxon based on similarity with *Effigia okeeffeae* (Nesbitt, 2007). The cervical rib (Figure 27a,b) has a distinct capitulum and tuberculum with oval articular facets. A clear anterior process is present and the long posterior portion tapers indicating that the ribs are longer than the vertebra it attaches to. The incompletely preserved trunk rib (Figure 27c,d) has two heads separated by a thin web of bone and the rib shaft is mediolaterally compressed with a nearly flat lateral surface, like that of *Effigia okeeffeae* (Nesbitt, 2007).

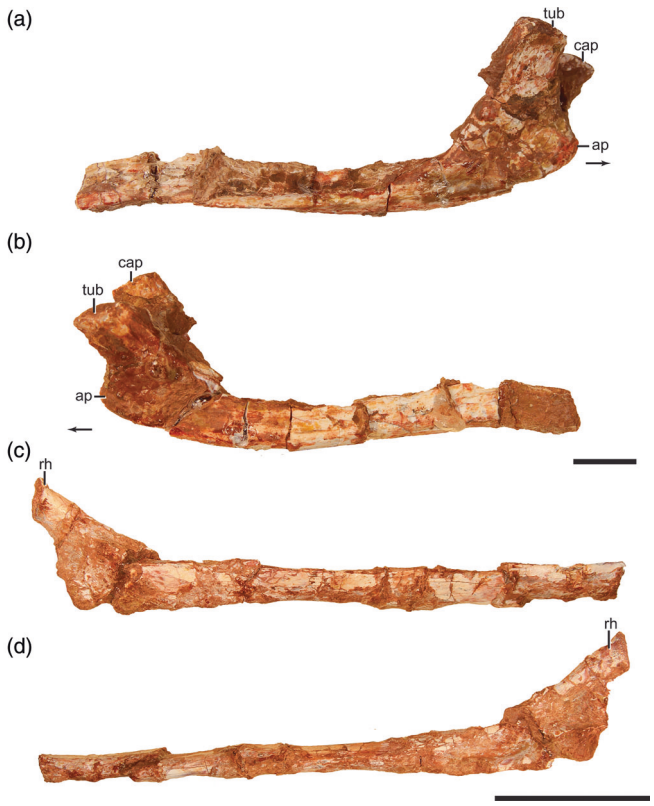

FIGURE 27 Ribs associated with partial skeletons of *Shuvosaurus inexpectatus*. A right cervical rib (TTU-P23903) in lateral (a) and medial (b) views. A trunk rib (TTU-P19577) in two views (c and d). ap, anterior process; cap, capitulum; rh, rib head; tub, tuberculum. Arrows indicate anterior direction. Scale bar equals 1 cm in (a) and (b), and 5 cm in (c) and (d).

3.2 | Pectoral girdle

Scapulocoracoid—The scapulocoracoid is represented as both left and right elements of the most complete postcranial skeleton (TTU-P9001; Figure 28), although most of the thin parts of the anterior portion of the scapula blade and much of the thin portions of the ventral and anterior portions are missing. None of the preserved scapulae or coracoids are complete among the sample of *Shuvosaurus inexpectatus*, but we rely on two right scapulae (TTU-P18424; Figure 29 and TTU-P 18425) to supplement that of TTU-P9001. The scapula-coracoid suture is open (sensu Brochu, 1996) in TTU-P9001, similarly to the reference scapulae (TTU-P18424; Figure 29 and TTU-P 18425) which also show no sign of coossification.

The preserved portions of the scapula of *Shuvosaurus inexpectatus* are nearly identical to that of *Effigia okeeffeae* (AMNH FR 30587) and much anteroposteriorly broader than originally described (Long & Murry, 1995). The scapula of *Shuvosaurus inexpectatus* possesses a broad scapular blade that is expanded anteriorly and dorsally as a similar mediolateral thickness. In lateral view, the proximal (= ventral) has a greater anteroposterior length than that of the more distal portion, giving the scapula blade a trapezoidal shape (Figure 29a,b), a character state that appears only in *Effigia okeeffeae* (AMNH FR 30587) among pseudosuchians. The posterior and, likely the anterior, edges of the scapular blade are straight proximodistally in lateral view and the posterior border is mediolaterally thicker than that of the rest of the scapular blade. The shape of the distal end in lateral view is not known. The proximal end mediolaterally expands to a glenoid region and the posteromedial surface of this region bears a shallow groove also present in *Arizonasaurus babbitti* (MSM P4590), *Poposaurus gracilis* (YPM 57100), and *Effigia okeeffeae* (AMNH FR 30587), although the feature in *Shuvosaurus inexpectatus* appears shallower than the aforementioned taxa. The glenoid faces posteroventrally like that of other paracrocodylomorphs (Nesbitt, 2011) and avian-line archosaurs (Nesbitt et al., 2017) where the glenoid articular surface is nearly hidden in lateral view (Figures 28a,d and 29a,b). The slightly concave surface of the glenoid has a well-defined glenoid rim, and the distolateral edge of the glenoid bears a clear rounded fossa (Figures 28 and 29); this feature is also present in *Effigia okeeffeae* (Nesbitt, 2007). A distinct scar lies on and contacts the distal (= dorsal) surface of the glenoid rim (Figures 28 and 29) like in *Effigia okeeffeae* (AMNH FR 30587). This scar is concave

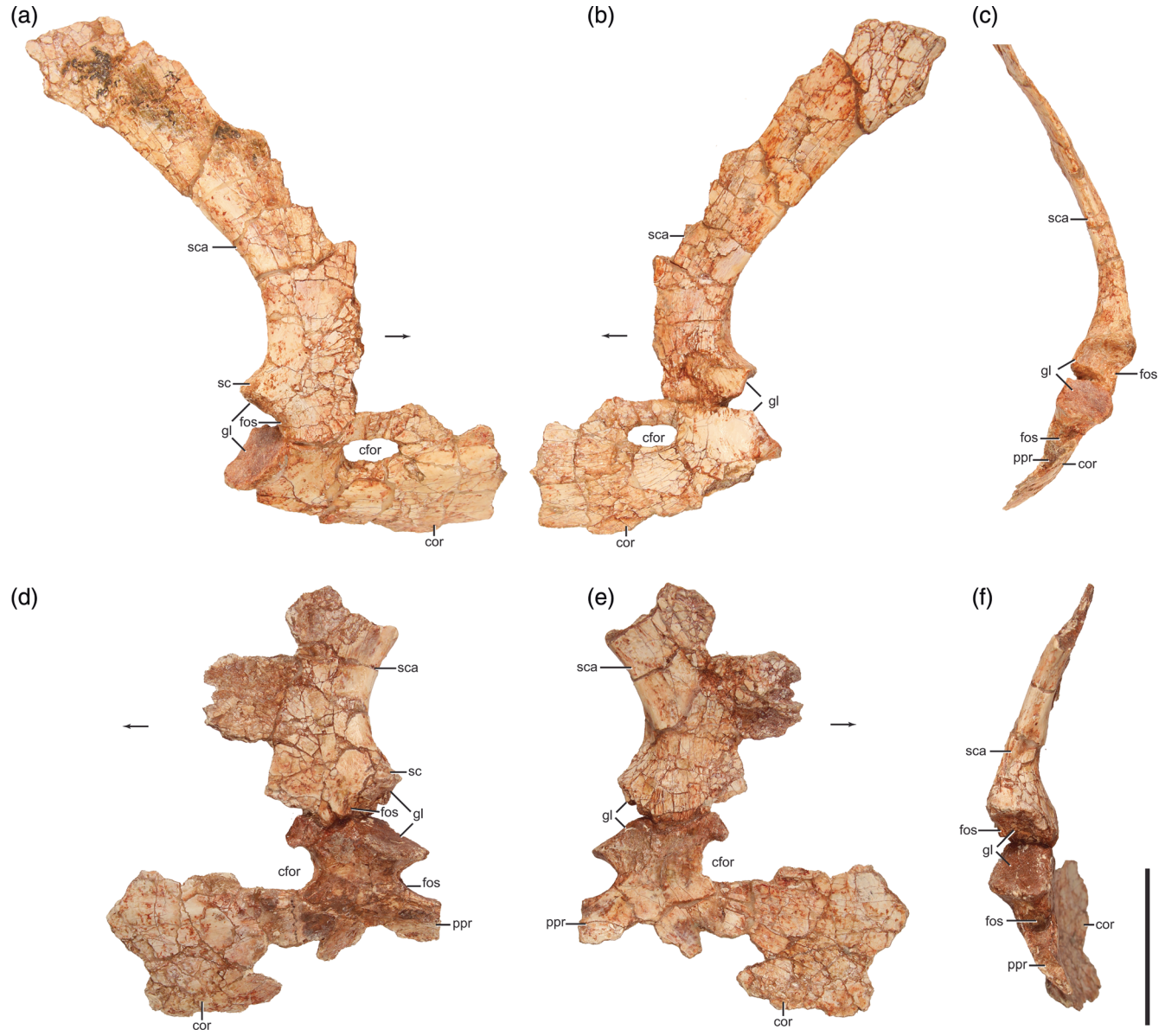

FIGURE 28 Scapulocoracoids of a referred specimen of *Shuvosaurus inexpectatus* (TTU-P9001). Right element in lateral (a), medial (b), and posteroventral (c) views. Left element in lateral (d), medial (e), and posteroventral (f) views. cfor, coracid foramen; cor, coracoid; fos, fossa; gl, glenoid; ppr, posterior process; sc, scar; sca, scapula. Arrows indicate anterior direction. Scale bar equals 5 cm.

with a rugose surface and contrasts with the raised and rugose scars in other poposauroids (e.g., *Poposaurus gracilis*, Schachner et al., 2020) and in some loricatans (e.g., *Batrachotomus kupferzellensis*). Furthermore, the position of the scar is on the rim of the glenoid in shuvosaurids in comparison with the more distally placed scar in other pseudosuchians (e.g., *Poposaurus gracilis*, Schachner et al., 2020, Gower & Schoch, 2009). The rugose articular surface with the coracoid is triangular and thins immediately anterior of the glenoid.

The anteroposteriorly elongate coracoid (Figure 28) is generally rectangular in ventrolateral view, but the anterior and posterior portions of the coracoid are not known in any preserved specimen. The posterodorsally oriented glenoid of the coracoid is slightly larger and expands more posteriorly than its counterpart of the scapula. The glenoid rim also tapers to its posteromedial side. Although broken, the coracoid of *Shuvosaurus inexpectatus* clearly bears an elongated post glenoid process and posteriorly opening fossa just ventral to the glenoid rim like that of *Effigia okeeffeae* (Nesbitt, 2007). As observed by Nesbitt (2007), the coracoid foramen of *Shuvosaurus inexpectatus* is proportionally much larger than that of *Effigia okeeffeae* (AMNH FR 30587), a clear difference in the two taxa. The medial surface of the glenoid region is flat.

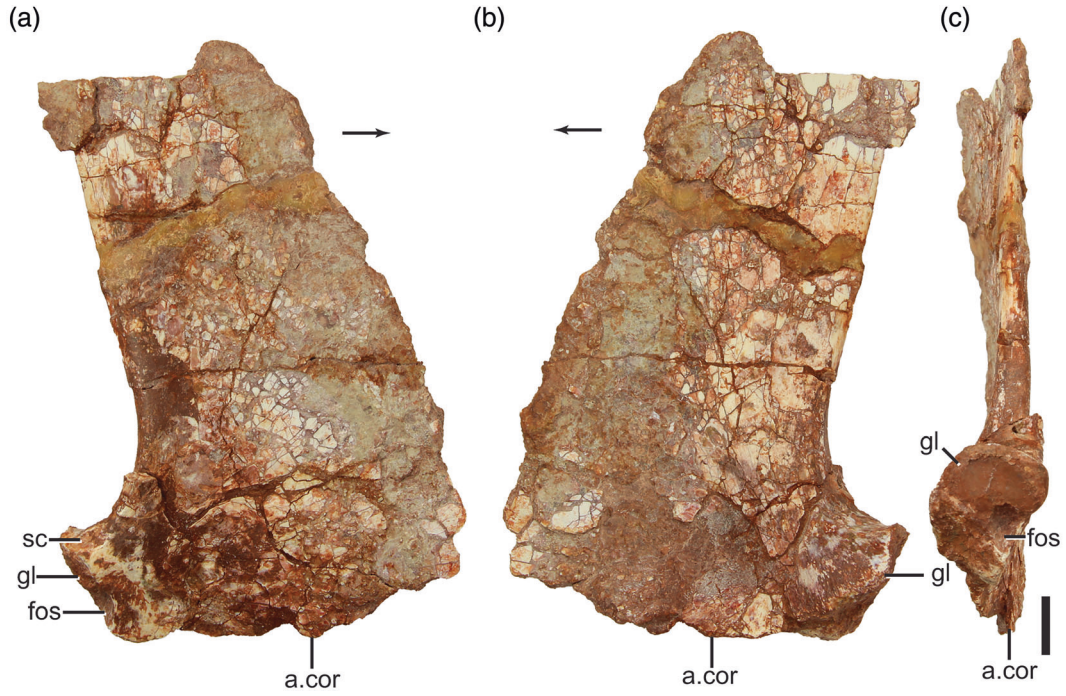

FIGURE 29 Right scapula of a referred specimen of *Shuvosaurus inexpectatus* (TTU-P18424) in lateral (a), medial (b), and posteroventral (c) views. a., articulates with; cor, coracoid; fos, fossa; gl, glenoid; ppr, posterior process; sc, scar. Arrows indicate anterior direction. Scale bar equals 1 cm.

3.3 | Forelimb

Humerus—A left humerus is present in the referred skeleton (TTU-P9001; Figure 30) and there are many complete and isolated humeri from the Post Quarry. Here, we focus the description of TTU-P9001 because of the exquisite preservation and preparation of the element. The overall shape of the humerus is slender with a slightly expanded proximal end and a little expanded distal end connected through a narrow shaft. A similarly narrow shaft is present in *Effigia okeeffeae* (AMNH FR 30587) and comparatively, the humeri of other poposauroids (e.g., *Poposaurus gracilis*, Schachner et al., 2020; *Qianosuchus mixtus*, Li et al., 2006) and loricatans (e.g., *Postosuchus kirkpatricki*, Chatterjee, 1985) have much more expanded proximal ends and wider midshafts than that of shuvosaurids (Nesbitt, 2007). The long humerus is ~66% the length of the femur (Long & Murry, 1995).

The proximal portion of the humerus expands mediolaterally from the shaft where the medial side is more expanded compared to the lateral side; the entire proximal portion is arched medially relative to the proximodistal orientation of the shaft. The humeral head occupies much of the proximal surface as in *Effigia okeeffeae* (AMNH FR 30587). The humeral head expands both proximally and posteriorly as a distinct rounded surface; small grooves occupy the proximal surface. Anteriorly, the humeral head is convex in proximal view and anterolaterally, the humeral head terminates in a broad process. A short medial process (~3–4 mm) lies on the posteromedial surface of the humeral head, and like in *Effigia okeeffeae* (AMNH FR 30587), this medial process is significantly shorter and more anteroposteriorly narrow than in *Poposaurus gracilis* (YPM 57100) and other paracrocodylomorphs (e.g., *Postosuchus kirkpatricki*, TTU-P9002). The concave anterior surface of the proximal end extends distally to the anterior peak of the deltopectoral crest and is constrained between the lateral end and the deltopectoral crest. The posterior side of the proximal end is largely convex with a proximodistally oriented expansion located near the lateral edge (Figure 30). The homology of this expansion is possibly the insertion of m. teres major and latissimus dorsi (Meers, 2003), however, the homologous expansion and pit in *Poposaurus gracilis* (Schachner et al., 2020, fig. 23e) and a ridge or pit in Crocodylia (e.g., *Alligator mississippiensis*; Meers, 2003) is more laterally located. The deltopectoral crest defines the lateral margin and extends anteriorly. The anteriormost expansion or "peak" of the structure occurs ~25 mm distal from the proximal surface and the crest continues distally 45 mm; the crest peak extends 18% and the entire crest extends 32%

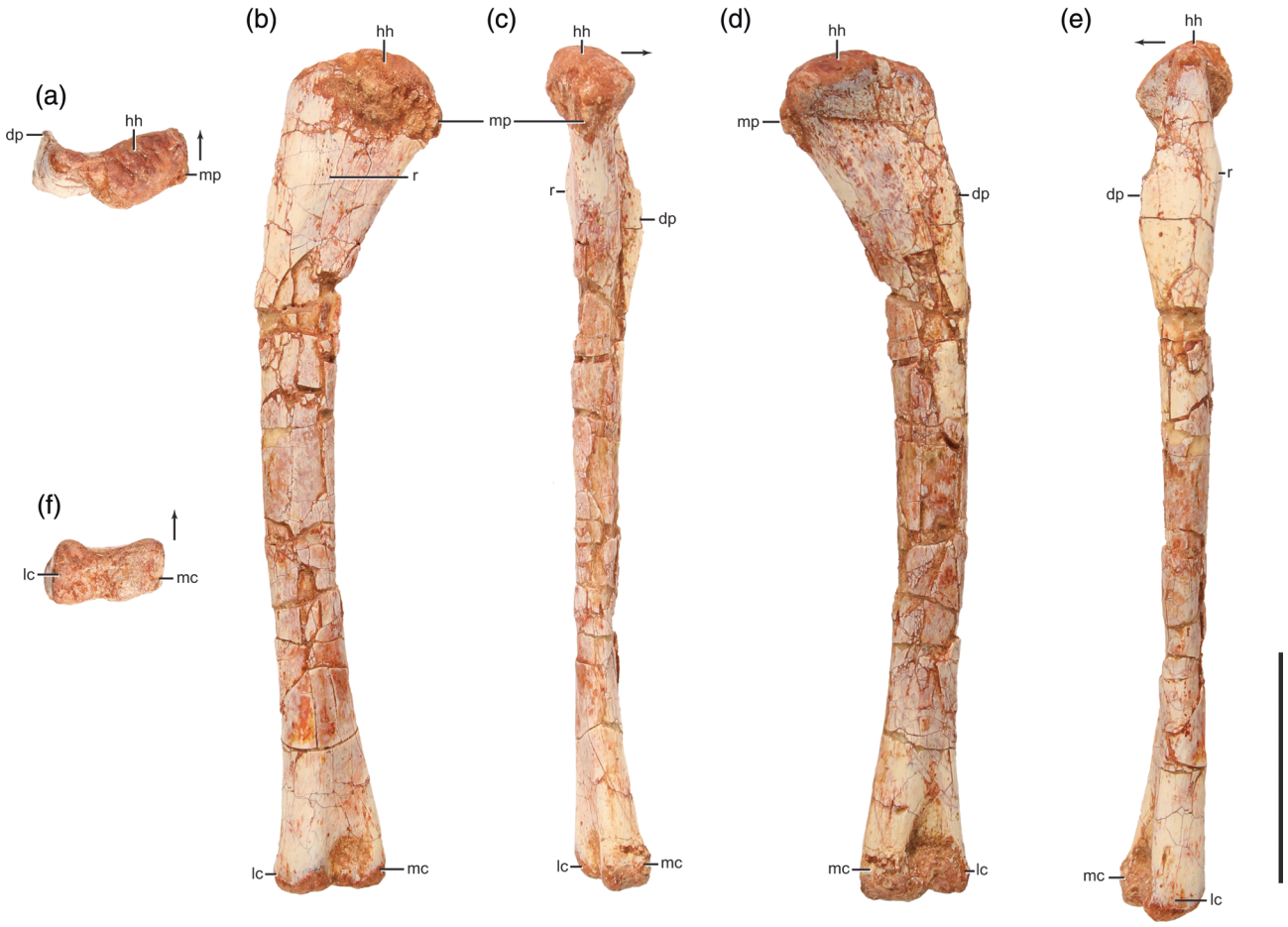

FIGURE 30 Left humerus of an associated referred specimen of *Shuvosaurus inexpectatus* (TTU-P9001) in proximal (a), posterior (b), medial (c), anterior (d), lateral (e), and distal (f) views. dp, deltopectoral crest; hh, humeral head; lc, lateral condyle; mc, medial condyle; mp, medial process; r, ridge. Arrows indicate anterior direction. Scale bars equal 5 cm.

distally the length of the humerus. In lateral view (Figure 30e), the mediolaterally thin crest arches gradually like in *Poposaurus gracilis* (YPM 57100) and lacks the distinct anterior pointed crest in loricatans like *Postosuchus kirkpatricki* (TTU-P9002) and *Hesperosuchus agilis* (AMNH FR 6758).

The midshaft is oval in cross section with a longer mediolateral axis than anteroposterior axis. The distal end only slightly expands relative to midshaft, like in other shuvosaurids (Nesbitt, 2007). Two distal condyles are present, a lateral one (ectepicondyle) and medial one (entepicondyle). Both condyles are about the same size and are separated by an anteroposteriorly oriented gap. The distal gap between the condyles extends onto the posterior side as a circular fossa (Figure 30d) whereas a rim of bone separates the condyles anteriorly from an oval fossa on the anterior surface. An ectepicondylar groove on the lateral side of the humerus of *Poposaurus gracilis* (Schachner et al., 2020) is absent in *Shuvosaurus inexpectatus* and *Effigia okeeffeae* (Nesbitt, 2007) and the medial surface of the distal end is also smooth.

3.4 | Pelvic girdle

Ilium—The ilium is represented by many partial specimens, a partial left ilium from the referred skeleton (TTU-P9001; Figure 31a–e) and a complete right ilium (TTU-P 9003; Figure 31f–i). The well-defined supraacetabular crest (= supraacetabular rim in Nesbitt, 2007) projects ventrolaterally so that in articulation, the femur is braced laterally by the crest. The supraacetabular crest originates on the lateral surface of the pubic peduncle, but it does not contact the articulation surface for the pubis and reaches just dorsal to the ischial peduncle. Small foramina are present on the dorsolateral surface of the crest (Figure 31a). Within the ventrally directed and concave acetabulum, the articulation surface with the femur is rugose; this surface extends laterally of the ischial peduncle to create a distinct surface (= antitrochanter). The pubic and ischial peduncles are well separated by a concave ventral margin indicating that the pubis and ischium did not contact each other similar to that of *Poposaurus gracilis* (Schachner et al., 2020).

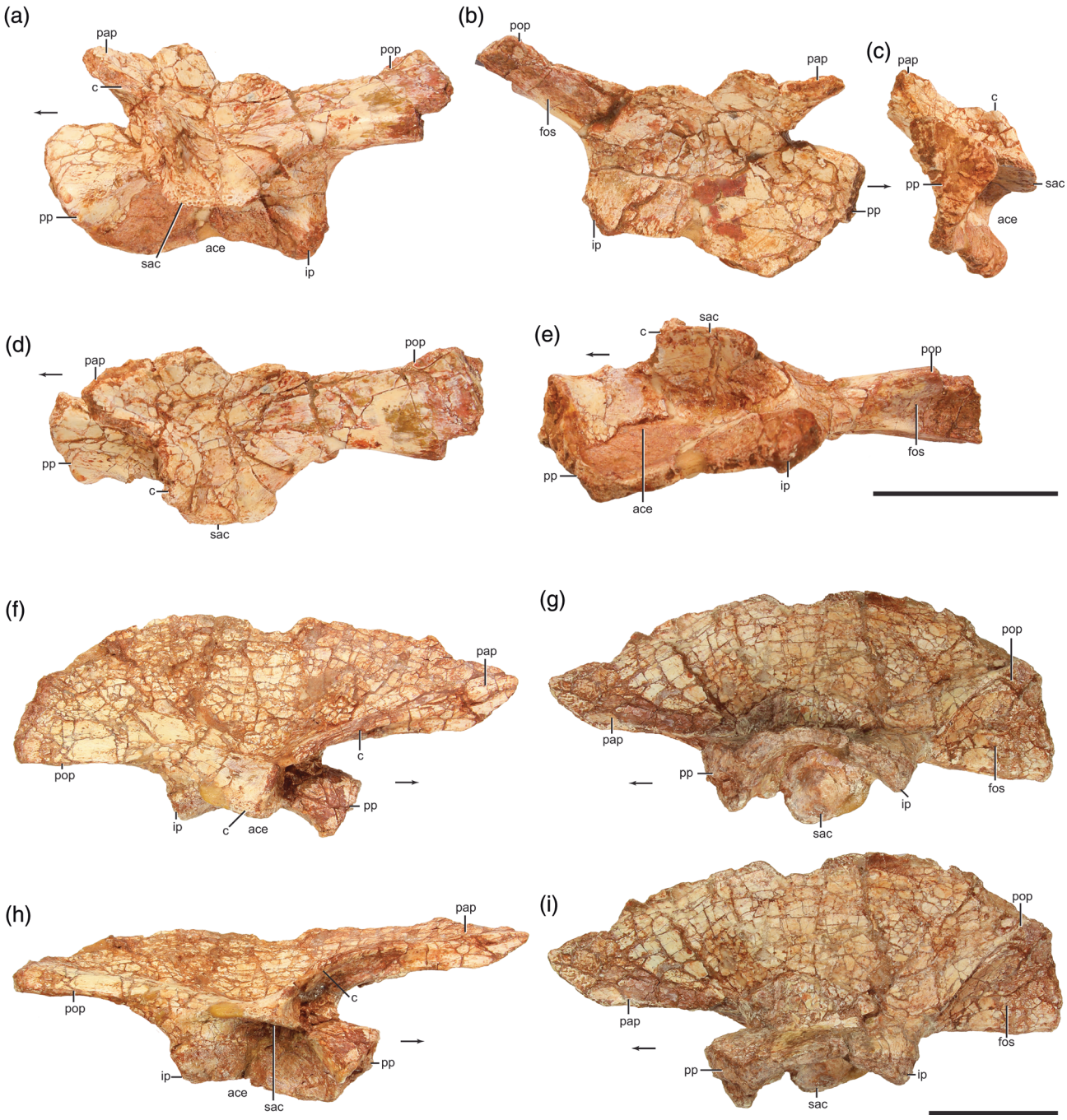

FIGURE 31 Ilia of referred specimens of *Shuvosaurus inexpectatus*. Left ilium (TTU-P9001) in lateral (a), medial (b), anterior (c), dorsal (d), and ventral (e) views. Right ilium (TTU-P9003) in dorsolateral (f), ventromedial (g), ventrolateral (h), and medial (i) views. ace, acetabulum; c, crest; fos, fossa; ip, ischial process/peduncle; pp, pubic process/peduncle; pap, preacetabular process; pop, postacetabular process; sac, supraacetabular crest. Arrows indicate anterior direction. Scale bars equal 5 cm.

Consequently, that acetabulum was perforated (= open) like that of *Poposaurus gracilis* (Schachner et al., 2020), dinosaurs (Langer & Benton, 2006; Nesbitt, 2007), and most crocodylomorphs (Nesbitt, 2011). The medial wall of the acetabulum is much thicker than that of dinosaurs (e.g., Figure 31). The rugose articular surface of the pubic peduncle is triangular and has a small anterior projection in the middle of the surface that corresponds to a depression of the proximal articular surface of the pubis.

The greatly expanded dorsal edge of the ilium dorsal to the supraacetabular crest of *Shuvosaurus inexpectatus* and other shuvosaurids is more similar to that of theropod dinosaurs than that of other pseudosuchians. This dorsal expansion bridges the elongated anterior process

(= preacetabular process) to the posterior process (= postacetabular process) and projects dorsally in a gradual arch creating a dorsal part of the ilium that is three times taller than the acetabulum height. A distinct crest (= supra-acetabular crest of Nesbitt, 2007; referred to a crest in characters 266 and 267 in Nesbitt, 2011) lies on the dorsal surface of the supraacetabular crest (Figure 31a,c,d,f,h) and arcs anteriorly similar to the homologous feature in *Poposaurus gracilis* (Schachner et al., 2020). The laterally expanded crest of *Shuvosaurus inexpectatus* originates on the anterior portion of the supraacetabular crest instead of the anteroposterior middle like *Arizonasaurus babbitti* (MSM P4590) and gently arcs anteriorly and creates a clear pocket framed by the crest and pubic peduncle. The anterior process of the ilium extends well anterior of the pubic peduncle like in *Effigia okeeffeae* (AMNH FR 30587) and *Poposaurus gracilis* (Schachner et al., 2020). The anteroposteriorly thin crest dorsal to the supraacetabular crest of *Shuvosaurus inexpectatus* bears a striated lateral surface that becomes smoother anterodorsally where the crest transitions smoothly into the anterior process. A change in angle (= kink; Figure 31) occurs on the ventral edge of the anterior process near the anterior extent of the feature. The main body of the dorsal expansion is concave laterally between the pre- and postacetabular processes. The posterior process has a laterally defining ridge that weakly contacts the posterior portion of the supraacetabular crest and reaches the posterior extent of the element. The entire posterior process is angled dorsomedially.

Medially, the surface adjacent to the acetabulum is smooth and is separated from the dorsal process by means of a concave region with an anteroposteriorly directed axis. The sacral rib scars are poorly defined in all specimens, except for one scar medial of the posterior end of the ischial peduncle. This lack of scars is in contrast to the close relative *Poposaurus gracilis* (Schachner et al., 2020) and other pseudosuchians with well-defined scars for the attachment of sacral ribs. This ventrally rimmed scar continues posteriorly as a sharp ridge (Figure 31g,i), but is poorly defined dorsally. This posterior ridge defines the anterior and dorsal extent of a slightly concave surface on the posterior process (iliac shelf of Nesbitt, 2007, fig. 32).

Pubis—The pubis is well represented in the referred skeleton (TTU-P9001; Figure 32) and preserved from both the right and left sides, but none of the specimens are complete; the medial portion of the pubic apron is broken in nearly all of the specimens with the exception of TTU-P18927 (Figure 32e). The proximal portion of the pubis is expanded in all directions relative to the pubic shaft. The lateral side of the proximal end bears a shallow depression that may mark the insertion of the ambiens musculature (Schachner et al., 2011) rather than any kind of ridge. A similar depression is also present in the same area in *Arizonasaurus babbitti* (MSM P4590) and *Poposaurus gracilis* (Schachner et al., 2020) in contrast to the much more prominent feature in *Batrachotomus kupferzellensis* (Gower & Schoch, 2009). The proximal articular surface is highly rugose and triangular in outline with prominent points directed dorsally, ventrally, and laterally. The ventral portion of the proximal end bears an extension of the acetabulum. This surface faces posterolaterally and a similar surface is present in *Poposaurus gracilis* (Schachner et al., 2020) but not in *Arizonasaurus babbitti* (MSM P4590). It is clear from the pubis and from the features of the ilium (see above) that the ischium and pubis did not contact each other in *Shuvosaurus inexpectatus*, similar to that of the close relative *Poposaurus gracilis* (Schachner et al., 2020; Weinbaum & Hungerbühler, 2007). An obturator foramen is not present in TTU-P9001 and in any other specimen as originally observed (Long & Murry, 1995). However, given this area is fragile and easily broken and that *Effigia okeeffeae* (Nesbitt, 2007, fig. 41) possesses them like other archosaurs, we cannot confirm the presence or absence of the feature.

The pubic shaft arches anteroventrally, but the exact orientation is not clear because of taphonomic distortion, preparation, and reconstruction. For example, TTU-P9001 was originally reconstructed as much more highly arched (Long & Murry, 1995, fig. 166a) versus the same element after repreparation (Figure 32). Other pubes from the Post Quarry and repreparation of TTU-P9001 indicates that the pubis was more straight than previously reconstructed, similar to that of *Effigia okeeffeae* (AMNH FR 30587). The shaft narrows immediately distal of the proximal end of the pubis and then gradually expands to the distal end. None of the recovered pubes of *Shuvosaurus inexpectatus* possess a complete medial portion of the apron because this part of the bone is thin and fragile, but TTU-P18927 (Figure 32e) preserves the proximal portion. Like other poposauroids (Nesbitt, 2007, 2011), the proximal portion of the midline symphysis is dorsoventrally thicker than the rest of the apron and creates a solid contact between the pubes. The lateral edge of the shaft possesses a sharp crest that parallels the shaft. This crest originates ~33% distal of the proximal end and terminates at the ventral expansion and a similar crest is only present in *Effigia okeeffeae* (AMNH FR 30587) among pseudosuchians.

The distal end of the pubis terminates in a large posterior expansion typically referred to as a "pubic boot" in other archosaurs (Nesbitt et al., 2013). The expansion in *Shuvosaurus inexpectatus* and *Effigia okeeffeae* (AMNH FR 30587) are proportionally larger than any other pseudosuchian, being about 50% the length of the long axis of

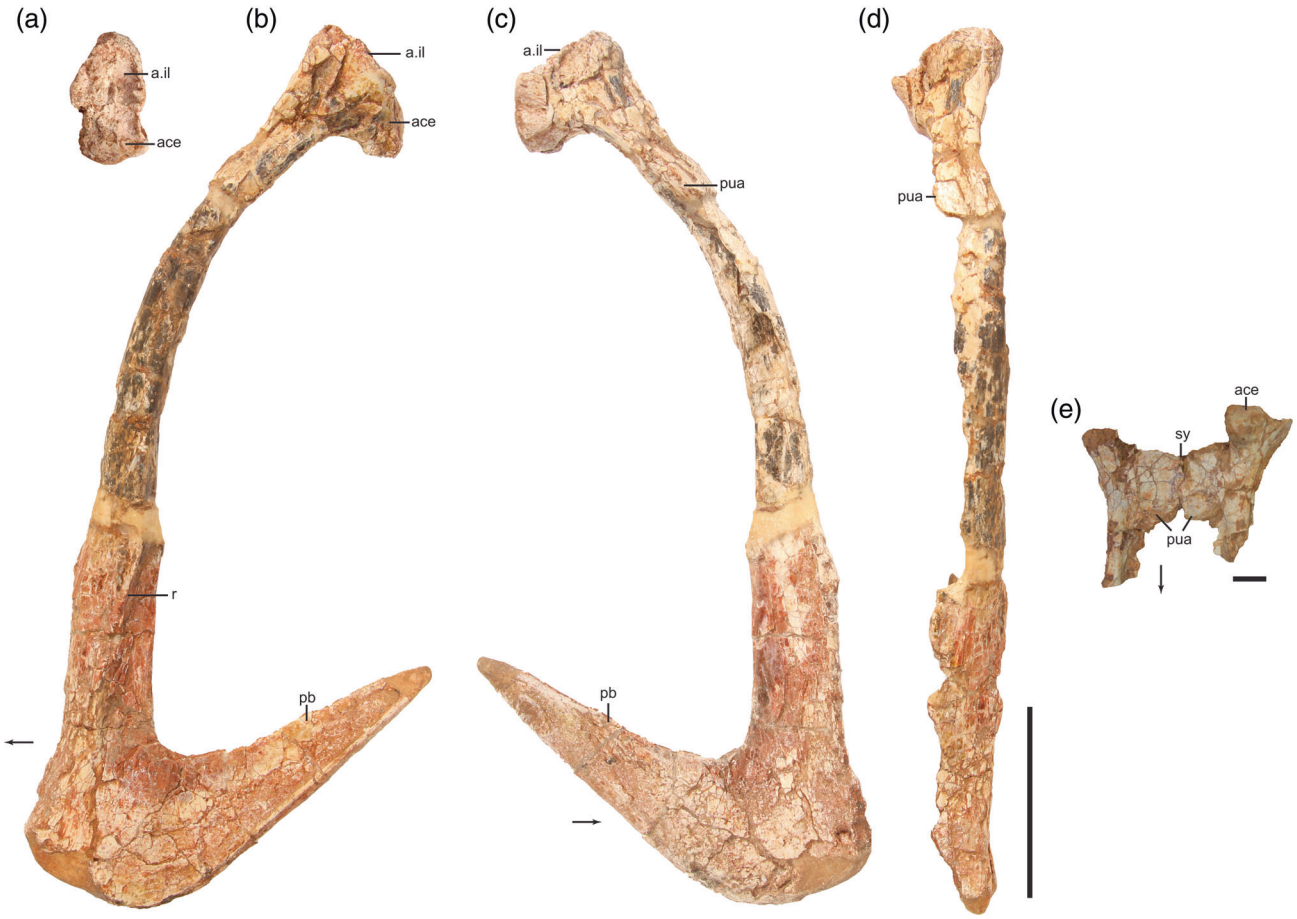

FIGURE 32 Pubis of a referred specimen of *Shuvosaurus inexpectatus* (TTU-P9001) in proximal (a), lateral (b), medial (c), and anterior (d) views. Left and right pubes of a referred specimen of *Shuvosaurus inexpectatus* (TTU-P18927) in ventral (e) view. a., articulates; ace, acetabulum; il, ilium; pb, pubic "boot"/ posterior expansion; pua, pubic apron; sy, symphysis. Arrows indicate anterior direction. Scale bar equals 5 cm in (a)–(d) and 1 cm in (e).

the pubis. The anteroventral portion of the expansion transitions from the pubic apron ventrally to a flat surface. The straight ventral margin possesses a defining ventral rim on the lateral side. Posteriorly, the "boot" tapers and the ventral margins of the structure contact each other along their length, similar to the condition in *Poposaurus gracilis* (Schachner et al., 2020). The orientation of the ventral edge relative to the anteroposterior axis of the body is not clear because of the taphonomic distortion of the pubic shaft, but the posterior tip of the expansion must have been directed posterodorsally rather than just posteriorly.

Ischium—The ischium is represented in the referred skeleton (TTU-P9001; Figure 33) and other well-preserved examples (TTU-P18414; Figure 34). TTU-P9001 is missing part of the shaft so the length of the element is reconstructed (Figure 33). In all cases, the left and right ischia are coossified at the midline along their length, like in *Effigia okeeffeae* (Nesbitt, 2007), *Poposaurus gracilis* (Schachner et al., 2020), and *Arizonasaurus babbitti* (Nesbitt, 2005b). A subtle division at the midline is present throughout the element and its depth is variable across the sample from the Post Quarry. The proximal portion consists of the laterally directed facet for articulation with the ilium and a more ventral acetabular rim. The rugose articulation surface with the ilium has a slightly concave surface, but not nearly as deep as that of *Poposaurus gracilis* (Weinbaum & Hungerbühler, 2007). The acetabular region has a sharp defining rim that weakens anteriorly. A slight concave gap, observable in ventral view, separates the anterior portions of the ischia.

The shafts of the ischia are generally D-shaped in cross section throughout their length where the flat portion represents the midline (Figure 34e). The ventral portion of the shaft bears a thin lamina at the midline in the proximal third of the element that disappears distally, identical to the condition of *Effigia okeeffeae* (Nesbitt, 2007). Distal to the thin lamina, a groove defines the midline to nearly the distal end. Dorsally, the shaft bears a "raised area" (sensu Nesbitt, 2007) that is also

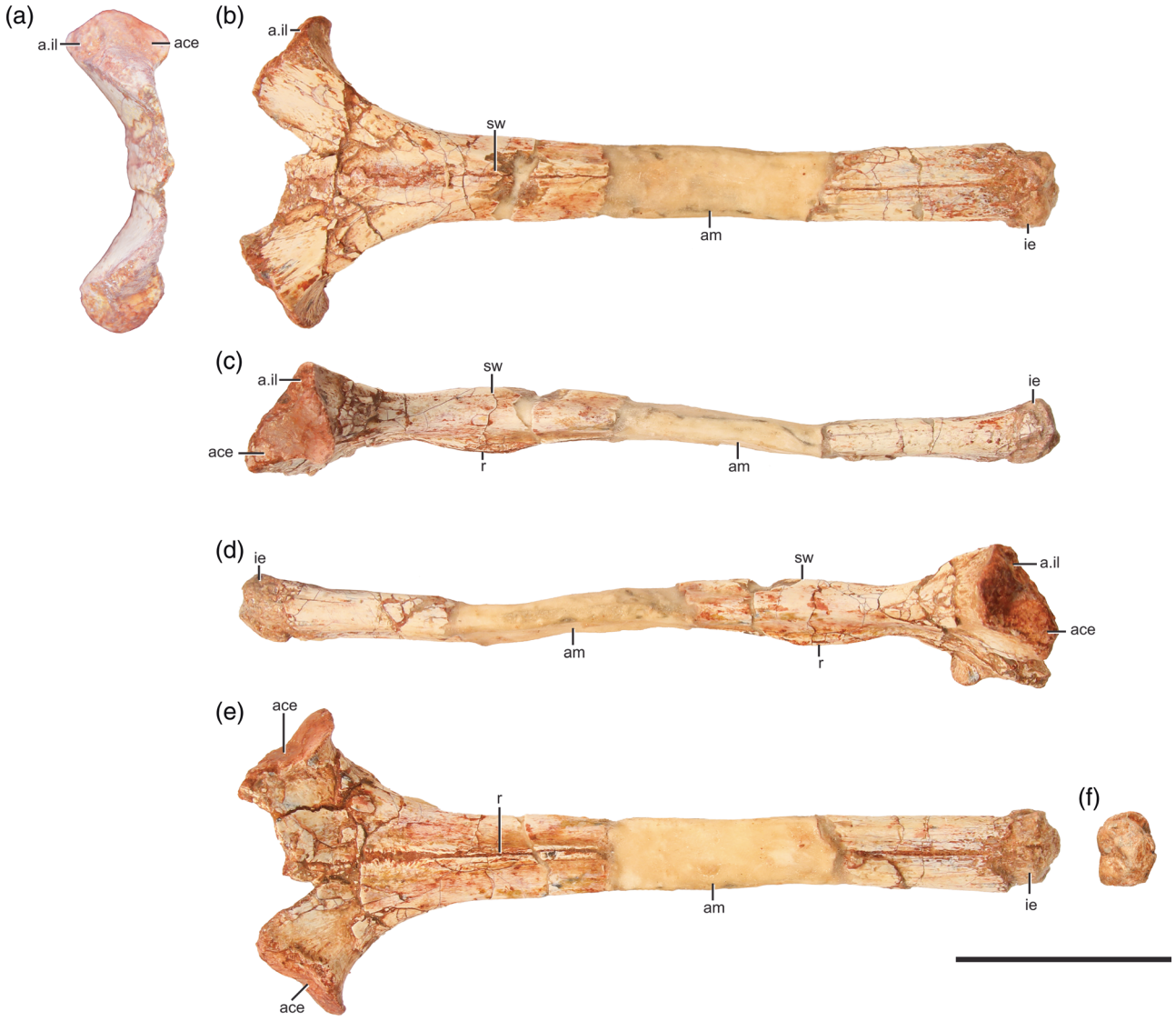

FIGURE 33 Ischia of a referred specimen of *Shuvosaurus inexpectatus* (TTU-P9001) in proximal (a), dorsal (b), left lateral (c), right lateral (d), ventral (e), and distal (f) views. a., articulates with; ace, acetabulum; am, added material; ie, ischium expansion; il, ilium; r, ridge; sw, swelling. Arrows indicate anterior direction. Scale bar equals 5 cm. Photograph in A by Bill Mueller.

present in *Effigia okeeffeae* (AMNH FR 30587) and *Silosuchus longicervix* (PVSJ 85). This dorsally expanded area integrates into the rest of the shaft and completely disappears by midshaft moving posteriorly. A slight groove also marks the midline on the dorsal surface in the distal half of the element. Distally, the ischium is slightly expanded dorsally and to a lesser extent ventrally, but not anywhere to the same degree as *Poposaurus gracilis* (Schachner et al., 2020) or *Arizonasaurus babbitti* (Nesbitt, 2005b). In lateral view, the distal end is rounded and in distal view the ischia are taller than wide with a small groove defining the midline. The size of the distal expansion is variable across the *Shuvosaurus* sample from the Post Quarry, ranging within ~15% of each other.

3.5 | Hindlimb

Femur—The femur is represented by many examples from the Post Quarry, but here we focus the description on a left example from the referred partial skeleton (TTU-P9001; Figure 35) and a newly prepared right femur (TTU 18309; Figure 36). The distinct proximal head hooks medially over the shaft, a character state in shuvosaurids more similar to that of dinosaurs than to other pseudosuchians. The femoral head bears two tubera on the posteromedial side, an anteromedial tuber and posterolateral tuber but none on the anterolateral side, like that of *Effigia okeeffeae* (Nesbitt, 2007). The anteromedial tuber is the most expanded from the shaft

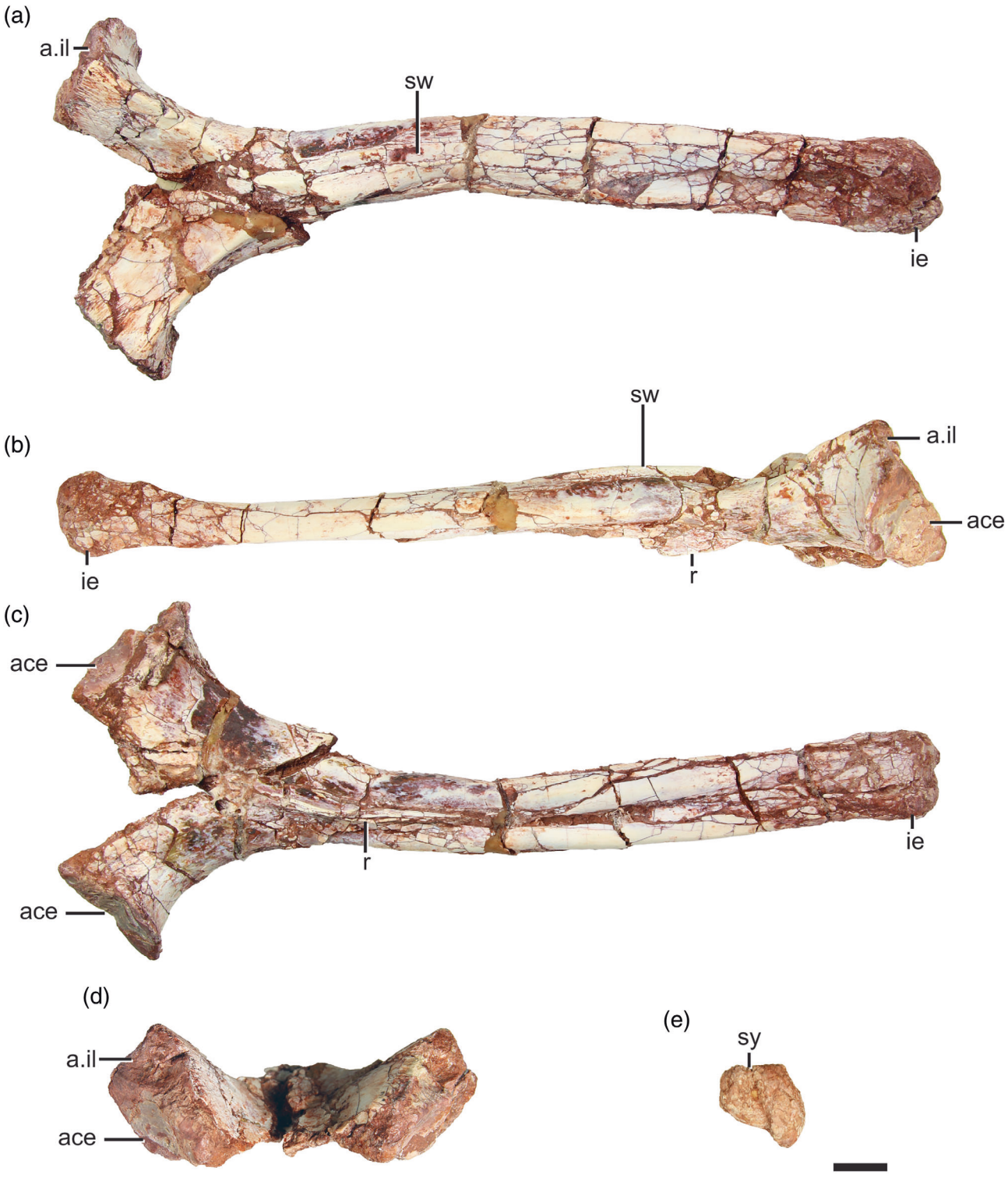

FIGURE 34 Ischia of a referred specimen of *Shuvosaurus inexpectatus* (TTU-P18414) in dorsal (a), right lateral (b), ventral (c), proximal (d), and distal (e) views. a., articulates with; ace, acetabulum; ie, ischium expansion; il, ilium; r, ridge; sw, swelling. Arrows indicate anterior direction. Scale bar equals 1 cm.

relative to the others and forms much of the medial "head" of the femur. The position of the anteromedial tuber is more medial than that of *Effigia okeeffeae* (AMNH FR 30588) and the posterolateral side of the tuber is not as clearly hooked in *Shuvosaurus inexpectatus* compared to that of *Effigia okeeffeae*; the hooked portion may be the result of complete preservation in *Effigia okeeffeae*. The distal "corner" on the mediodistal portion

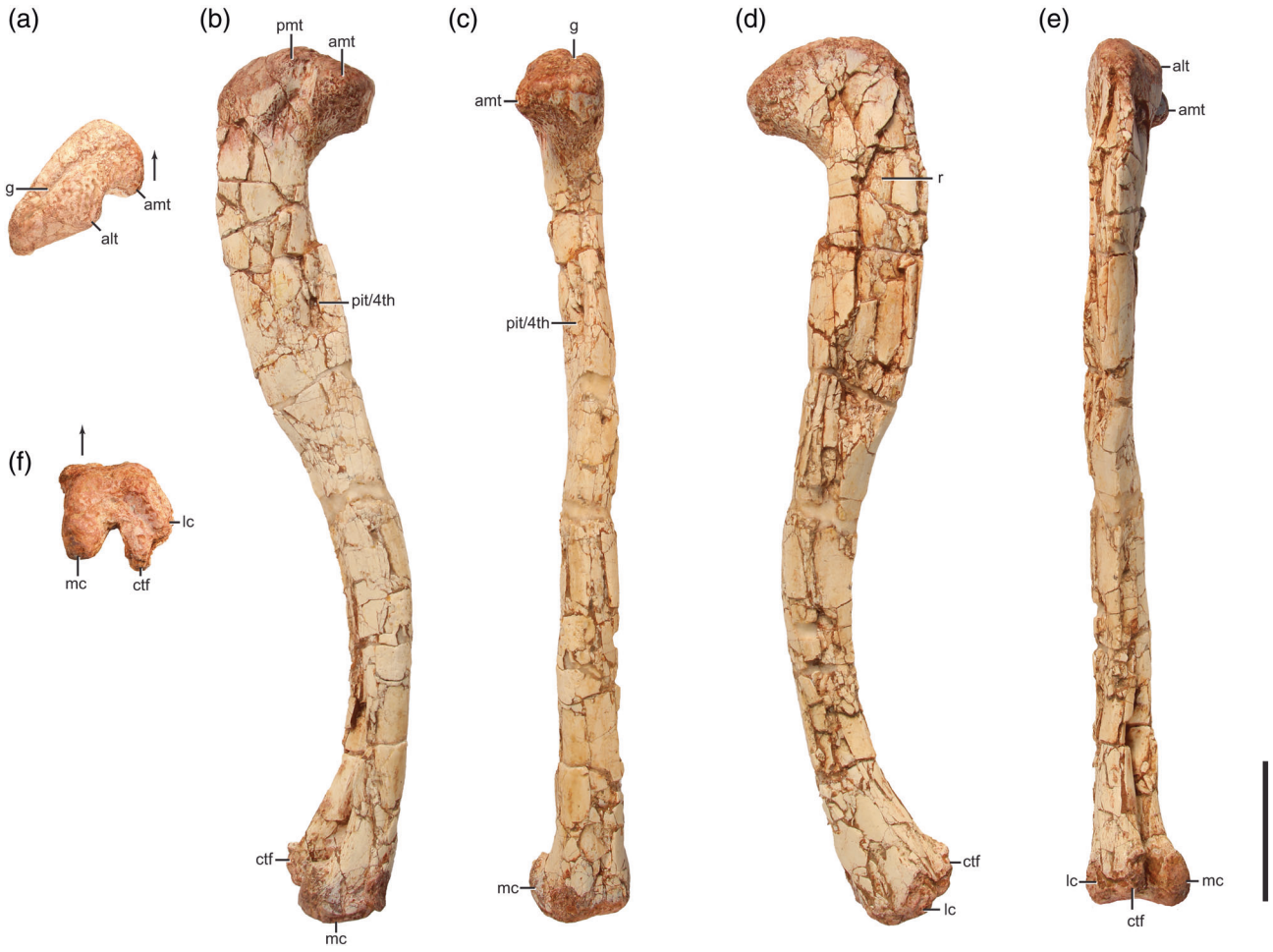

FIGURE 35 The left femur of a referred specimen of *Shuvosaurus inexpectatus* (TTU-P9001) in proximal (a), posteromedial (b), anteromedial (c), anterolateral (d), posterolateral (e), and distal (f) views. amt, anteromedial tuber; alt, anterolateral tuber; ctf, crista tibiofibularis; g, groove; lc, lateral condyle; mc, medial condyle; pit/4th, fourth trochanter/insertion of the caudifemoralis musculature; r, ridge. Arrows indicate anterior direction. Scale bar equals 5 cm.

of the anteromedial tuber is not as sharp in *Shuvosaurus inexpectatus* as *Effigia okeeffeae*, but this could also be the result of the lack of perfect preservation of this region in the femora of *Shuvosaurus inexpectatus*. A wide proximodistally oriented depression separates the anteromedial and posteromedial tubera. The posteromedial tuber has a distolaterally oriented ridge on it and the bone surface distal to this ridge is porous. The proximal surface arcs from the medial to the lateral portion with the most proximally expanded region in mediolateral center (Figure 35a). A straight and narrow groove is present on the rugose proximal surface but does not reach the medial or lateral edge (Figure 35a). The proximal surface extends distally on the posterolateral edge like that of *Effigia okeeffeae* and dinosauriforms (Nesbitt, 2007). Distal to the posteromedial tuber, *Shuvosaurus inexpectatus* lacks the prominent proximodistally oriented ridge present in *Effigia okeeffeae* (AMNH FR 30588). Anteriorly, the proximal portion of the femur is nearly flat. Medially on the anterior surface, there is a rounded and arched ridge that connects the "head" to the rest of the shaft (Figures 35 and 36). More distally, there is a proximodistally oriented ridge that is only visible in carefully cleaned surfaces (Figure 35d). A scarred surface is also present in *Effigia okeeffeae* (AMNH FR 30588) and some other pseudosuchians like crocodylomorphs (e.g., *Hesperosuchus agilis*, AMNH FR 6758).

The shafts of all of the *Shuvosaurus inexpectatus* femora are compressed and distorted depending on their orientation within the Post Quarry (i.e., crushed in different anatomical planes). Like other shuvosaurids and the Moenkopi poposauroid (Nesbitt, 2005a; Schoch et al., 2010), the attachment for the caudifemoralis musculature occurs only in a fossa and there is no attachment ridge (= 4th trochanter). The depression, located ~25% distal from the proximal surface, bears internal striations and opens medially. Furthermore, the shaft expands anteromedially in profile to accommodate the deep fossa (Figures 35 and 36). A ridge defines the lateral edge of

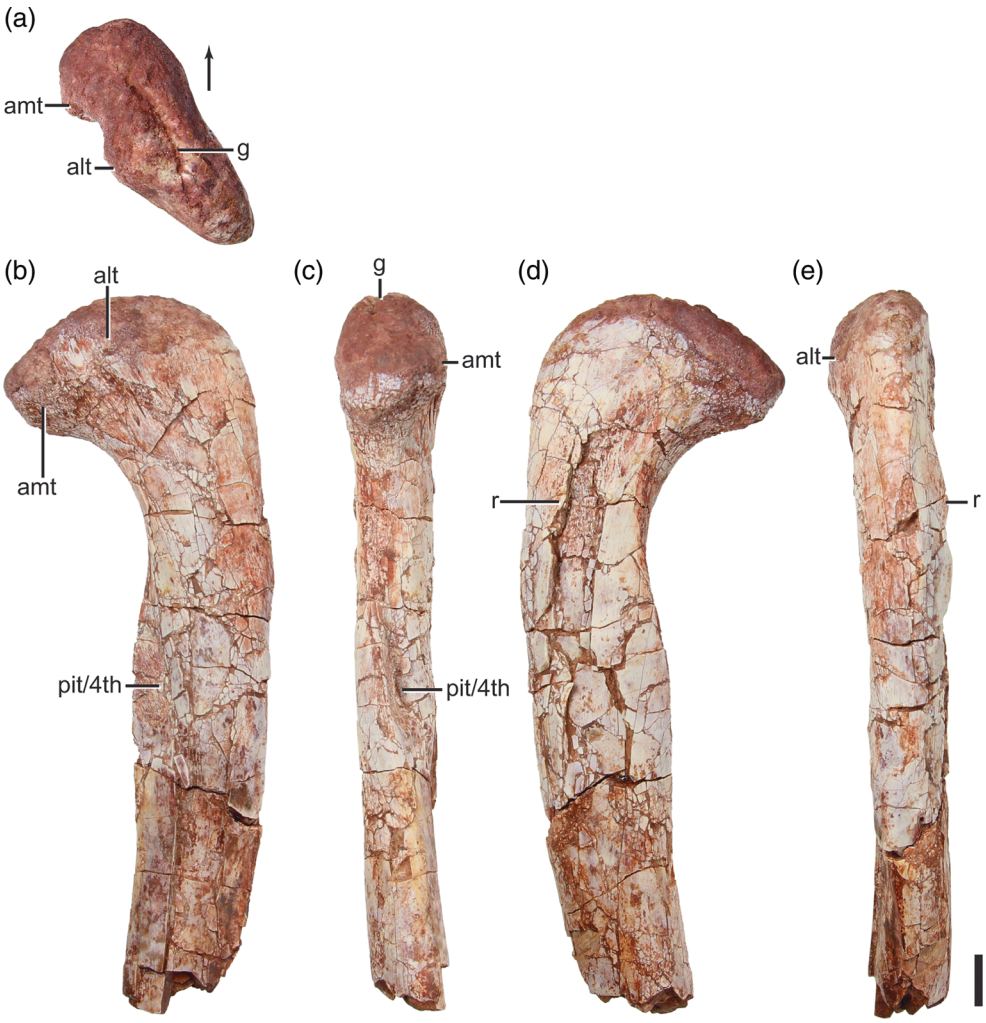

FIGURE 36 The right partial femur of a referred specimen of *Shuvosaurus inexpectatus* (TTU-P18309) in proximal (a), posteromedial (b), anteromedial (c), anterolateral (d), and posterolateral (e) views. amt, anteromedial tuber; alt, anterolateral tuber; g, groove; pit/4th, fourth trochanter/insertion of the caudifemoralis musculature; r, ridge. Arrows indicate anterior direction. Scale bars equal 1 cm.

the shaft starting ~50% distal from the proximal surface and extending to the distal end, similar to that in *Effigia okeeffeae* (AMNH FR 30587).

The distal end of the femur is known from many examples, but many are compressed in different anatomical planes (e.g., TTU-P9001; Figure 35). The distal end expands into a medial (tibial) condyle, a crista tibiofibularis posteriorly and a lateral (fibular) condyle (Figure 35f). The medial side of the medial condyle and the lateral side of the lateral condyle are smooth. The proximal portion of the posterior expansion of the medial terminates in a slight hook. The crista tibiofibularis expands posteriorly beyond the other condyles like in other poposauroids (e.g., *Poposaurus gracilis*, YPM 57100; *Effigia okeeffeae* AMNH FR 30587) and projects slightly posteriorly at its tip. The lateral condyle is the smallest of the three and in distal view, forms a near right angle with the lateral side of the crista tibiofibularis. The anterior surface of the distal end is gently convex. In distal view, a shallow but defined groove separates the lateral condyle and the crista tibiofibularis, as in other poposauroids and in some other archosaurs (Nesbitt, 2007, 2011).

Tibia—The tibia is best represented from the referred skeleton (TTU-P9001) from both tibiae (Figure 37). The tibia is shorter than the femur (86%; Long & Murry, 1995). The proximal end bears a posterior and lateral expansion and a short anteriorly direct cnemial crest similar to other suchians (e.g., *Poposaurus gracilis*, YPM 57100; *Postosuchus kirkpatricki*, TTU-P9000; *Riojasuchus tenuisceps*, PVL 3827; Von Baczko et al., 2019). The proximal surface of the lateral condyle is depressed like that of other suchians (Nesbitt, 2011). A proximodistally oriented ridge is present just distal to the lateral condyle on the lateral surface; the same feature is more prominent in *Effigia okeeffeae* (Nesbitt, 2007). The midshaft is circular in cross section and there is a proximally opening foramen on the anterior portion of the lateral surface.

The distal end slightly expands relative to midshaft and bears a complex articulation surface with the astragalus. The posterior portion extends distally whereas the medial surface expands proximally to accept the proximally expanded process of the astragalus. A slight groove

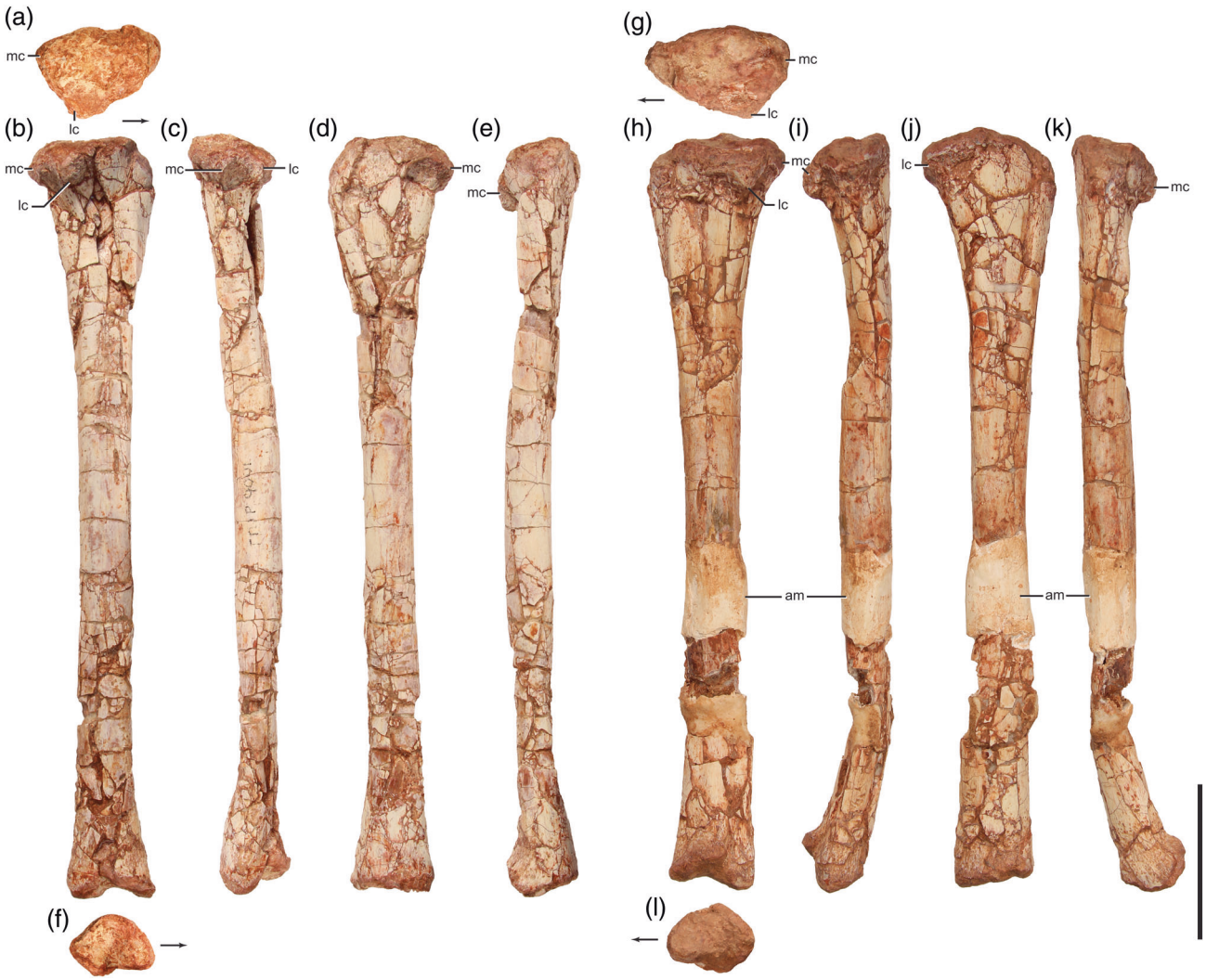

FIGURE 37 The tibiae of an associated referred specimen of *Shuvosaurus inexpectatus* (TTU-P9001). Right tibia in proximal (a), lateral (b), posterior (c), medial (d), anterior (e), and distal (f) views. Left tibia in proximal (g), lateral (h), posterior (i), medial (j), anterior (k), and distal (l) views. am, added material; lc, lateral condyle; mc, medial condyle. Arrows indicate anterior direction. Scale bar equals 5 cm.

on the lateral surface separates the posterior and lateral articulation surfaces. In distal view, the shape is subcircular whereas in *Poposaurus gracilis* (YPM 57100) the same view is L-shaped with a more laterally expanded process. The anterior, medial, and posterior side lack any rugosity or crests, unlike the condition in *Poposaurus gracilis* where there is a clear proximodistally oriented crest on the posteromedial portion of the distal end (Schachner et al., 2020).

Fibula—The fibula is represented by many examples from the Post Quarry; here we focus on the well-preserved right element from the referred skeleton (TTU-P9001; Figure 38). The expanded proximal end is highly asymmetrical in lateral view; the anterior edge is nearly straight whereas the posterior edge gradually expands from midshaft to terminate in a rounded point. In proximal view, the proximal surface is mediolaterally compressed and comma shaped with an anteromedial pointed end and a rounded posterior end. This compressed shape is also present in *Effigia okeeffeae* (AMNH FR 30587), *Poposaurus gracilis* (Schachner et al., 2020) and avemetatarsalians (e.g., the dinosauriform *Asilisaurus kongwe*; Nesbitt et al., 2019), but differs from the more rounded proximal portion of suchians (e.g., *Batrachotomus kupferzellensis*, Gower & Schoch, 2009; *Mandasuchus tanyauchen*, Butler et al., 2018). The lateral surface of the proximal end of the fibula of *Shuvosaurus inexpectatus* is convex anteroposteriorly whereas the medial surface is concave anteroposteriorly. In medial view, the posterior portion of the proximal portion has a distally elongated depression whereas the more anterior portion is flat (Figure 38). The proximalmost portion of the iliofibularis crest originates on the anterior edge ~25 mm from the proximal surface and in lateral view, the anterior edge bows anteriorly here. The

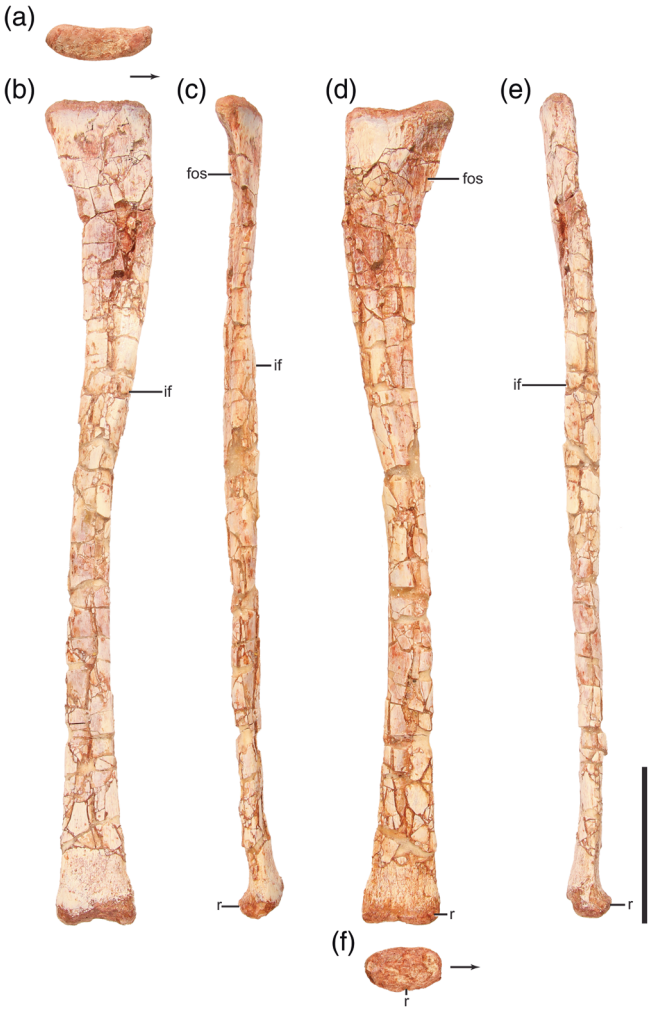

FIGURE 38 Right fibula of an associated referred specimen of *Shuvosaurus inexpectatus* (TTU-P9001) in proximal (a), lateral (b), posterior (c), medial (d), anterior (e), and distal (f) views. fos, fossa; if, iliofibularis crest; r, ridge. Arrows indicate anterior direction. Scale bar equals 5 cm.

low iliofibularis crest wraps onto the lateral side and continues posterodistally until about midshaft. The bone at midshaft is oval in cross section with a longer anteroposterior axis than mediolateral axis.

The distal end expands anteriorly and posteriorly relative to the midshaft but only expands just less than the maximum width of midshaft. In lateral view, the distal end is nearly symmetrical whereas in the poposauroid *Poposaurus gracilis* (YPM 57100) and loricatan *Batrachotomus kupferzellensis* (SMNS 80277), the distal end is asymmetrical with a more distally expanded posterior edge relative to the anterior end. The distal surface of the fibula of *Shuvosaurus inexpectatus* is concave in lateral view. The medial edge of the distal end possesses a medially expanded rim that is also present in *Effigia okeeffeae* (AMNH FR 30587), which seems to be unique among paracrocodylomorphs.

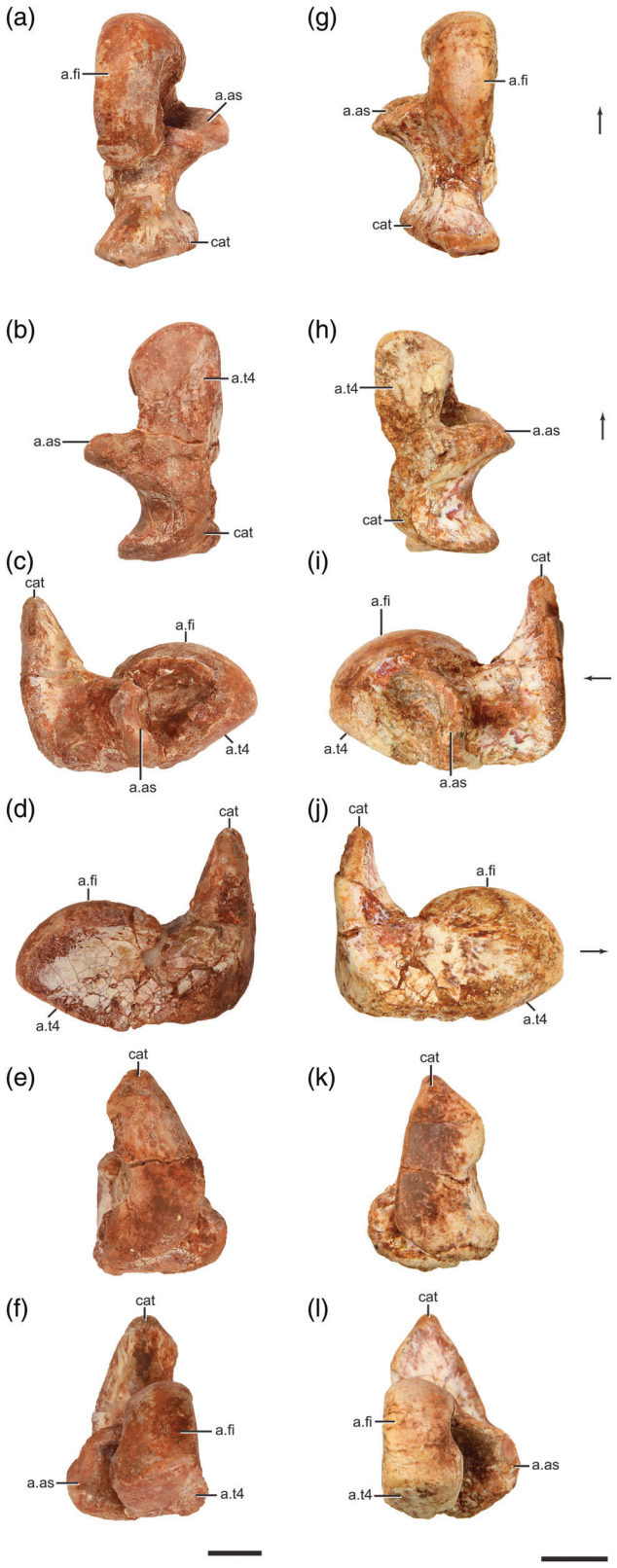

FIGURE 39 Calcanea of *Shuvosaurus inexpectatus*. Left calcaneum (TTU-P9001) (a–f) and right calcaneum (TTU-P18322) (g–l) in proximal (a, g), distal (b, h), medial (c, i), lateral (d, j), posterior (e, k), and anterior (f, l) views. a., articulates with; as, astragalus; cat, calcaneum tuber; fi, fibula; t4, distal tarsal four; ti, tibia. Arrows indicate anterior direction. Scale bars equal 1 cm.

Calcaneum—The calcaneum is represented by numerous examples, but we focus on exquisite examples from the referred skeleton (TTU-P9001, Figure 39a–f), and two other examples (TTU-P18322; Figure 39g–l; TTU-P18384). The main body of the calcaneum is mediolaterally compressed like that of *Poposaurus gracilis* (Schachner et al., 2020; YPM 57100) and this shape is in contrast to the much more mediolaterally wide calcanea of early diverging poposauroids (*Qianosuchus mixtus*, Li et al., 2006), other pseudosuchians (*Nundasuchus songeaensis* NMT RB48), early diverging loricatans (e.g., *Prestosuchus*), aetosauriforms (*Revueltosaurus callenderi*, PEFO 34561), and early diverging crocodylomorphs (NCSM 21722). The articular facet with the fibula is distinctly concave anteroposteriorly in lateral view and slightly concave in mediolateral view. This mediolaterally restricted articular surface is continuous and not divided as in *Effigia okeeffeae* (Nesbitt, 2007) or other pseudosuchians (*Revueltosaurus callenderi*, PEFO 34561). Anteriorly, the fibular facet meets the articular surface with a distal tarsal four at an obtuse angle ~120°. Posteriorly, the facet tapers and meets the rest of the calcaneum at a small lip. The pit for articulation with the astragular peg excavates the medial surface of the fibular facet, like in other suchians (*Postosuchus kirkpatricki*, TTU-P9000; *Poposaurus gracilis*, Schachner et al., 2020). The lateral surface between the facets with the fibula and distal tarsal four is slightly concave and made of compact bone.

The medial portion of the calcaneum protrudes as a tongue that fits the astragular peg (Figure 39). The rim of the process is thin dorsally and medially, but thickens distally. Within the articular surface with the astragular peg, the surface is convex anteriorly; this surface matches the concave surface found on the posterior and distal surface of the astragular peg of the astragalus. The lateral extent of the articular surface with the astragular peg excavates the medial side of the region just ventral to the fibular facet (Figure 39c,i); this fossa is oval in all examples. The distolateral portion of the articular surface with the astragular peg is expanded into a small platform in all examples of *Shuvosaurus inexpectatus* (Figure 38) and in *Effigia okeeffeae* (AMNH FR 30587), but absent in other pseudosuchians.

The prominent calcaneum tuber of *Shuvosaurus inexpectatus* (Figure 38) is distinct among pseudosuchians (unknown in *Effigia okeeffeae*). The shaft of the tuber is taller than wide whereas most other pseudosuchians have similar height: width ratios (e.g., *Poposaurus gracilis*, YPM 57100; *Nundasuchus songeaensis*, NMT RB48; *Postosuchus kirkpatricki*, TTU-P9000; early diverging crocodylomorphs, NCSM 21722) or are much wider than tall (*Revueltosaurus callenderi*, PEFO 34561; early diverging loricatans). Ventrally, the shaft of the calcaneum tuber of *Shuvosaurus inexpectatus* is completely connected to the rest of the body like in *Poposaurus gracilis* (YPM 57100), rather than separated by a clear concave region prominent in other pseudosuchians (*Revueltosaurus callenderi*, PEFO 34561; *Nundasuchus songeaensis*, NMT RB48). All of the calcanea of *Shuvosaurus inexpectatus* are slightly damaged in this area, but none show an area of finished bone (compacta) like the pseudosuchians mentioned above. The calcaneum tuber expands proximally but not distally; this morphology is in contrast to the tubera that expand proximally and distally in many pseudosuchians like *Postosuchus kirkpatricki* (TTU-P9000), *Poposaurus gracilis* (YPM 57100), and early diverging Crocodylomorpha (e.g., NCSM 21722). Starting distally and moving proximally, the posterior surface of the tuber expands anterolaterally, the surface tapers medially, then tapers proximally to an acute point. The flat posterior surface lacks the proximodistally oriented groove found in *Postosuchus kirkpatricki* (TTU-P9000), *Poposaurus gracilis* (YPM 57100), and early diverging crocodylomorphs (NCSM 21722). The proximal expansion of the tuber extends well proximal of the fibular facet and the proximal extent of the tuber is posteriorly expanded with a rugose surface (Figure 38c,i). The slight lateral expansion of the distal surface of the posterior surface is similar to a much more prominent feature in *Nundasuchus songeaensis* (NMT RB48) and *Revueltosaurus callenderi* (PEFO 34561), but absent in the close relative *Poposaurus gracilis* (YPM 57100).

Astragalus—Like calcanea, numerous astragali are represented in the sample of *Shuvosaurus inexpectatus* from the Post Quarry (see referred specimen list above); this description relies on the left element from the referred skeleton (TTU-P9001; Figure 40a–f) and another well-preserved right element (TTU-P18304; Figure 40g–l). The distinct astragalus bears a number of exaggerated projections and well defined articular surfaces synapomorphic of *Shuvosaurus inexpectatus* and *Effigia okeeffeae* among pseudosuchians (Nesbitt, 2007). The articular surface with the tibia occupies most of the proximal surface and stretches from the fibular facet to the medial extent of the element. This tibial facet has two surfaces divided by a convex and low ridge. The more medial surface is deeper and lacks the area of non-articular surface of some pseudosuchians (e.g., *Revueltosaurus callenderi*, *Poposaurus gracilis*, Crocodylomorpha) (Nesbitt, 2011). A rounded rim defines the edges of the medial portion of the tibial facet. The more lateral surface slopes proximally on the posterior side to reach the posterior edge of the articular surface. The division of the lateral and medial sides is common in pseudosuchians (Nesbitt, 2011), but the condition in shuvosaurids appears more exaggerated than other members of the larger clade. The proximal articulation with the fibula (= fibula facet) stretches from the anterior to the

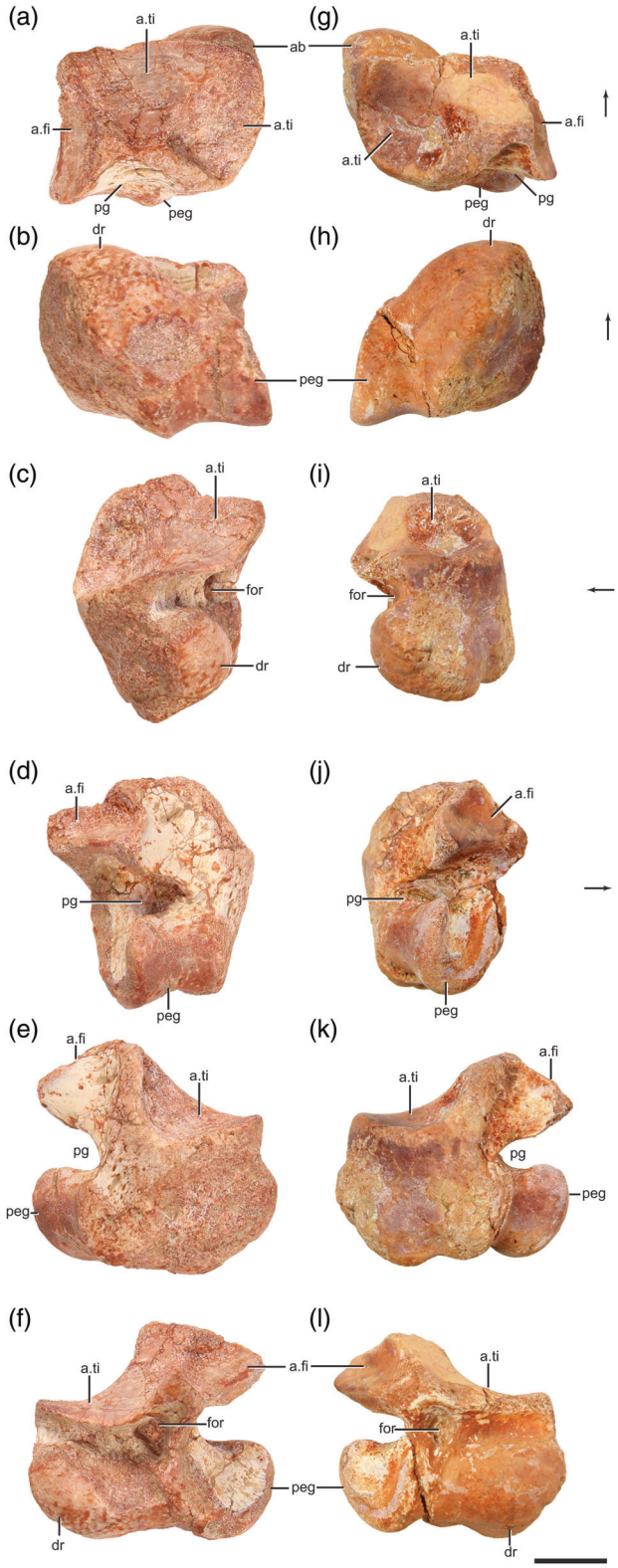

FIGURE 40 Astragali of *Shuvosaurus inexpectatus*. Left astragalus (TTU-P9001) (a–f) and right astragalus (TTU-P18304) (g–l) in proximal (a, g), distal (b, h), medial (c, i), lateral (d, j), posterior (e, k), and anterior (f, l) views. a., articulates with; dr, distal roller; for, foramen/anterior hollow; fi, fibula; peg, peg of the astragalus; pg, posterior groove; ti, tibia. Arrows indicate anterior direction. Scale bar equals 1 cm.

posterior side of the proximal surface and a sharp ridge separates the tibial and fibular facets. This ridge has peaks anteriorly and posteriorly connected through a thin sunken ridge and this is in contrast with the much more exaggerated anterior peak more in the anteroposterior center of the articulation surface present in *Poposaurus gracilis* (YPM 57100) and some early diverging crocodylomorphs (NCSM 21722). The fibular facet largely contacts the medial side of the fibula and the facet extends posterior of the tibial facet.

Anteriorly, the astragalus of *Shuvosaurus inexpectatus* bears a large rounded structure at its mediodistal margin (Figure 40). This rounded surface (= distal roller, Brochu, 1992) extends anteriorly much more than that of other pseudosuchians (*Revueltosaurus callenderi*, PEFO 34561; *Nundasuchus songeaensis*, NMT RB48), but similar to that of early diverging Crocodylomorpha (NCSM 21722). Proximal and lateral to the anteriorly projecting rounded surface, there is a deep concave area surrounded by thin but projected ridges on its proximal and lateral side. We interpret this area as homologous with the anterior hollow of other pseudosuchians. The anterior hollow of *Shuvosaurus inexpectatus* bears a large and well defined foramen in the medial portion of the structure and a similar, but a proportionally smaller foramen is present in some early diverging crocodylomorphs (NCSM 21722). The anterior hollow is present on the anterior surface where the tibial and fibular facets meet. The lateral side of the anterior surface is concave and forms the lateral side of the astragular peg that fits into the calcaneum.

Distally, the surface of the astragalus is divided in a rounded surface medially. This rounded surface is divided into the distal roller medially and the astragular peg laterally (Figure 40). The largely convex astragular peg has a long axis directed anteromedially and has a concave surface perpendicular to the long axis; the concave surface corresponds to a convex surface with the calcaneum. The astragular peg is similar in relative size and shape to that of other suchians (e.g., *Revueltosaurus callenderi*, PEFO 34561; early diverging crocodylomorphs, NCSM 21722) rather than that of earlier diverging pseudosuchians (e.g., phytosaurs, USNM 18131; *Nundasuchus songeaensis*, NMT RB48). The posterolateral tip of the astragular peg is hooked in *Shuvosaurus inexpectatus* but seems not to be in *Effigia okeeffeae*, early diverging crocodylomorphs (NCSM 21722), or *Revueltosaurus callenderi* (PEFO 34561).

Posteriorly, much of the medial side is slightly rounded and nearly featureless, whereas the lateral side bears the posterior surface of the astragalar peg and the posterior side of the articulation surface with the fibula and tibia (Figure 40). A small projection on the surface from the medial side defines the posterior margin of the articular surface with the tibia and this projection reaches the fibular articulation surface like in *Effigia*

okeeffeae (= articular ridge in Nesbitt, 2007, fig. 49D) (Figure 40). The posterior groove (= Sereno, 1991) separates the astragular peg from the more proximal portion that articulates with the tibia and the fibula.

Distal tarsal three—Distal tarsal three was not recovered from the largely complete referred skeleton (TTU-P9001), but we recognized a well-preserved example from the *Shuvosaurus inexpectatus* collection from the Post Quarry (TTU-P24024; Figure 41a–d) from its similarity to that of *Effigia okeeffeae* (AMNH FR 30587). Given that TTU-P24024 was found disarticulated, we are not certain of the orientation and side, but our comparisons with *Effigia okeeffeae* (AMNH FR 30587) suggest that TTU-P24024 is from the left side and that there is a lateral process. The "bean"-shaped element caps metatarsal III and contacts distal tarsal four laterally with its lateral process. The distal surface is concave anteroposteriorly and the proximal surface is nearly flat. The anterior portion is more broad than the posterior portion and a nonarticular facet lies distal to the lateral process.

Distal tarsal four—The distal tarsal four of *Shuvosaurus inexpectatus* was commonly found among the Post Quarry remains, but was always found isolated with the exception of the one associated with the left pes of TTU-P9001 (Figure 41e–h). Therefore, the exact orientation and the articulation surfaces are assumed based on comparisons with *Effigia okeeffeae* (Nesbitt, 2007), *Poposaurus gracilis* (Schachner et al., 2020), and *Postosuchus alisonae* (Peyer et al., 2008).

The proximal surface is nearly flat with a slightly concave anteroposterior center. The posterior portion of the proximal surface tapers posteromedially. In lateral view, distal tarsal four extends distally into a mediolaterally tongue. The posterolateral portion of this expanded distal portion articulates with metatarsal V and this surface is nearly flat. Medially, a nonarticulation surface with finished bone occupies much of the surface. It is not clear if this surface and the more posterior surface both articulate with metatarsal IV. Overall, distal tarsal four of *Shuvosaurus inexpectatus* is nearly identical to that of *Effigia okeeffeae* with the exception of proportions; the distally expanded tongue is proportionally shorter and shifted more posteriorly than that of *Effigia okeeffeae* (AMNH FR 30587).

Metatarsals—Partially articulated or associated pedes of *Shuvosaurus inexpectatus* are rare within the Post Quarry with only an unambiguous example from the left foot of the referred skeleton (TTU-P9001; Chatterjee, 1985, fig. 22) and another left partial foot (TTU-P23995). Nearly all of the metatarsals were compressed and contorted (Figure 42) to some degree from the fossilization process. For the purposes of the description below, we will focus on the unambiguously associated foot from TTU-P9001.

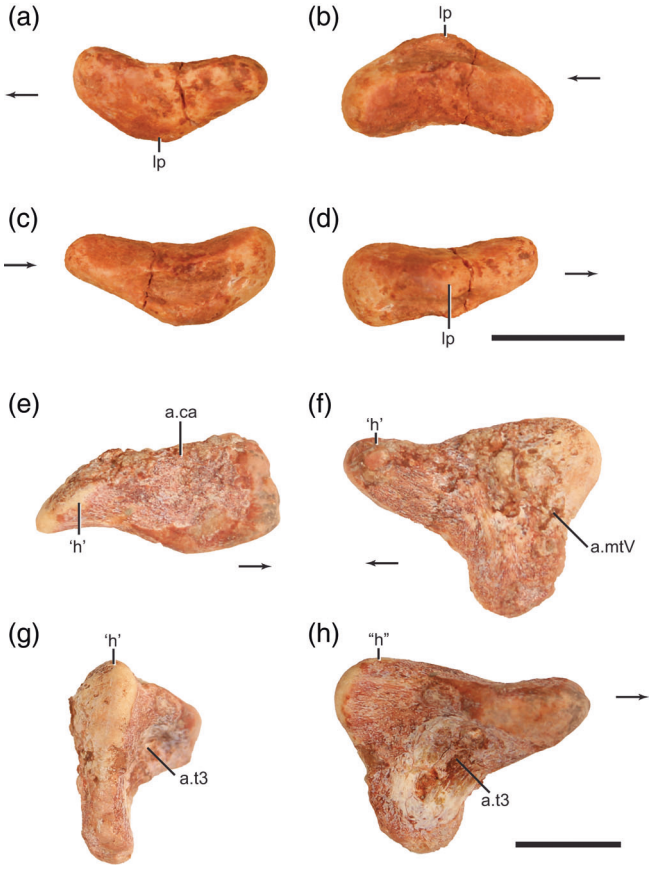

FIGURE 41 Distal tarsals of *Shuvosaurus inexpectatus*. Left distal tarsal three (TTU-P24024) in proximal (a), distal (b), lateral (c), and lateral (d) views. Left distal tarsal four (TTU-P9001) in proximal (e), lateral (f), posterior (g), and medial (h) views. a., articulates with; ca, calcaneum; "h," heal; lp, lateral process; mtV, metatarsal V; t3, distal tarsal three. Arrows indicate anterior direction. Scale bar equals 1 cm.

Metatarsal I—Subequal in length to metatarsal IV, metatarsal I (Figure 42a) possesses the smallest diameter at the midshaft compared to the other metatarsals. Proximally, metatarsal I expands relative to the shaft in both the anterolateral and posteromedial directions. The long axis of the proximal surface is oriented anterolateral and the anterolateral termination is more expanded than the tapered posteromedial termination. In medial view, the posteromedial portion overlies the shaft at a small kink 6 mm from the proximal surface. The anteromedial surface of the proximal end is smoothly convex whereas the posterolateral surface bears a rounded ridge at the proximal surface that spans the entire proximal edge; a shallow concavity lies just distal to this ridge and this feature is absent in *Effigia okeeffeae* (AMNH FR 30587) and *Poposaurus gracilis* (YPM 57100). The shaft gently tapers distally toward the distal end but remains oval in cross

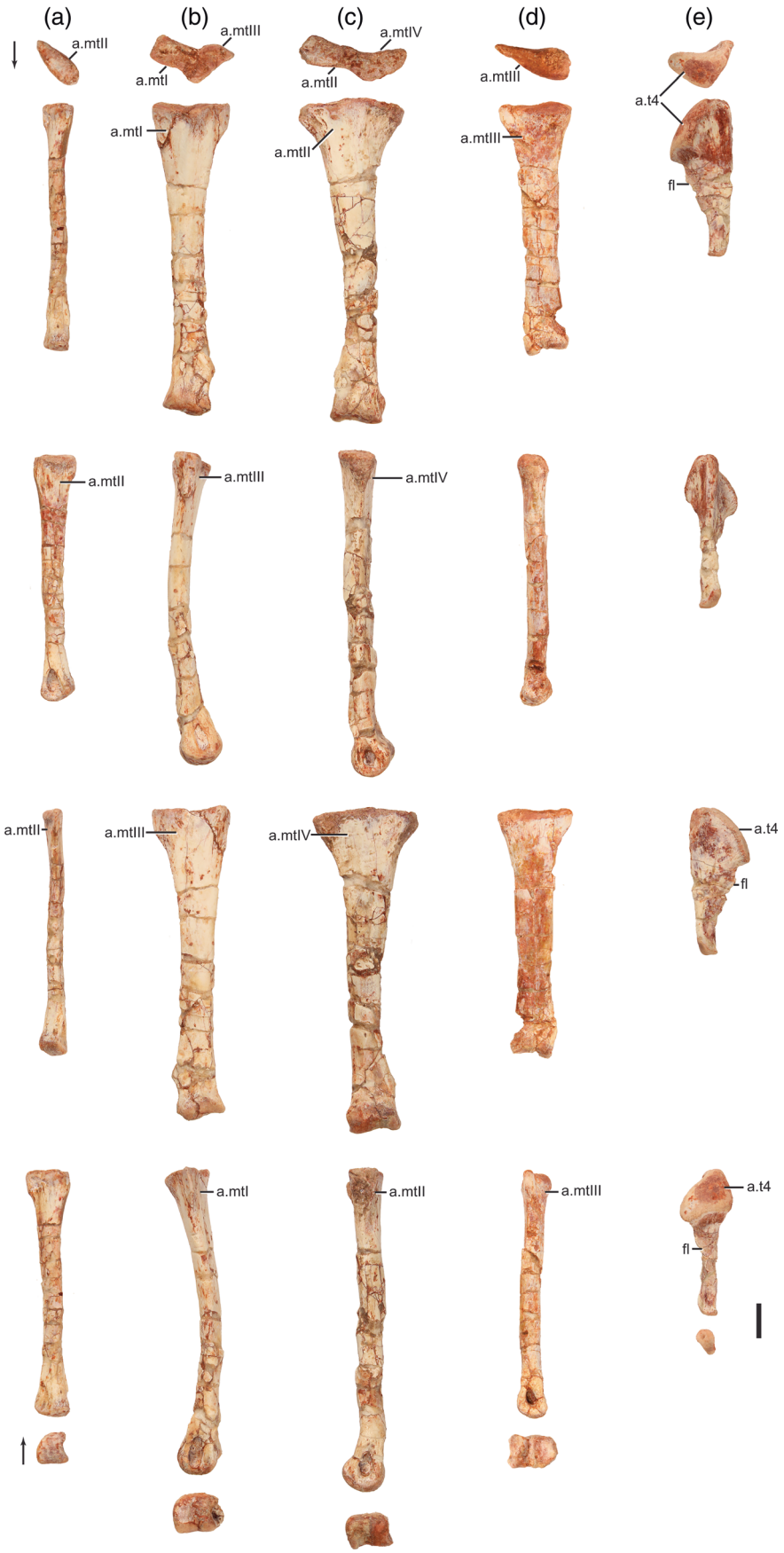

FIGURE 42 Left metatarsals (a–e) of an associated skeleton referred to *Shuvosaurus inexpectatus* (TTU-P9001) including metatarsal I (a), metatarsal II (b), metatarsal III (c), metatarsal IV (d), and metatarsal V (e). From the top of each column: proximal, dorsal, lateral, ventral, medial, and distal. a., articulates with; fl, flange; mt1, metatarsal I; mtII, metatarsal 2; mtIII, metatarsal III; mtIV, metatarsal IV; t4; 4th distal tarsal. Arrows indicate anterior direction. Scale bar equals 1 cm.

section with an anterolateral long axis. The distal end expands asymmetrically where the medial side expands more anteriorly than the lateral side and the distal surface is rounded anteriorly to posteriorly. This shape is generally similar to the asymmetric distal end of metatarsal IV of dinosauriforms (Langer & Benton, 2006; Novas, 1996). The posterior edge of the distal end is mediolaterally straight in *Shuvosaurus inexpectatus* whereas this same edge is concave in metatarsal IV of dinosauriforms (e.g., *Asilisaurus kongwe* NMT RB159). The medial surface bears a shallow fossa whereas the lateral side bears a deep (~3 mm) pit that invades the shaft proximally. *Effigia okeeffeae* (AMNH FR 30587) possesses a similarly deep medial pit, but in other pseudosuchians (*Poposaurus gracilis* YPM 57100; *Postosuchus alisonae*, NCSM 13731), this pit is much shallower. The anterior surface of the distal end transitions from the distal articular surface smoothly without any anterior expansion like that in *Effigia okeeffeae* (AMNH FR 30587) and the greater anterior expansion of *Poposaurus gracilis* (YPM 57100).

Metatarsal II—Metatarsal II is the second longest of the pes (Figure 42b; Table 2). The proximal portion expands twice as wide as the midshaft. The medial side of the shaft expands gradually from the midshaft whereas the lateral side is nearly straight until it reaches ~15 mm to the proximal surface; here the shaft expands posterolaterally until it reaches a point 7 mm to the proximal surface where the medial edge is vertical again. A nearly exact configuration is present in *Effigia okeeffeae* (AMNH FR 30587), whereas both lateral and medial sides gradually expand in *Poposaurus gracilis* (YPM 57100). Like metatarsal I, the long axis is oriented anterolaterally and posteromedially. A pronounced ridge expands anteriorly from the proximal edge. This ridge, which is present in *Shuvosaurus inexpectatus*, *Effigia okeeffeae*, and *Poposaurus gracilis* among poposauroids, separates the anterolateral surface from the more medial articular facet for metatarsal I. This more medial surface is slightly concave and the more lateral surface is straight in proximal view in all three taxa. The posterolateral surface is more concave in proximal view in *Shuvosaurus inexpectatus* compared to that of *Effigia okeeffeae* (AMNH FR 30587). This concave surface is more exaggerated in *Shuvosaurus inexpectatus* largely because the posterolateral edge is expanded more comparatively with *Effigia okeeffeae* (AMNH FR 30587) and *Poposaurus gracilis* (YPM 57100). Consequently, the articulation surface between metatarsal II and III has a higher degree of concave, convex relationship than in that of *Effigia okeeffeae*. The cross section at midshaft is oval with a mediolaterally oriented long axis. Distally, metatarsal II expands slightly asymmetrically where the lateral side is slightly more distal and expanded than the medial side; the condition is similar in *Effigia okeeffeae* (AMNH FR 30587) and *Poposaurus gracilis* (YPM 57100). The articular surface wraps onto the anterior surface with little anterior expansion and a depression lies just proximal to the termination of the articular surface. Both the lateral and medial sides bear rimmed pits whereas the lateral pit is deeper (~4 mm). The distal surface is nearly flat in the mediolateral center whereas a slight anteroposteriorly oriented groove is present in the same location in *Effigia okeeffeae* (AMNH FR 30587).

Metatarsal III—Metatarsal III is the longest and has the greatest proximal expansion compared to the other metatarsals (Figure 42c); this condition is also present in *Effigia okeeffeae* (AMNH FR 30587) and *Poposaurus gracilis* (YPM 57100). The proximal end expands asymmetrically where the lateral side has a more gradual expansion than the medial side. The posteromedial termination tapers into a clear process in *Shuvosaurus inexpectatus* (TTU-P9001) and *Effigia okeeffeae* (AMNH FR 30587) whereas there is no similar feature in *Poposaurus gracilis* (YPM 57100). In proximal view, the proximal portion is expanded mediolaterally, but this appears to be the result of taphonomic distortion given that the long axis orientation should be more anterolateral like that of the other metatarsals and the conditions in *Effigia okeeffeae* (AMNH FR 30587) and *Poposaurus gracilis* (YPM 57100). In proximal view, the posterior surface is largely concave. A ridge on the anterior surface separates the more medial surface for articulation with metatarsal II from that of the lateral surface. In proximal view, the more medial surface for articulation with metatarsal II is concave. Comparatively, the articular facet for metatarsal II on metatarsal III is shorter in *Shuvosaurus inexpectatus* (TTU-P9001) and *Effigia okeeffeae* (AMNH FR 30587) in comparison with that of *Poposaurus gracilis* (YPM 57100). Like metatarsal II, the oval cross section at midshaft has a mediolateral orientation.

In anterior view, the distal end of metatarsal III of *Shuvosaurus inexpectatus* (TTU-P9001) is nearly symmetrical mediolaterally, whereas these same surfaces are asymmetrical in *Effigia okeeffeae* (AMNH FR 30587; this is possibly distorted) and *Poposaurus gracilis* (YPM 57100). The anterior surface of the distal end of metatarsal III is not expanded and proximally terminated in a clear fossa whereas the posterior portion is clearly expanded from the shaft. Posteriorly, there is a slight proximally-distally oriented broad groove between the medial and lateral sides and the posteromedial edge of the articular surface slightly twists medially. A clear fossa is present just proximal to the termination of the distal articular surface. Both the medial and lateral surfaces bear deep pits whereas the medial one expands more proximally to form a tear-drop shape.

Metatarsal IV—Metatarsal IV is subequal in length to metatarsal I (Figure 42d), like that of *Effigia okeeffeae* (AMNH FR 30587) and in contrast to that of *Poposaurus gracilis* (YPM 57100) where metatarsal IV is much longer than metatarsal I and subequal to metatarsal III. Overall, metatarsal IV appears slightly compressed taphonomically and is missing some small pieces near the distal end. The proximal portion expands both medially and laterally whereas the medial side tapers to a more acute point. In proximal view, the medial side tapers to a thin point whereas the lateral side is rounded; this results in a teardrop shape. Much of anterior/dorsal surface of the proximal end articulates with the posterolateral surface of metatarsal III. Consequently, most of metatarsal IV lies posterior/ventral to that of metatarsal III. Comparisons between the proximal portions of metatarsal IV of *Shuvosaurus inexpectatus* and *Effigia okeeffeae* (AMNH FR 30587) are limited because of the poor preservation of the element in the later.

The distal end of metatarsal IV slightly expands relative to the oval cross section at midshaft in all directions, but it is clear that the distal end is expanded mediolaterally whereas the distal end of *Effigia okeeffeae* (AMNH FR 30587) is more expanded anteroposteriorly. The lateral surface bears a pit but the shape of the opening is damaged whereas the medial surface bears a deep pit. The distal articular surface extends from the anterior/dorsal surface, wraps around the distal end and slightly extends onto the posterior surface. Anteriorly, the articular surface terminated in a shallow fossa.

Metatarsal V—Metatarsal V (Figure 42e) is the shortest of the series and is about half the length of metatarsal III (Long & Murry, 1995). The convex proximal surface is expanded relative to the rest of the element and the distal end gradually tapers to a blunt point. In proximal view, metatarsal V expands medially and anteriorly and the posterior portion expands into a distinct process. The process marks the posterior and lateral margin of the element. The posterior process is present in *Effigia okeeffeae* (AMNH FR 30587) and *Postosuchus alisonae* (NCSM 13731), but absent in *Poposaurus gracilis* (YPM 57100). A medially projecting and anteroposterior compressed flange of bone lies just distal to the proximal surface (Figure 42e); an identical flange of bone is also present in *Effigia okeeffeae* (Nesbitt, 2007). On the posteromedial edge of the shaft, there is a slight rounded expansion in *Shuvosaurus inexpectatus*, *Effigia okeeffeae* (AMNH FR 30587), and *Postosuchus alisonae* (NCSM 13731), but absent in *Poposaurus gracilis* (YPM 57100). A shallow proximodistally oriented groove separates the rounded expansion from the anterior edge, as in *Effigia okeeffeae* (Nesbitt, 2007). The distal end terminates in a flat articulation surface that extends proximally on the posterior portion as in *Effigia okeeffeae* (Nesbitt, 2007).

In overall appearance, metatarsal V of *Shuvosaurus inexpectatus* and *Effigia okeeffeae* (AMNH FR 30587) are remarkably similar but a few differences are present including: the distal surface of *Shuvosaurus inexpectatus* is more tapered than that of *Effigia okeeffeae*; the proximal surface of *Effigia okeeffeae* is more circular in proximal view when compared to the more oval surface of *Shuvosaurus inexpectatus*; and the posterior process of the proximal end is mediolaterally narrower in *Shuvosaurus inexpectatus* than in *Effigia okeeffeae*.

Pedal phalanges—The pedal phalanges (Figure 43) are present at each digit in TTU-P9001, but a full set of pedal phalanges is not present in any of the specimens. Previously, a phalangeal formula of 2-3-4-5-0 was described for the referred skeleton (TTU-P9001; Long & Murry, 1995). However, since repreparation of the referred skeleton (TTU-P9001) and after publication by Long and Murry (1995), a full set of phalanges are not present anymore and are either lost or mixed with other Post Quarry specimens. Furthermore, the unguals attributed to TTU-P9001 originally are not unambiguously from *Shuvosaurus inexpectatus* (see below). From the original quarry map, some of the phalanges were articulated to each other, but these associations were not obviously recorded after preparation with one possible exception (see digit 1 below). Metatarsal V was cited as having no phalanges (Long & Murry, 1995), and the close relative *Effigia okeeffeae* also lacks any clear phalanges of digit V. However, the feet of *Shuvosaurus inexpectatus* and *Effigia okeeffeae* were not found completely articulated and other paracrocodylomorphs with a tapered metatarsal V have tiny phalanges that could be easily lost after burial or recovery (e.g., *Poposaurus gracilis*, Schachner et al., 2020; *Postosuchus alisonae*, Peyer et al., 2008). Therefore, the phalangeal formula of *Shuvosaurus inexpectatus* can only be cited as 2-1+-3+-2+-?

The phalanges (Figure 43) are unremarkable and not easily differentiated from other archosaurs when the position is not known. The proximal articular surfaces are typically taller than wide (Figure 43, top) whereas the distal articular surfaces are wider than tall (Figure 43, bottom). Most of the phalanges are symmetrical across their midlines in dorsal and ventral views. The distal ends expand laterally and medially and deep pits flank that sides. The distal surface is concave between the lateral and medial portions in dorsal and ventral views.

Unguals are represented by a once articulated element from digit I of the referred skeleton (TTU-P9001; Figure 44a–e) and by other examples from the Post Quarry (TTU-P9297; TTU-P9296; Figure 44). The unguals of *Shuvosaurus inexpectatus* (Figure 44) and *Effigia okeeffeae* (AMNH FR 30587) are distinct within Pseudosuchia in that they are highly dorsoventrally compressed with

TABLE 2 Measurements of a postcranial skeleton referred to *Shuvosaurus inexpectatus* (TTU P9001).

Element	Measurement	Length (mm)
Axis	Anteroposterior length	43.4
Sacral vertebra 1	Anteroposterior length	31.9
Sacral vertebra 2	Anteroposterior length	29.6
Sacral vertebra 3	Anteroposterior length	26.1
Humerus (left)	Proximodistal length	142.1
	Length of proximal end (long axis)	26.8
	Length of distal end (long axis)	17.9
	Midshaft width (max)	12.2
	Midshaft circumference	32
Femur (left)	Proximodistal length	234.7
	Length of proximal end (long axis)	43.3
	Length of distal end (long axis)	26.8
	Midshaft width (max)	20.8
	Midshaft circumference	55
Tibia (right)	Proximodistal length	198.2
	Length of proximal end (long axis)	32.8
	Length of distal end (long axis)	23.7
	Midshaft width (max)	13.8
Fibula (right)	Proximodistal length	201.9
	Length of proximal end (long axis)	27.1
	Length of distal end (long axis)	19.5
	Midshaft width (max)	9.8
Calcaneum (left)	Anteroposterior length	42.8
	Tuber height	31.6
Astragalus (left)	Proximal width	26.4
Metatarsal I (left)	Proximodistal length	65.3
	Length of proximal end (long axis)	12.9
	Length of distal end (long axis)	8.3
	Midshaft width (max)	6.1
Metatarsal II (left)	Proximodistal length	77.9
	Length of proximal end (long axis)	20.6
	Length of distal end (long axis)	12.2
	Midshaft width (max)	9.6
Metatarsal III (left)	Proximodistal length	85.6
	Length of proximal end (long axis)	28.5
	Length of distal end (long axis)	14.4
	Midshaft width (max)	9.6
Metatarsal IV (left)	Proximodistal length	62.7
	Length of proximal end (long axis)	20
	Length of distal end (long axis)	11.6
	Midshaft width (max)	10.3
Metatarsal V (left)	Proximodistal length	41.6
	Length of proximal end (long axis)	21.1
	Length of distal end (long axis)	7.9

pointed tips. *Poposaurus gracilis* (YPM 57100) also has dorsoventrally compressed unguals, but not to the same degree as that of shuvosaurids (Schachner et al., 2020). All unguals of *Shuvosaurus inexpectatus* are asymmetrical from dorsal view, and the one associated ungual with a digit (TTU-P9001, digit I; Figure 44a–e) indicates the unguals curved medially at their tips. The articular ends are concave and wider than tall.

Other than the single ungual from TTU-P9001, the position of the other unguals of *Shuvosaurus inexpectatus* is not known and the same is also true of *Effigia okeeffeae* (AMNH FR 30587). In the original description of TTU-P9001, Long and Murry (1995, fig. 170) assigned much larger, but highly dorsoventrally compressed unguals to digits II–IV. The identity of these three unguals is not clear because there is no documented association during preparation, the unguals were removed from TTU-P9001 during repreparation after the original description and, these unguals do not match those from digit I (TTU-P9001; Figure 44a–e) of *Shuvosaurus inexpectatus* and *Effigia okeeffeae* (AMNH FR 30587). Therefore, the referral of these unguals to *Shuvosaurus inexpectatus* is ambiguous and they could possibly be from another taxon.

3.6 | Previously attributed material to *Shuvosaurus inexpectatus*

Shuvosaurus inexpectatus emanates from a multitaxic bonebed (Chatterjee, 1984, 1985; Martz et al., 2013) and a number of postcranial bones were previously attributed to the taxon. In light of our new work presented here and the discovery of other Upper Triassic tetrapods, we review those bones. The type series of *Shuvosaurus inexpectatus* (TTU-P9280) originally contained the following

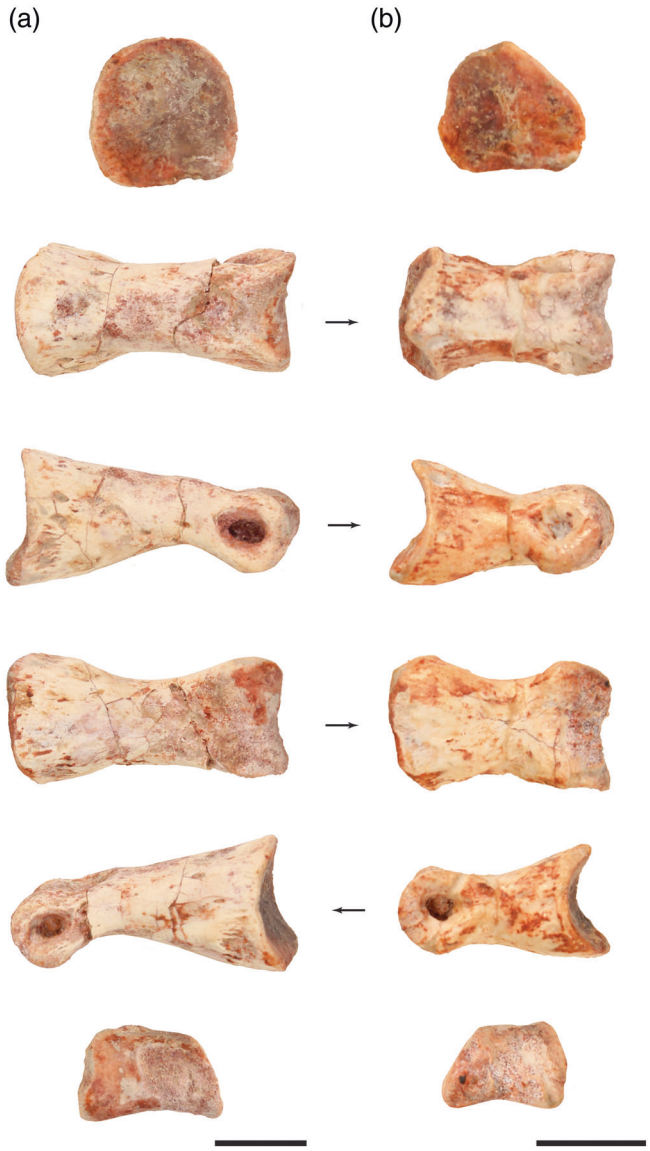

FIGURE 43 Pedal phalanges of an associated skeleton referred to *Shuvosaurus inexpectatus* (TTU-P9001) likely phalanx III-1 (a) and phalanx I-1 (b). From the top of each column: proximal, dorsal, lateral or medial, ventral, lateral or medial, distal. Arrows indicate anterior direction. Scale bar equals 1 cm.

FIGURE 44 Unguals of *Shuvosaurus inexpectatus*. Complete pedal ungual from a left digit I of a partial skeleton referred to *Shuvosaurus inexpectatus* (TTU-P9001) in lateral or medial (a and b), proximal (c), dorsal (d), and ventral (e) views. Complete pedal ungual from an unknown digit referred to *Shuvosaurus inexpectatus* (TTU-P9297) in lateral or medial (f and g), proximal (h), dorsal (i), and ventral (j) views and another referred to *Shuvosaurus inexpectatus* (TTU-P9296). Arrows indicate anterior direction. Scale bar equals 1 cm.

postcrania, a trunk vertebra (TTU-P9280; Figure 45e,f), partial atlas (TTU-P9281; TTU-P9282; Figure 45g–j), and a scapula (TTU-P9281; Figure 45a,b). A theropod tibia (TTU-P11044; Figure 45c,d) was informally assigned to *Shuvosaurus inexpectatus* in Chatterjee (1993). With the exception of the partial atlas (see above), all of these bones do not match those bones of the referred postcranial skeleton (TTU-P9001) or other referred specimens. Instead, these other bones are diagnosable to other taxa.

The previously identified trunk vertebra (previously TTU-P9280, now TTU-P24875; Figure 45e,f) is reidentified here as a posterior cervical vertebra based on the presence of a parapophysis located at the anteroventral edge of the centrum combined with a ridge on the ventral midline of the centrum. A large diapophysis well separated from the parapophysis and slightly procoelous condition (concave anterior articular facet of the centrum and slight convex rim of

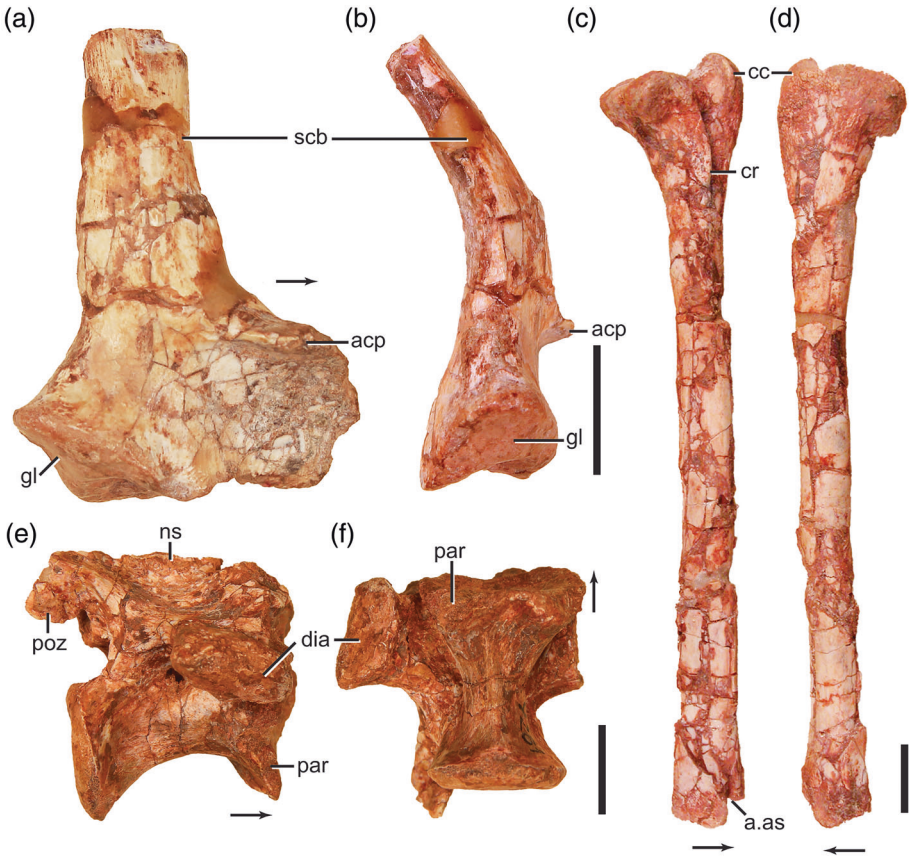

FIGURE 45 Bones previously assigned to *Shuvosaurus inexpectatus*. Archosaur right scapula (TTU-P11045) in lateral (a) and posteroventral (b) views. Right neotheropod tibia (TTU-P11044) in lateral (c) and medial (d) views. Azendohsaurid posterior cervical vertebra (TTU-P24875) in right lateral (e) and ventral (f) views. a., articulates with; acp, acromion process; as, astragalus; cc, cnemial crest; cr, crest; dia, diapophysis; gl, glenoid; ns, neural spine; par, parapophysis; poz, postzygapophysis. Arrows indicate anterior direction. Scale bars equal 1 cm.

the posterior articular facet of the centrum) are consistent with, but not unambiguously synapomorphic with, azendohsaurid archosauromorphs (Nesbitt et al., 2021). Other cervical vertebra remains of azendohsaurids were documented as "?*Malerisaurus langstoni*" in Martz et al. (2013) from the Post Quarry and malerisaurine azendohsaurids are abundant in the Dockum Group (Nesbitt et al., 2021).

The right scapula (previously TTU-P9281 now TTU-P11045; Figure 45a,b) bears a posteroventrally directed glenoid, a well pronounced acromion process that sits dorsal to a large depression, and a constricted base of the scapula blade. The pronounced acromion process is diagnostic of archosaurs (Nesbitt, 2011). However, the combination of its suite of character states are consistent with many archosaur clades (see Ezcurra, 2016; Nesbitt, 2011), but not obviously diagnostic to a certain clade because of convergence of character state combinations. The constriction of the base of the scapula blade is more common in ornithodirans (Ezcurra et al., 2020), so an assignment to that clade is reasonable, but not well supported. Ornithodirans including lagerpetids (*Dromomeron*), silesaurids (*Technosaurus smalli*), and dinosaurs (Nesbitt & Chatterjee, 2008) were recovered from the Post Quarry (Martz et al., 2013).

Lastly, the theropod tibia (TTU-P11044; Figure 45c,d) that was informally assigned to *Shuvosaurus inexpectatus* in Chatterjee (1993), bears diagnostic features of neotheropods (e.g., cnemial crest present and proximally expanded) and has been discussed elsewhere (Martz et al., 2013; Nesbitt & Chatterjee, 2008). This specimen represents the voucher for presence of a neotheropod from the Post Quarry (Marsh & Parker, 2020; Martz et al., 2013).

4 | DISCUSSION

4.1 | What is *Shuvosaurus*?

Late Triassic archosaurs with largely hollowed bones, long-limb proportions, and possibly changes in the dentition were historically assigned to dinosaurs (Benton, 1990b, 2004), given that dinosaurs originated in the Triassic (e.g., Colbert, 1958; Langer et al., 2018; Rogers et al., 1993). This was the case with a number of important discoveries from the Upper Triassic strata of the Dockum Group where partial skeletons with the aforementioned characteristics were assigned to various dinosaurian groups (e.g., *Postosuchus kirkpatricki* to Carnosauria Chatterjee, 1985; *Technosaurus smalli* to Ornithischia Chatterjee, 1984; and later *Shuvosaurus inexpectatus* to ?Ornithomimosauria within Theropoda

Chatterjee, 1993). Following these discoveries, the emergence of larger archosaur phylogenetic analyses capturing whole skeletons and additional discoveries of many Triassic archosaurs specimens and new species, changed the picture of archosaur evolution in the Triassic Period. From these advances in our understanding of archosaur evolution, a number of patterns emerged including: (1) dinosaurs were not as abundant in the Triassic as previous thought (e.g., Nesbitt et al., 2007); (2) convergence was rampant in archosaurs and their closest relatives (Nesbitt, 2007; see Stocker et al., 2016); (3) partial skeletons were much more reliable for identification rather than isolated bones (Nesbitt, 2011; Nesbitt et al., 2007); and (4) apomorphy-based identifications yielded a clear picture of occurrences of taxa in time and space (Lessner et al., 2018; Nesbitt & Stocker, 2008). *Shuvosaurus inexpectatus* is a perfect candidate illustrating this change in our understanding of archosaur evolution given our progress over the last 30 years of research. We now know that *Shuvosaurus inexpectatus* is a member of the highly divergent clade Shuvosauridae within Pseudosuchia (Figure 46), but possesses many uncanny character states previously exclusive to dinosaurs and their subgroups. Yet, differentiating *Shuvosaurus inexpectatus* from other close relatives and other archosaurs has not been detailed.

Our critical revision of the assignment of bones and detailed osteology of *Shuvosaurus inexpectatus* necessitated a complete revision of the diagnosis of the species (given above). Here we detail our diagnosis strategy given the complex history of the specimens. In general, we quantified previously unquantified relative terms (e.g., long, elongated), added in more comparative taxa that are closely related, and made the diagnoses as explicit as possible based on the holotype skull, the paratype and referred skull material, and then the postcrania separately.

Given our revision of the skull anatomy and the recognition that some of the originally assigned skull bones to *Shuvosaurus inexpectatus* may pertain to other skeletal elements, we completely revise the diagnosis of the skull. For example, we could not confirm the identification of the maxilla, so character states detailing the relationships of cranial opening related to the maxilla or contacting

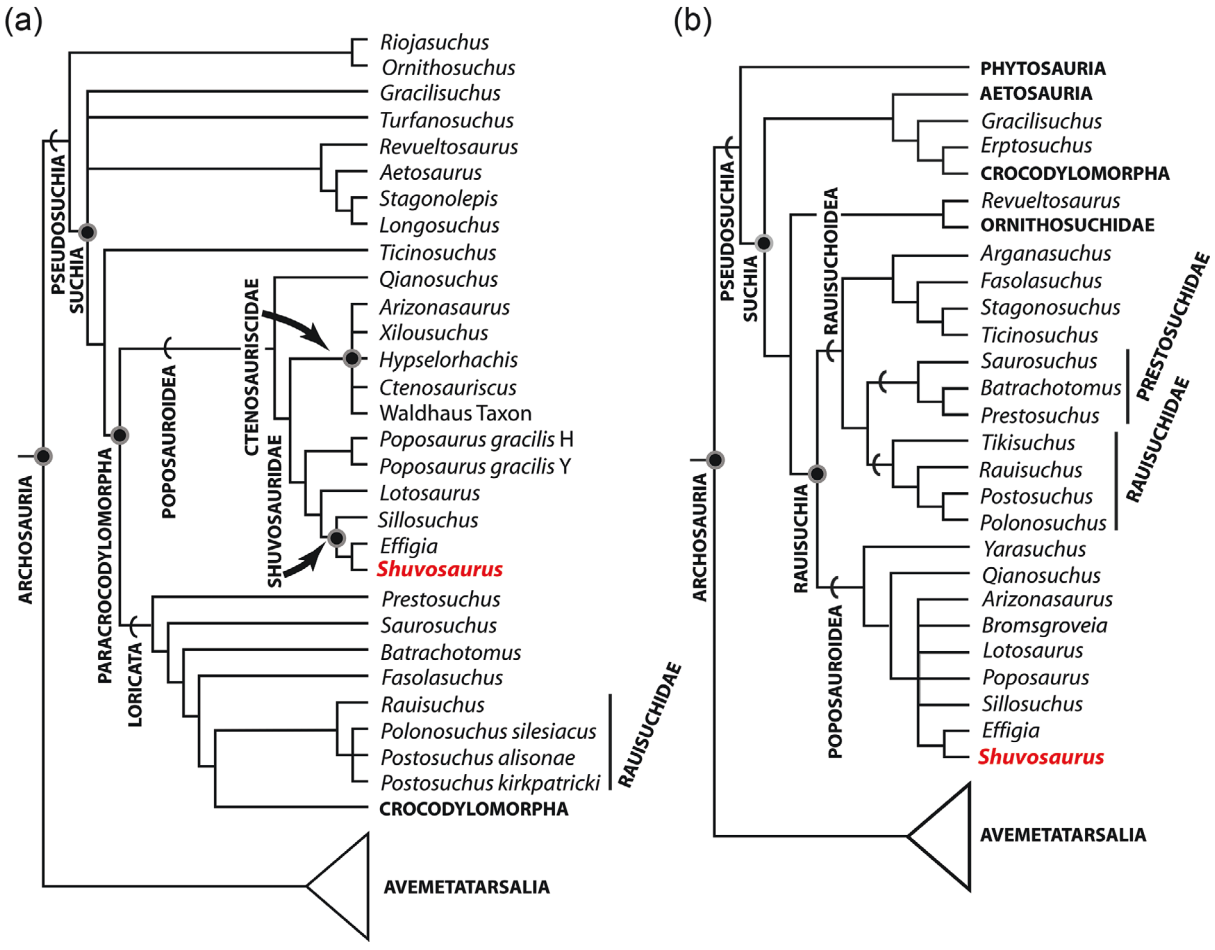

FIGURE 46 Hypotheses of the relationships of *Shuvosaurus inexpectatus* within Archosauria of Nesbitt (2011) (a) and Brusatte et al. (2010) (b). Some larger clades have been simplified (e.g. Avemetatarsalia, Crocodylomorpha) from the original analyses. H, holotype; Y, YPM 57100.

skull elements were not included. Similarly, any character states associated with the originally identified palatal elements (in Chatterjee, 1993; Lehane, 2023) were modified because each of those bones were reidentified (Table 1). Moreover, the size and shapes of the cranial openings played heavily into the original diagnosis based on the reconstructed skull (Chatterjee, 1993). We now think that these parts of the diagnosis are not repeatable with the reprepared material. Therefore, we did not include the shape of the naris, antorbital fenestra, orbit, or temporal openings as well as length of parts of the skull (e.g., preorbital region). We also incorporated the information and modification in the critical examination by Lucas et al. (2010) of the differences between *Shuvosaurus inexpectatus* and *Effigia okeeffeae* presented in Nesbitt and Norell (2006) and clarified by Nesbitt (2007).

Lastly, we focused the comparative statements to more closely related taxa confirmed in phylogenetic analyses (Brusatte et al., 2010; Nesbitt, 2007, 2011; Nesbitt & Norell, 2006), rather than previously proposed close relatives (i.e., theropod dinosaurs). It is clear that *Shuvosaurus inexpectatus* and *Effigia okeeffeae* are closely related (Lucas et al., 2010; Nesbitt, 2007; Nesbitt & Norell, 2006; Figure 46), so we relied heavily on their similarities relative to other pseudosuchians and then differentiated the two.

Postcranially, the original diagnosis of "*Chatterjeea elegans*" by Long and Murry (1995) was based on TTU-P9001, the same skeleton we largely rely on for the description above. Furthermore, the original diagnosis included comparison to other taxa (e.g., *Poposaurus gracilis*), that are confirmed as close relatives. Much of their diagnosis for the species is now diagnostic of either Shuvosauridae or the clade that contains *Shuvosaurus inexpectatus* and *Effigia okeeffeae*. We do revise their diagnosis further after further preparation, the incorporation of more referable specimens from the Post Quarry, and based on different comparisons with new taxa named after 1995, but clarify that *Chatterjeea elegans* is a junior synonym of *Shuvosaurus inexpectatus*.

This revised diagnosis implies that *Shuvosaurus inexpectatus* is only known from the Post Quarry currently (see below) and we urge future workers to compare to the revised type series and use the postcranium of TTU-P9001 for comparison with other taxa.

4.2 | The *Shuvosaurus inexpectatus* population

Shuvosaurus inexpectatus partial skeletons are abundant within the Post Quarry with nine partial skeletons recognized originally (Chatterjee, 1985). We evaluated the shuvosaurid material, now organized by element, and located and counted the most abundant element by side. From this process, we found hindlimb elements were the best represented and that there were at least 14 right partial femora (TTU-P15186; TTU-P18305; TTU-P18306; TTU-P18307; TTU-P18308; TTU-P18309; TTU-P18310; TTU-P18311; TTU-P18312; TTU-P18316; TTU-P18480; TTU-P18481; TTU-P18483; TTU-P18490; TTU-P18493), 12 left (TTU-P9001; TTU-P18323; TTU-P18368; TTU-P18380; TTU-P18381; TTU-P18382; TTU-P18383; TTU-P19010; TTU-P19012; TTU-P19275; TTU-P19575; TTU-P22577, TTU-P22578), 10 right calcanea, and 8 left and 12 right astragali. The numerous femora indicate a minimum number of 14 individuals in the quarry. This population represents one of the best samples of all Triassic pseudosuchians from one singular time-slice, and a study of variation and growth dynamics of this group will be published separately.

Although femora and robust hindlimb elements like the ankle are abundant, other parts of the skeleton are curiously missing from this sample of the population. Among the presacral vertebrae, only a few neural arches were found attached to the vertebrae (e.g., Figure 19) or isolated (Figure 22). Moreover, among the axial skeleton, cervical and trunk ribs are almost completely absent from the collection, and no confirmed chevron could be identified. Most curiously, we observed that no elements, or potential fragments, of the antebrachium (i.e., radius and ulna) or the hand are present among the Post Quarry material. This is more odd given that there are at least eight humeri present from the quarry. Admittedly, the ulna and radius are thin and delicate, and the manus is incredibly small and delicate (as indicated by those of *Effigia okeeffeae*, Nesbitt & Norell, 2006; Nesbitt, 2007) and could have washed away seemingly like the neural arches, ribs, and chevrons. Alternatively, it is possible that these elements may have been highly reduced, partially absent, or completely absent in *Shuvosaurus inexpectatus*, like that of some theropods (e.g., *Limusaurus inextricabilis*, Xu et al., 2009) or avialans (e.g., *Hesperornis regilis* and relatives, Bell & Chiappe, 2020; paleognaths such as *Apteryx australis*). The distal end of the humerus is complete with distinct condyles, and generally similar to other archosaurs, but little modification of the distal end does not correlate well with the reduction of loss of other forelimb elements (see Xing et al., 2009 for *Limusaurus inextricabilis*).

4.3 | Distribution of *Shuvosaurus inexpectatus*

During the original description of the postcrania of *Shuvosaurus inexpectatus* ("*Chatterjee elegans*" at the time), Long and Murry (1995) referred tens of bones and partial skeletons

to the taxon throughout the stratigraphic sequences of the Chinle Formation and the Dockum Group in the western United States. After the recognition of another shuvosaurid from stratigraphically high in the sequence (i.e., *Effigia okeeffeae*), it became clear that the assignment of all of the *Shuvosaurus inexpectatus*-like material represents a long-lived clade ("clade y" = Shuvosauridae; Nesbitt, 2007, 2011). Alternatively, Lucas et al. (2010) assigned all of the named taxa (i.e., *Effigia okeeffeae* and *Shuvosaurus inexpectatus*) to *Shuvosaurus* after concluding that the diagnosis presented in Nesbitt and Norell (2006) and updated in Nesbitt (2007) did not justify a new genus for AMNH FR 30587.

Shuvosaurid skeletal material is diagnostic throughout the skull (e.g., premaxilla, squamosal, hemimandible) and postcranium (e.g., pectoral and pelvic girdles, forelimbs and hindlimbs, particularly the femur) given the groups divergence with other pseudosuchians and its closest relatives. However, differentiating members *within* Shuvosauridae from the Chinle Formation and Dockum Group is not easy based on isolated bones from across the skeleton, even though the skeletons for *Effigia okeeffeae* and *Shuvosaurus inexpectatus* are now more differentiated (see diagnosis). From this evidence, we conclude that assignments to species, whether new or existing, can only reliably be made from partial, clearly associated skeletons or possibly scattered bones within a quarry of a presumably single species. Thus, we restrict all assignable remains of *Shuvosaurus inexpectatus* to specimens from the Post Quarry and do not recognize any occurrence outside of the bonebed.

AUTHOR CONTRIBUTIONS

Sterling Nesbitt: Conceptualization; investigation; funding acquisition; visualization; writing – review and editing; writing – original draft; data curation; resources; methodology. **Sankar Chatterjee:** Conceptualization; investigation; funding acquisition; writing – review and editing; resources.

ACKNOWLEDGMENTS

We are indebted to Kendra Dean-Wallace and John Henry Voss for curatorial help (TTU), finding original pictures of the Post Quarry, and locating specimens. We thank Bryan Small for discussing the Post Quarry excavation and providing other pictures of the excavation. We thank the late R. C. Miller for access to his ranch, Sibani Chatterjee, Bryan Small, Mike Nickell, J.B. Moring, and David Proctor for field assistance, and Bryan Small, Shuvo Chatterjee, Kendra Dean-Wallace, James Lehane, Vicki Yarborough, and many volunteers for the preparation of the material in the laboratory. We are thankful for discussions about the anatomy of the taxon and other taxa with Michelle Stocker, Adam Marsh, Randall Irmis, Jonathon Weinbaum, Jun Liu, and Doug Cunningham. We especially thank Doug Cunningham for discussion about the full skeletal mount that he put together. Adam Marsh and William Parker provided thorough and helpful reviews that greatly improved the observations and communication of the paper. Finally, we thank our funders, National Geographic (to S.C.) for a series of grants to support the excavations and subsequent research and the National Science Foundation (EAR 1943286 to S.J.N.).

ORCID

Sterling J. Nesbitt https://orcid.org/0000-0002-7017-1652

REFERENCES

Alcober, O., & Parrish, M. J. (1997). A new poposaurid from the Upper Triassic of Argentina. *Journal of Vertebrate Paleontology*, *17*, 548–556.

Bailleul, A. M., Scannella, J. B., Horner, J. R., & Evans, D. C. (2016). Fusion patterns in the skulls of modern archosaurs reveal that sutures are ambiguous maturity indicators for the Dinosauria. *PLoS One*, *11*, e0147687.

Bates, K., & Schachner, E. (2012). Disparity and convergence in bipedal archosaur locomotion. *Journal of the Royal Society Interface*, *9*, 1339–1353.

Bell, A., & Chiappe, L. M. (2020). Anatomy of *Parahesperornis*: Evolutionary mosaicism in the Cretaceous Hesperornithiformes (Aves). *Life*, *10*, 62.

Benton, M. J. (1986). The Late Triassic reptile *Teratosaurus* a rauisuchian not a dinosaur. *Palaeontology*, *29*, 293–301.

Benton, M. J. (1990a). Phylogeny of the major tetrapod groups: Morphological data and divergence dates. *Journal of Molecular Evolution*, *30*, 409–424.

Benton, M. J. (1990b). Origin and interrelationships of dinosaurs. In D. B. Weishampel, P. Dobson, & H. Osmolska (Eds.), *The Dinosauria* (pp. 11–30). University of California Press.

Benton, M. J. (2004). Origins and relationships of Dinosauria. In D. B. Weishampel, P. Dobson, & H. Osmolska (Eds.), *Dinosauria II* (pp. 7–24). University of California Press.

Benton, M. J., & Clark, J. M. (1988). Archosaur phylogeny and the relationships of the Crocodylia. In M. J. Benton (Ed.), *The phylogeny and classification of the tetrapods. Vol 1: Amphibians and reptiles* (pp. 295–338). Clarendon Press.

Bestwick, J., Jones, A., Nesbitt, S. J., Lautenschlager, S., Rayfield, E., Cuff, A., Button, D., Barrett, P. M., Porro, L., & Butler, R. J. (2021). Cranial functional morphology of the pseudosuchian *Effigia* and implications for its ecological role in the Triassic. *The Anatomical Record*, *305*, 2435–2462.

Britt, B. B. (1993). *Pneumatic postcranial bones in dinosaurs and other archosaurs*. University of Calgary.

Brochu, C. A. (1992). Ontogeny of the postcranium in crocodylomorph archosaurs. In *Geological Sciences*. University of Texas. https://repositories.lib.utexas.edu/items/a0c8722b-0b86-4368-aba7-e8348c995d65

Brochu, C. A. (1996). Closure of neurocentral sutures during crocodilian ontogeny: Implications for maturity assessment in fossil archosaurs. *Journal of Vertebrate Paleontology*, *16*, 49–62.

Brusatte, S. L., Benton, M. J., Desojo, J. B., & Langer, M. C. (2010). The higher-level phylogeny of Archosauria (Tetrapoda: Diapsida). *Journal of Systematic Palaeontology*, *8*, 3–47.

Butler, R. J., Brusatte, S. L., Reich, M., Nesbitt, S. J., Schoch, R. R., & Hornung, J. J. (2011). The sail-backed reptile *Ctenosauriscus* from the latest Early Triassic of Germany and the timing and biogeography of the early archosaur radiation. *PLoS One*, *6*, 1–28.

Butler, R. J., Nesbitt, S. J., Charig, A. J., Gower, D. J., & Barrett, P. M. (2018). *Mandasuchus tanyauchen* gen. et sp. nov., a pseudosuchian archosaur from the Manda beds of Tanzania. In: Sidor CA, Nesbitt SJ, editors. Vertebrate and climatic evolution in the Triassic rift basins of Tanzania and Zambia. Society of Vertebrate Paleontology Memoir 17. *Journal of Vertebrate Paleontology*, *37*(Suppl 6), 96–121.

Chatterjee, S. (1984). A new ornithischian dinosaur from the Triassic of North America. *The Science of Nature*, *71*, 630–631.

Chatterjee, S. (1985). *Postosuchus*, a new thecodontian reptile from the Triassic of Texas and the origin of tyrannosaurs. *Philosophical Transactions of the Royal Society of London B*, *309*, 395–460.

Chatterjee, S. (1993). *Shuvosaurus*, a new theropod. *National Geographic Research and Exploration*, *9*, 274–285.

Colbert, E. H. (1958). Tetrapod extinctions at the end of the Triassic period. *Proceedings of the National Academy of Sciences*, *44*, 973–977.

Cope, E. D. (1869). Synopsis of the extinct Batrachia, Reptilia and Aves of North America. *Transactions of the American Philosophical Society, New Series*, *14*, 1–252.

Dzik, J. (2003). A beaked herbivorous archosaur with dinosaur affinities from the early Late Triassic of Poland. *Journal of Vertebrate Paleontology*, *23*, 556–574.

Ezcurra, M. D., Nesbitt, S. J., Bronzati, M., Dalla Vecchia, F. M., Angolin, F. L., Benson, R. B. J., Egli, F. B., Cabreura, S. F., Evers, S. W., Gentil, A. R., Irmis, R. B., Martinelli, A. G., Novas, F. E., da Silva, L. R., Smith, N. D., Stocker, M. R., Turner, A. H., & Langer, M. C. (2020). Enigmatic dinosaur precursors bridge the gap to the origin of Pterosauria. *Nature*, *588*, 445–449.

Ezcurra, M. D. (2016). The phylogenetic relationships of basal archosauromorphs, with an emphasis on the systematics of proterosuchian archosauriforms. *PeerJ*, *4*, e1778.

Gauthier, J., & Padian, K. (1985). Phylogenetic, functional, and aerodynamic analyses of the origin of birds and their flight. In M. K. Hecht, J. H. Ostrom, G. Viohl, & P. Wellnhofer (Eds.), *The beginning of birds* (pp. 185–197). Freunde des Jura Museums.

Gauthier, J. A. (1986). Saurischian monophyly and the origin of birds. *Memoirs of the California Academy of Science*, *8*, 1–55.

Gower, D. J. (1999). The cranial and mandibular osteology of a new rauisuchian archosaur from the Middle Triassic of southern Germany. *Stuttgarter Beitraege zur Naturkunde Serie B (Geologie und Palaeontologie)*, *280*, 1–49.

Gower, D. J. (2002). Braincase evolution in suchian archosaurs (Reptilia: Diapsida): Evidence from the rauisuchian Batrachotomus kupferzellensis. *Zoological Journal of the Linnean Society*, *136*, 49–76.

Gower, D. J., & Nesbitt, S. J. (2006). The braincase of *Arizonasaurus babbitti*—Further evidence of the non-monophyly of Rauisuchia. *Journal of Vertebrate Paleontology*, *26*, 79–87.

Gower, D. J., & Schoch, R. R. (2009). Postcranial anatomy of the rauisuchian archosaur *Batrachotomus kupferzellensis*. *Journal of Vertebrate Paleontology*, *29*, 103–122.

Griffin, C. T., Stocker, M. R., Colleary, C., Stefanic, C. M., Lessner, E. J., Riegler, M., Formosa, K., Koeller, K., & Nesbitt, S. J. (2020). Assessing ontogenetic maturity in extinct saurian reptiles. *Biological Reviews*, *96*, 470–525.

Heckert, A. B., & Lucas, S. G. (1998). Global correlation of the Triassic theropod record. *GAIA: Revista de Geociências*, *1998*, 63–74.

Hunt, A. (2001). The vertebrate fauna, biostratigraphy and biochronology of the type Revueltian land-vertebrate faunachron. Bull Canyon Formation (Upper Triassic), East-Central New Mexico: New Mexico Geological Society. *Guidebook*, *52*, 123–151.

Hunt, A. P., Lucas, S. G., Heckert, A. B., Sullivan, R. M., & Lockley, M. G. (1998). Late Triassic dinosaurs from the western United States. *Geobios*, *31*, 511–531.

Irmis, R. B. (2007). Axial skeleton ontogeny in the Parasuchia (Archosauria: Pseudosuchia) and its implications for ontogenetic determination in archosaurs. *Journal of Vertebrate Paleontology*, *27*, 350–361.

Irmis, R. B., Mundil, R., Martz, J. W., & Parker, W. G. (2011). High-resolution U–Pb ages from the Upper Triassic Chinle Formation (New Mexico, USA) support a diachronous rise of dinosaurs. *Earth and Planetary Science Letters*, *309*, 258–267.

Juul, L. (1994). The phylogeny of basal archosaurs. *Palaeontologia Africana*, *31*, 1–38.

Langer, M. C., Ramezani, J., & Da Rosa, Á. A. (2018). U–Pb age constraints on dinosaur rise from South Brazil. *Gondwana Research*, *57*, 133–140.

Langer, M. C., & Benton, M. J. (2006). Early dinosaurs: A phylogenetic study. *Journal of Systematic Palaeontology*, *4*, 309–358.

Lehane, J. (2005). *Anatomy and relationship of Shuvosaurus, a basal theropod from the Triassic of Texas*. Texas Tech University.

Lehane, J. R. (2023). Cranial anatomy of *Shuvosaurus inexpectatus*, an edentulous poposauroid pseudosuchian from the Late Triassic of Texas. *Historical Biology*, 1–26.

Lessner, E. J., Parker, W. G., Marsh, A. D., Nesbitt, S. J., Irmis, R. B., & Mueller, B. D. (2018). New insights into Late Triassic dinosauromorph bearing assemblages from Texas using apomorphy-based identifications. *PaleoBios*, *35*, 1–41.

Li, C., Wu, X.-C., Cheng, Y.-N., Sato, T., & Wang, L. (2006). An unusual archosaurian from the marine Triassic of China. *Naturwissenschaften*, *93*, 200–206.

Long, R. A., & Murry, P. A. (1995). Late Triassic (Carnian and Norian) tetrapods from the southwestern United States New Mexico. *New Mexico Museum of Natural History and Science Bulletin*, *4*, 1–254.

Lucas, S. G., Spielmann, J. A., & Hunt, A. P. (2010). Taxonomy of *Shuvosaurus*, a Late Triassic archosaur from the Chinle group, American southwest. In S. G. Lucas & J. A. Spielmann (Eds.), *The Global Triassic: New Mexico Museum of Natural History and Science Bulletin* (pp. 259–261).

Marsh, A. D., & Parker, W. G. (2020). New dinosauromorph specimens from Petrified Forest National Park and a global biostratigraphic review of Triassic dinosauromorph body fossils. *PaleoBios*, *37*, 50859.

Martz, J., & Parker, W. (2017). Revised formulation of the Late Triassic land vertebrate "Faunachrons" of western North America:

Recommendations for codifying nascent systems of vertebrate biochronology. In *Terrestrial depositional systems* (pp. 39–125). Elsevier.

Martz, J. M., Mueller, B., Nesbitt, S. J., Stocker, M. R., Parker, W. G., Atanassov, M., Fraser, N., Weinbaum, J. C., & Lehane, J. (2013). A taxonomic and biostratigraphic re-evaluation of the post quarry vertebrate assemblage from the Cooper Canyon Formation (Dockum group, Upper Triassic) of southern Garza County, western Texas. *Earth and Environmental Science Transactions of the Royal Society of Edinburgh*, *103*, 339–364.

Meers, M. B. (2003). Crocodylian forelimb musculature and its relevance to Archosauria. *The Anatomical Record Part A: Discoveries in Molecular, Cellular, and Evolutionary Biology: An Official Publication of the American Association of Anatomists*, *274*, 891–916.

Nesbitt, S. J., & Stocker, M. R. (2008). The vertebrate assemblage of the Late Triassic Canjilon Quarry (northern New Mexico, USA), and the importance of apomorphy-based assemblage comparisons. *Journal of Vertebrate Paleontology*, *28*, 1063–1072.

Nesbitt, S. J. (2005a). A new archosaur from the upper Moenkopi Formation (Middle Triassic) of Arizona and its implications for rauisuchian phylogeny and diversification. *Neues Jahrbuch für Geologie Und Paläeontologie Monatshefte*, *2005*, 332–346.

Nesbitt, S. J. (2005b). The osteology of the Middle Triassic pseudosuchian archosaur *Arizonasaurus babbitti*. *Historical Biology*, *17*, 19–47.

Nesbitt, S. J. (2007). The anatomy of *Effigia okeeffeae* (Archosauria, Suchia), theropod convergence, and the distribution of related taxa. *Bulletin of the American Museum of Natural History*, *302*, 1–84.

Nesbitt, S. J. (2011). The early evolution of Archosauria: Relationships and the origin of major clades. *Bulletin of the American Museum of Natural History*, *352*, 1–292.

Nesbitt, S. J., Brusatte, S. L., Desojo, J. B., Liparini, A., Gower, D. J., França, M. A. G., & Weinbaum, J. C. (2013). Rauisuchia. In S. J. Nesbitt, J. B. Desojo, & R. B. Irmis (Eds.), *Anatomy, phylogeny, and palaeobiology of early archosaurs and their kin* (Special volume) (pp. 241–274). Geological Society.

Nesbitt, S. J., Butler, R. J., Ezcurra, M. D., Barrett, P. M., Stocker, M. R., Angielczyk, K. D., Smith, R. M. H., Sidor, C. A., Niedźwiedzki, G., Sennikov, A., & Charig, A. J. (2017). The earliest bird-line archosaurs and assembly of the dinosaur body plan. *Nature*, *544*, 484–487.

Nesbitt, S. J., Irmis, R. B., & Parker, W. G. (2007). A critical re-evaluation of the Late Triassic dinosaur taxa of North America. *Journal of Systematic Palaeontology*, *5*, 209–243.

Nesbitt, S. J., Langer, M. C., & Ezcurra, M. D. (2019). The anatomy of *Asilisaurus kongwe*, a dinosauriform from the Lifua Member of the Manda beds (∼Middle Triassic) of Africa. *Anatomical Record*, *303*, 813–873.

Nesbitt, S. J., Liu, J., & Li, C. (2011). A sail-backed suchian from the Heshanggou Formation (Early Triassic: Olenekian) of China. *Earth and Environmental Science Transactions of the Royal Society of Edinburgh*, *101*, 271–284.

Nesbitt, S. J., Patellos, E., Kammerer, C. F., Ranivoharimanana, L., Wyss, A. R., & Flynn, J. J. (2023). The earliest-diverging avemetatarsalian: A new osteoderm-bearing taxon from the ?earliest Late Triassic of Madagascar and the composition of avemetatarsalian assemblages prior to the radiation of dinosaurs. *Zoological Journal of the Linnean Society*, *199*, 327–353.

Nesbitt, S. J., Stocker, M. R., Ezcurra, M. D., Fraser, N. C., Heckert, A. B., Parker, W. G., Mueller, B., Sengupta, S., Bandyopadhyay, S., Pritchard, A. C., & Marsh, A. D. (2021). Widespread azendohsaurids (Archosauromorpha: Allokotosauria) from the Late Triassic of the western United States and India. *Papers in Palaeontology*, *8*, e1413.

Nesbitt, S. J., & Chatterjee, S. (2008). Late Triassic dinosauriforms from the Post Quarry and surrounding areas, West Texas, U.S.A. *Neues Jahrbuch für Geologie und Paläeontologie Abhandlungen*, *2008*, 143–156.

Nesbitt, S. J., & Norell, M. A. (2006). Extreme convergence in the body plans of an early suchian (Archosauria) and ornithomimid dinosaurs (Theropoda). *Proceedings of the Royal Society of London B*, *273*, 1045–1048.

Nopcsa, F. (1923). Die Familien der Reptilien. *Fortschritte der Geologie und Paläontologie*, *2*, 1–210.

Novas, F. E. (1996). Dinosaur monophyly. *Journal of Vertebrate Paleontology*, *16*, 723–741.

Osmólska, H. (1997). Ornithomimosauria. In P. J. Currie & K. Padian (Eds.), *Encyclopedia of dinosaurs* (pp. 499–503). Academic Press.

Parrish, J. M. (1993). Phylogeny of the Crocodylotarsi, with reference to archosaurian and crurotarsan monophyly. *Journal of Vertebrate Paleontology*, *13*, 287–308.

Peyer, K., Carter, J. G., Sues, H.-D., Novak, S. E., & Olsen, P. E. (2008). A new suchian archosaur from the Upper Triassic of North Carolina. *Journal of Vertebrate Paleontology*, *28*, 363–381.

Plateau, O., & Foth, C. (2021). Common patterns of skull bone fusion and their potential to discriminate different ontogenetic stages in extant birds. *Frontiers in Ecology and Evolution*, *9*, 737199.

Ramezani, J., Hoke, G. D., Fastovsky, D. E., Bowring, S. A., Therrien, F., Dworkin, S. I., Atchley, S. C., & Nordt, L. C. (2011). High-precision U–Pb zircon geochronology of the Late Triassic Chinle Formation, Petrified Forest National Park (Arizona, USA): Temporal constraints on the early evolution of dinosaurs. *Bulletin*, *123*, 2142–2159.

Rasmussen, C., Mundil, R., Irmis, R. B., Geisler, D., Gehrels, G. E., Olsen, P. E., Kent, D. V., Lepre, C., Kinney, S. T., & Geissman, J. W. (2021). U–Pb zircon geochronology and depositional age models for the Upper Triassic Chinle Formation (Petrified Forest National Park, Arizona, USA): Implications for Late Triassic paleoecological and paleoenvironmental change. *Bulletin*, *133*, 539–558.

Rauhut, O. W. M. (1997). Zur Schädelanatomie von *Shuvosaurus inexpectatus* (Dinosauria; Therapoda). In S. Sachs, O. W. M. Rauhut, & A. Weigert (Eds.), *Treffen der deutschsprachigen Palaeoherpetologen* (pp. 17–21). Dusseldorf.

Rauhut, O. W. M. (2003). The interrelationships and evolution of basal theropod dinosaurs. *Special Papers in Palaeontology*, *69*, 1–214.

Rogers, R. R., Swisher, C. C., III, Sereno, P. C., Monetta, A. M., Forster, C. A., & Martínez, R. N. (1993). The Ischigualasto tetrapod assemblage (Late Triassic, Argentina) and $^{40}Ar/^{39}Ar$ dating of dinosaur origins. *Science*, *260*, 794–797.

Sarigül, V. (2017). New theropod fossils from the Upper Triassic Dockum Group of Texas, USA, and a brief overview of the Dockum theropod diversity. *PaleoBios*, *34*, 1–18.

Schachner, E. R., Irmis, R. B., Huttenlocker, A. K., Sanders, R. K., Cieri, R. L., & Nesbitt, S. J. (2020). Osteology of the Late Triassic bipedal archosaur *Poposaurus gracilis* (Archosauria: Pseudosuchia). *Anatomical Record*, *303*, 874–917.

Schachner, E. R., Manning, P. L., & Dodson, P. (2011). Pelvic and hindlimb myology of the basal archosaur *Poposaurus gracilis* (Archosauria: Poposauroidea). *Journal of Morphology*, *272*, 1464–1491.

Schoch, R., Nesbitt, S. J., Muller, J., Fastnacht, M., Lucas, S. G., & Boy, J. A. (2010). The reptile assemblage from the Moenkopi Formation (Middle Triassic) of New Mexico. *Neues Jahrbuch für Geologie und Paläontologie, Abhandlungen*, *255*, 245–369.

Sereno, P. C. (1991). Basal archosaurs: Phylogenetic relationships and functional implications. *Journal of Vertebrate Paleontology*, *10*(Suppl 3), 1–53.

Sereno, P. C., & Arcucci, A. B. (1990). The monophyly of crurotarsal archosaurs and the origin of bird and crocodile ankle joints. *Neues Jahrbuch für Geologie und Paläeontologie Abhandlungen*, *180*, 21–52.

Sidor, C. A., Peecook, B. R., Beightol, C. V., Kaye, T., Kulick, Z. T., Livingston, G., Parker, W. G., Olroyd, S. L., & Whitney, M. R. (2018). *A multitaxic bonebed featuring a new shuvosaurid (Archosauria, Poposauroidea) from the Sonsela Member of the Chinle Formation at Petrified Forest National Park*. Journal of Vertebrate Paleontology, Program and Abstracts, 2018, 216.

Stefanic, C. M., & Nesbitt, S. J. (2018). The axial skeleton of *Poposaurus langstoni* (Pseudosuchia: Poposauroidea) and its implications for accessory intervertebral articulation evolution in pseudosuchian archosaurs. *PeerJ*, *6*, e4235.

Stocker, M. R., Nesbitt, S. J., Criswell, K. E., Parker, W. G., Witmer, L. M., Rowe, T. B., Ridgely, R., & Brown, M. A. (2016). A dome-headed stem archosaur exemplifies convergence among dinosaurs and their distant relatives. *Current Biology*, *26*, 2674–2680.

Von Baczko, M. B., Desojo, J. B., & Ponce, D. (2019). Postcranial anatomy and osteoderm histology of *Riojasuchus tenuisceps* and a phylogenetic update on Ornithosuchidae (Archosauria, Pseudosuchia). *Journal of Vertebrate Paleontology*, *39*, e1693396.

Weinbaum, J. C., & Hungerbühler, A. (2007). A revision of *Poposaurus gracilis* (Archosauria: Suchia) based on two new specimens from the Late Triassic of the southwestern U.S.A. *Paläontologische Zeitschrift*, *81*(2), 131–145.

Wilson, J. A. (1999). A nomenclature for vertebral laminae in sauropods and other saurischian dinosaurs. *Journal of Vertebrate Paleontology*, *19*, 639–653.

Witmer, L. M. (1997). The evolution of the antorbital cavity of archosaurs: A study in soft-tissue reconstruction in the fossil record. *Journal of Vertebrate Paleontology Memoir*, *3*, 1–73.

Xu, X., Clark, J. M., Mo, J., Choiniere, J., Forster, C. A., Erickson, G. M., Hone, D., Sullivan, C., Eberth, D. A., Nesbitt, S. J., Zhao, Q., Hernandez, R., Jia, C.-K., Han, F.-L., & Guo, Y. (2009). A Jurassic ceratosaur from China bearing on theropod digit reduction and avian digital homologies. *Nature*, *459*, 940–944.

Zhang, F. K. (1975). A new thecodont *Lotosaurus*, from the Middle Triassic of Hunan. *Vertebrata Palasiatica*, *13*, 144–147.

How to cite this article: Nesbitt, S. J., & Chatterjee, S. (2024). The osteology of *Shuvosaurus inexpectatus*, a shuvosaurid pseudosuchian from the Upper Triassic Post Quarry, Dockum Group of Texas, USA. *The Anatomical Record*, 1–64. https://doi.org/10.1002/ar.25376